SCREENING OF *Clostridium* sp. FOR BIOHYDROGEN PRODUCTION FROM SYNTHETIC WASTEWATER

Miss Chonticha Srimawong

A Dissertation Submitted in Partial Fulfillment of the Requirements
for the Degree of Doctor of Philosophy in Biotechnology
FACULTY OF SCIENCE
Chulalongkorn University
Academic Year 2022

การคัดกรอง *Clostridium* sp. เพื่อใช้ในการผลิตไบโอไฮโดรเจนจากน้ำเสียสังเคราะห์

น.ส.ชลธิชา ศรีมาวงษ์

วิทยานิพนธ์นี้เป็นส่วนหนึ่งของการศึกษาตามหลักสูตรปริญญาวิทยาศาสตรดุษฎีบัณฑิต
สาขาวิชาเทคโนโลยีชีวภาพ ไม่สังกัดภาควิชา/เทียบเท่า
คณะวิทยาศาสตร์ จุฬาลงกรณ์มหาวิทยาลัย
ปีการศึกษา 2565

Thesis Title	SCREENING OF *Clostridium* sp. FOR BIOHYDROGEN PRODUCTION FROM SYNTHETIC WASTEWATER
By	Miss Chonticha Srimawong
Field of Study	Biotechnology
Thesis Advisor	Professor WARAWUT CHULALAKSANANUKUL, Ph.D.

Accepted by the FACULTY OF SCIENCE, Chulalongkorn University in Partial Fulfillment of the Requirement for the Doctor of Philosophy

..... Dean of the FACULTY OF SCIENCE
(Professor POLKIT SANGVANICH, Ph.D.)

DISSERTATION COMMITTEE

..... Chairman
(Associate Professor SEHANAT PRASONGSUK, Ph.D.)

..... Thesis Advisor
(Professor WARAWUT CHULALAKSANANUKUL, Ph.D.)

..... Examiner
(Associate Professor SUCHADA CHANPRATEEP NAPATHORN, Ph.D.)

..... Examiner
(Assistant Professor CHOMPUNUCH GLINWONG, Ph.D.)

..... External Examiner
(Surisa Suwannarangsee, Ph.D.)

ชลธิชา ศรีมาวงษ์ : การคัดกรอง *Clostridium* sp. เพื่อใช้ในการผลิตไบโอไฮโดรเจนจากน้ำเสียสังเคราะห์. (SCREENING OF *Clostridium* sp. FOR BIOHYDROGEN PRODUCTION FROM SYNTHETIC WASTEWATER) อ.ที่ปรึกษาหลัก : ศ. ดร.วรวุฒิ จุฬาลักษณานุกูล

ในงานวิจัยมีความมุ่งหมายเพื่อคัดแยกเชื้อคลอสทริเดียมสปีชีส์ใหม่เพื่อนำมาผลิตไฮโดรเจนให้ได้ผลผลิตสูงและสามารถใช้สารตั้งต้นที่หลากหลายได้ รวมถึงของเสียอินทรีย์ เช่น ของเสียจากอุตสาหกรรมเกษตร เป็นต้น โดยงานนี้ได้ทำการแยกเชื้อกลุ่มที่สามารถผลิตเอนโดสปอร์จากแหล่งธรรมชาติและจากของเสียจากโรงงานอุตสาหกรรม ได้แก่ ป่าชายเลน น้ำพุร้อน และโรงงานมะพร้าว ซึ่งจากผลการวิเคราะห์ลำดับนิวคลีโอไทด์ของยีน 16S rRNA พบว่าเชื้อที่แยกมาได้มี *Clostridium* spp. และ *Paenibacillus* spp. จำนวนมาก เมื่อเปรียบเทียบค่าไฮโดรเจนที่เชื้อผลิตจากการหมักแบบกะ (batch fermentation) จึงเลือกเชื้อสองสายพันธุ์ที่สามารถผลิตไฮโดรเจนได้ดีที่สุดมาศึกษาต่อ ได้แก่ สายพันธุ์ CUEA01 และ CUEA03 หลังจากทำการหาลำดับนิวคลีโอไทด์ของจีโนมของเชื้อพบว่า CUEA01 เป็นเชื้อสปีชีส์ใหม่ ซึ่งได้ตั้งชื่อว่า *C. hydrogenum* และขณะที่เชื้อ CUEA03 คือเชื้อ *C. felsineum* โดยเชื้อทั้งสองสามารถโตและผลิตไฮโดรเจนได้ดีในสภาวะที่เป็นด่าง ผลการศึกษาจีโนมของเชื้อทั้งสองพบว่ามียีนที่สามารถถอดรหัสได้เอนไซม์ที่เกี่ยวข้องกับกระบวนการผลิตไฮโดรเจน และการใช้แหล่งคาร์บอนชนิดต่างๆ และจากผลการศึกษาหาสภาวะที่เหมาะสมต่อการผลิตไฮโดรเจนของเชื้อทั้งสองพบว่าสภาวะที่เหมาะสมต่อการผลิตไฮโดรเจนของเชื้อ CUEA01 คือ 37 °C, pH 8, และความเข้มข้นน้ำตาลที่ 10 g/L ขณะที่สายพันธุ์ CUEA03 คือที่ 30 °C pH 9, ความเข้มข้นน้ำตาลที่ 35 g/L ซึ่งจะให้ค่าไฮโดรเจนสะสมสูงสุดต่อลิตรเท่ากับ 3264 mL/L (3.11 $mol_{H2}/mol_{glucose}$) และ 5425 mL/L (1.70 $mol_{H2}/mol_{glucose}$) ตามลำดับ นอกจากนี้เชื้อทั้งสองยังสามารถใช้สารตั้งต้นที่หลากหลายในการผลิตไฮโดรเจนได้ เช่น ไซโลส แมนโนส อะราบิโนส แมนโนส ซูโครส อวิเซล แป้งมันสำปะหลัง เป็นต้น นอกจากนี้ได้มีการนำเอาของผลพลอยได้จากอุตสาหกรรมและวัสดุเหลือทิ้งทางการเกษตร ได้แก่ กากน้ำตาล กากมันสำปะหลัง และ ฟางข้าว มาใช้เป็นสารตั้งต้นในการผลิตไฮโดรเจนแทนแหล่งคาร์บอน โดยพบว่าเชื้อ CUEA01 สามารถผลิตไฮโดรเจนจากของเสียทั้งสามได้และสามารถผลิตไฮโดรเจนให้ปริมาณไฮโดรเจนสะสมที่ 4639 mL/L จากกากน้ำตาล และ 4024 mL/L จากกากมันสำปะหลัง ในขณะที่ CUEA03 สามรถผลิตไฮโดรเจนจากกากน้ำตาลได้ไฮโดรเจนสะสมผลผลิตที่ 5187 mL/L ดังนั้นแสดงให้เห็นว่าเชื้อทั้งสองมีศักยภาพที่จะนำมาใช้ในการผลิตไฮโดรเจนจากของเสียของเสียอินทรีย์ที่จะช่วยลดขั้นตอนทางกระบวนการทางชีวภาพและยังเป็นการบำบัดของเสียร่วมกับการผลิตพลังงานสะอาดซึ่งเป็นเป้าหมายของพลังงานในอนาตค

สาขาวิชา	เทคโนโลยีชีวภาพ	ลายมือชื่อนิสิต .....
ปีการศึกษา	2565	ลายมือชื่อ อ.ที่ปรึกษาหลัก .....

5872840823 : MAJOR BIOTECHNOLOGY

KEYWORD: Biohydrogen, Hydrogen fermentation, Clostridium hydrogenum, Clostridium felsinuem, CUEA01, CUEA03

Chonticha Srimawong : SCREENING OF *Clostridium* sp. FOR BIOHYDROGEN PRODUCTION FROM SYNTHETIC WASTEWATER . Advisor: Prof. WARAWUT CHULALAKSANANUKUL, Ph.D.

In this work, bacteria that can produce endospores were isolated from natural sources and industrial wastes, including mangrove forests, hot springs, and coconut factories. The bacterial isolates were identified as *Clostridium* spp. and *Panibacillus* spp. based on 16S RNA gene. When comparing the H_2 produced by batch fermentation, two of the isolates with the best H_2 production were selected for further study, namely CUEA01 and CUEA03. After genomics analysis, it was discovered that CUEA01 is a novel species named *C. hydrogenum*, and CUEA03 is *C. felsineum*. Both are capable of growing and producing H_2 in alkaline conditions. The genomics data reveal that they contain genetic information capable of encoding a variety of enzymes that aid in the process of H_2 production and also carbon source utilization. Following optimization of the H_2 production conditions for the two species, it was discovered that CUEA01 produced the highest cumulative H_2 yield of 3264 mL/L (3.11 $mol_{H2}/mol_{glucose}$) at 37 °C, pH 8, and 10 g/L of the initial carbon source, while CUEA03 is 5425 mL/L (1.70 $mol_{H2}/mol_{glucose}$) at 72 h of incubation was obtained from an initial glucose concentration of 35 g/L, pH 9, and an incubation temperature of 30 °C. Furthermore, different carbon sources were used as substrates to evaluate their feasibility of usage, and the results demonstrated that these species could secrete an effective enzyme capable of digesting various carbon sources to produce H_2 gas. Moreover, industrial by-products and agricultural residues have been employed as feedstocks to produce H_2 instead of simple sugar. It was found that CUEA01 was able to produce H_2 from the three wastes and was able to produce H_2 at an amount of 4639 mL/L from molasses and 4024 mL/L from cassava pulp, while CUEA03 could produce 5187 mL/L from molasses. Thus, this study indicates that both microorganisms have the potential to be used to produce H_2 from organic wastes, which will help integrate bioprocesses into waste treatment and clean energy production, which can help fulfill future fuel generation goals.

Field of Study:	Biotechnology	Student's Signature .....
Academic Year:	2022	Advisor's Signature .....

ACKNOWLEDGEMENTS

First of all, I would like to express my sincere gratitude and high appreciation to my advisor, Professor Dr. Warawut Chulalaksananukul, for his valuable encouragement, guidance, suggestions, and supervision throughout the period of the dissertation. My sincere thanks to Professor Dr. Christophe Gwendoline for her useful suggestion as well as her support to facilitate my experimental work at the Polytech Clermont-Ferrand, Clermont Auvergne University.

I would like to extend my gratitude to the chairman, Associate Professor Dr. Sehanat Prasongsuk. My sincere thanks to Associate Professor Dr. Suchada Chanprateep, Assistant Professor Dr. Chompunuch Glinwong, and Dr. Surisa Suwannarangsee for being on my committee and providing valuable advice.

My Sincere thanks to the Department of Botany, Faculty of Science, Chulalongkorn University, for offering the good laboratory facilities required for my research.

I would like to acknowledge the Research and Researchers for Industries (RRi) scholarship by Thailand Research Fund (TRF) [grant numbers PHD58I0084], Energy Absolute Public Company Limited (EA), and Chulalongkorn University for financial support as well as helping me with my mobility to Polytech Clermont-Ferrand, Clermont Auvergne University.

Additionally, I really would like to acknowledge and thank all of the fantastic members of the Biofuel by Biocatalyst Research Unit for their friendship, kind support, and help. I would not have done this without them.

Finally, I would like to express my sincere gratitude to my parents, sister, and my friends for supporting me and cheering me on in both good and terrible times.

Chonticha Srimawong

TABLE OF CONTENTS

Page

LIST OF TABLES

Page

LIST OF FIGURES

Page

LIST OF ABRREVIATIONS

CHP	Cumulative H_2 production
HPR	H_2 production rate
HPB	H_2 producing bacteria
VFA	Volatile fatty acid
SCE	Substrate conversion efficiency
MCC	Microcrystalline cellulose
LCB	locally collinear blocks
CDS	Protein-coding sequences
COD	Chemical Oxygen Demand
BOD	Biochemical Oxygen Demand
OD_{600}	Optical density at 600 nm
CDW	Cell dry weight
SEM	Scanning electron microscopy
TEM	Transmission electron microscopy

CHAPTER I

INTRODUCTION

Background

Currently, the growing demand for energy, notably electric power, combined with the depletion of fossil fuels has heightened interest in alternative bioenergy, including that used in electric vehicles. One of the most promising substitutes is Hydrogen (H_2), a carbon-free energy, which when burned produces a 2.75-fold higher energy density (122 kJ/g) than fossil fuels without emitting any harmful pollutants like carbon dioxide (CO_2), carbon monoxide (CO), fine particulate matter (PM 2.5), acidic pollutant gases (SOx and NOx), or carcinogenic acetaldehyde (Elbeshbishy et al., 2017). Additionally, it can directly generate electricity when combined with fuel cells. Dark fermentation is one of the biological processes that can produce H_2 in a sustainable manner under mild conditions. This method produces more H_2 per unit of time (HPR) than other methods. Furthermore, dark fermentation is applicable to a wide variety of complicated organic substrates and requires a simple system construction. A variety of H_2-producing bacteria have been investigated for H_2 fermentation. Nevertheless, the H_2 yield from various isolates ranged from around 2% to 60% of the theoretical yield (Yin & Wang, 2017).

The best candidates for H_2 producers among the many H_2-producing bacterial species are *Clostridium* spp., which produce H_2 at levels closer to the theoretical yield and with good compatibility with various carbon sources (Jayasinghearachchi et

al., 2010; Pan et al., 2008; Yin & Wang, 2017). Furthermore, it is the dominant species that supports H_2 generation during anaerobic digestion in the microflora of mixed cultures (Huang et al., 2010; Lin & Hung, 2008; Sivagurunathan et al., 2014). *Clostridium* spp. are generally obligate anaerobic bacteria of the family Clostridiaceae and genus *Clostridium*. They are spore-forming, Gram-positive bacteria.

A pure culture is also crucial for evaluating the characteristics of the isolated species and determining the most favorable condition for H_2 production, even though a mixed culture typically has the advantage in a practical application at an industrial scale. Additionally, a pure culture can be applied in alternative ways, such as in the bioaugmentation of a natural mixed culture or the establishment of a synthetic mixed culture to increase H_2 production. Previous research has shown that inoculating a mixed culture with an exogenous species can improve stability (Poirier et al., 2020), and bioaugmentation with *Clostridium* strains can improve H_2 yield from lignocellulosic biomass (Öner et al., 2018; Valdez-Vazquez et al., 2019). Previous findings have shown that numerous bacterial species screened from freshwater environments such as household landfills, sewage sludge, and dung can produce H_2. While the bacteria from marine environments have high biodiversity, they have rarely been mentioned in this context. Mangrove ecosystems are coastal wetland forests that play a crucial role in nutrient recycling by diverse microbial communities among other marine environments (Sahoo & Dhal, 2009). Mangrove sediments are rich in nutrients, have low oxygen levels, and contain a lot of highly decomposed plant

matter. As a result, they comprise fermentable bacteria that can effectively be employed to produce bio-H_2 by dark fermentation (Mullai et al., 2013; Zhu et al., 2008).

Accordingly, this study screened for *Clostridium* spp. from mangrove and hot spring sediments, which are natural resources and had never been screened before, compared with screening from coconut factory wastewater, which is an unnatural source. This led to the discovery of a novel *Clostridium* species with significant biotechnological potential for high-yield H_2 production from organic waste, which was named *C. hydrogenum* sp. nov. strain CUEA01 and *C. felsineum* strain CUEA03, and is hereafter referred to as CUEA01 and CUEA03. Whole genome sequencing (WGS) is a method that is continuously developing and can be used to access an organism's whole genetic information. The genomic sequences of CUEA01 and CUEA03 were determined using next generation sequencing (NGS) technology. The genomic sequences were subsequently analyzed, and genes involved in H_2 evolution and carbon utilization were identified. Furthermore, the optimum conditions for H_2 production by CUEA01 and CUEA03 in terms of batch culture temperature, pH, NaCl concentration, and initial glucose content were studied. The ability of CUEA01 and CUEA03 to produce H_2 from various carbon sources, including industrial by-products and agricultural residues, were also investigated, and the H_2 yield, substrate conversion efficiency (SCE), and energy recovery (ER) were compared to that of other *Clostridium* species.

Problem statement

Up to now, the highest H_2 yield (3.47 $mol_{H2}/mol_{glucose}$) has been obtained from *C. butyricum* 10702 (Yin & Wang, 2017) which is considerably below the theoretical yield (4 $mol_{H2}/mol_{glucose}$). Furthermore, the H_2 yield alone is insufficient to demonstrate H_2 production efficiency; cumulative H_2 production (CHP) and SCE should also be addressed. The cost of the substrate is one of the main limitations of H_2 fermentation, which has led to the development of second and third generation bio-H_2 production using organic waste and biomass as the substrate (Cheng et al., 2011). This will increase the possibilities for generating H_2 fuel from renewable sources. As a result, the search for novel *Clostridium* sp. that can secrete an enzyme cocktail, allowing for a wider variety of organic waste and biomass substrates as feedstock, is valuable.

Objectives

1. To isolate and characterize of a H_2 producing *Clostridium* sp. which have a H_2 producing ability for bioH2 production

2. To produce bioH_2 by fermentation from the screened and selected *Clostridium* sp. using synthetic wastewater as feedstock

Dissertation structure

This thesis is composed of 5 chapters. An overview shown in Fig. I-1 and I-2.

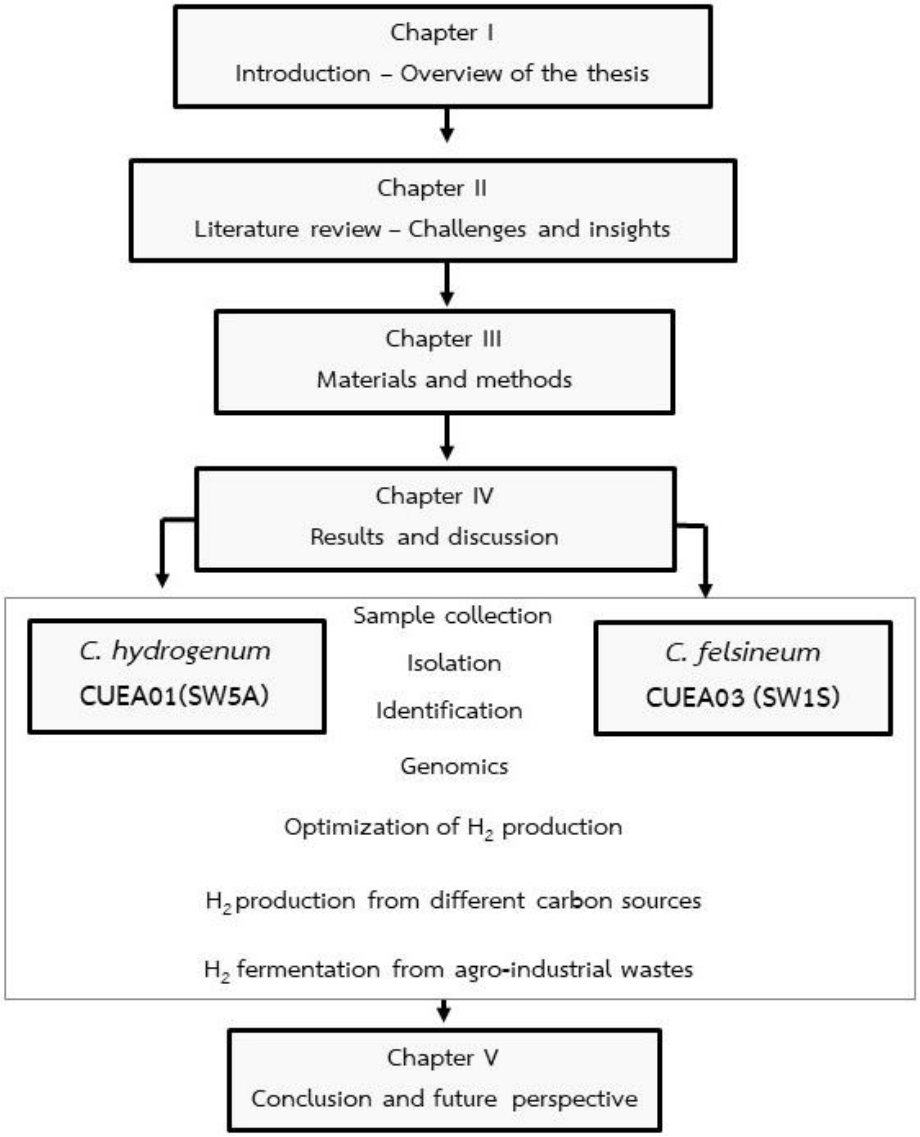

Figure I-1 Overview of chapter in dissertation.

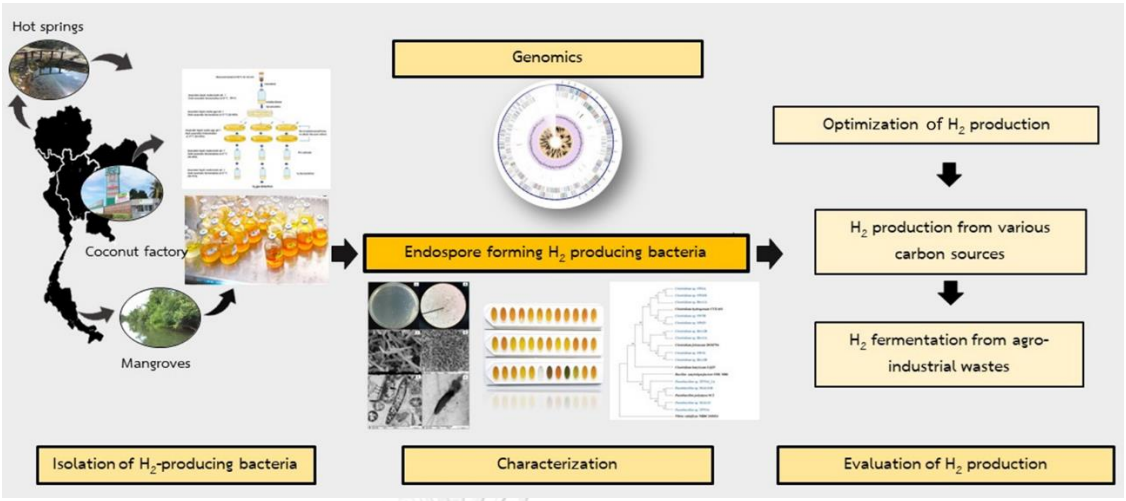

Figure I-2 Overview of a methodology in dissertation.

CHAPTER II

LITERATURE REVIEW

Researchers have been searching for alternative and renewable energy sources due to the depletion of fossil fuels and energy-related environmental pollution. H_2 (H_2), a clean energy, is regarded as one of the most promising substitutes because of its combustion yields 2.75 times more energy (122 kJ/g) than fossil fuels without the emission of CO_2, CO, fine particles such as carcinogenic acetaldehyde (Elbeshbishy et al., 2017). Currently, most of H_2 is produced via steam reforming of fossil fuels or natural gas. The aforementioned process exploit the petroleum-derived fuels energy which emits greenhouse gases (GHGs) (Chandrasekhar et al., 2015) and requires both high temperature and pressure of operation, leading to a high operational cost and some difficulties in operation (Smitkova et al., 2011).

Table II-1 Comparing the energy values of different fuels.

Fuel type	Energy/unit (MJ/Kg)	Energy/Vol. (MJ/L)	Kg of C release/Kg fuel
H_2 gas	120	2	0
H_2 liquid	120	8.5	0
Coal	15-30		0.6
Natural gas	33-50	9	0.46
Petrol	40-43	31	0.86
Oil	42-45	38	0.84
Diesel	43	35	0.9
Biodiesel	37	33	0.5
Ethanol	21	23	0.5
Charcoal	30		0.5
Agric. residues	10-17		0.5
Wood	15		0.5

(Bhutto et al., 2011)

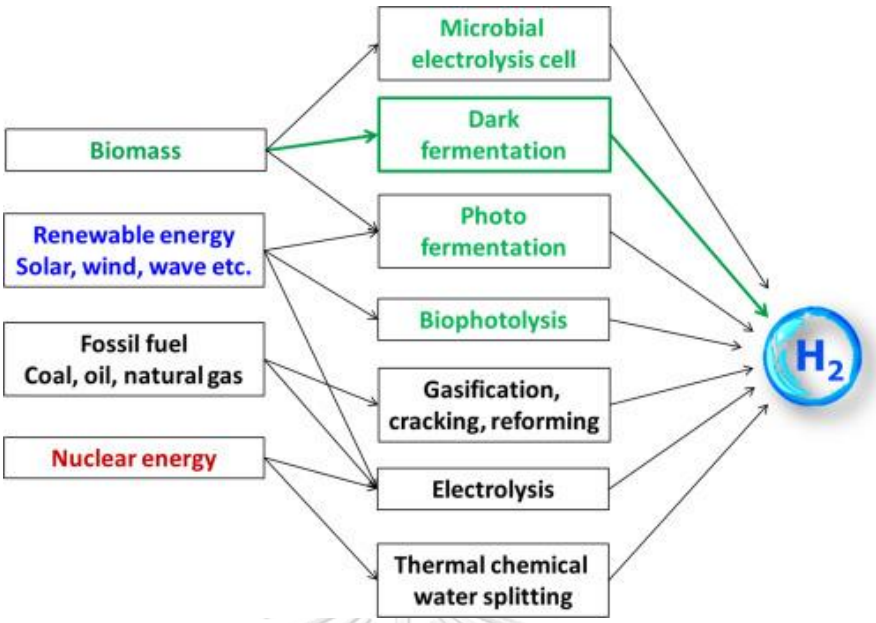

Figure II-1 H_2 production by various methods (Wang & Yin, 2018).

2.1 Biological H_2 production

Biological H_2 production produces bioH_2 by using microorganisms as biocatalysts. This process can generate H_2 at ambient temperature and pressure (Sinha et al., 2016). BioH_2 production is classified into biophotolysis by algae or cyanobacteria; and fermentation by bacteria and archaea which can be classified further as photo-fermentation or dark-fermentation (Sen et al., 2008). Among these processes, dark-fermentation seems to be the most attractive because of its light-independent process, high H_2 production rates and the requirements of the simple bioreactor (Ma et al., 2015; Nissilä et al., 2014). Moreover, a wide range of complex form of organic substrates can be used in this process (Elbeshbishy et al., 2017) including organic wastes (Singh et al., 2010).

Table II-2 Biological pathways for H_2 production and the technical limitations.

Type of Bioprocess	Technical challenges
Dark fermentation	▪ Ineffective substrate conversion ▪ Low yield of H_2 ▪ Thermodynamic limits ▪ H_2 and CO_2 gas mixture, which needs to be separated
Photofermentation	▪ An external light source is required. ▪ The process is constrained by day and night cycles (the light source being sunlight). ▪ Low H_2 yield as a result of extremely poor light conversion efficiency
Direct biophotolysis	▪ PS II activity leads to the production of O_2. ▪ Customized photobioreactors are required. ▪ Low H_2 yield as a result of extremely poor light conversion efficiency.
Indirect biophotolysis	▪ Lower H_2 yield caused by hydrogenase(s) ▪ External light source is required. ▪ The total light conversion efficiency was extremely low.

(Chandrasekhar et al., 2015)

2.1.1 Dark-fermentation

Dark-fermentation is the conventional anaerobic fermentation which is the metabolism process for energy production in heterotrophic microorganisms. This process generates exceeding electrons from oxidizing carbohydrate for energy production. Some organisms dispose electron by H_2 evolution for maintaining electron flow (Lee et al., 2011). Major microorganisms which produce H_2 from this process including obligate anaerobic (*Clostridium* spp.) and facultative anaerobic bacteria (*Enterobacter* spp. *Bacillus* spp. *E. coli.)* (Chandrasekhar et al., 2015).

The primary reaction shows in equation (1) which is a complete conversion from one mole of glucose generates maximum H_2 yield at 12 moles (stoichiometric equation) however, different resulting amounts of H_2 yield depending on the fermentative pathway and end products (Chandrasekhar et al., 2015). For instance, if glucose presents only in acetic acid pathway, the maximum theoretical H_2 yield will be 4 moles as shown in equation (2) (Chandrasekhar et al., 2015; Sen et al., 2008). However, in practical, the maximum H_2 yield is only 3.47 $mol_{H2}/mol_{glucose}$ obtained from *Clostridium butyricum* DSM 10702 (Yin & Wang, 2017).

$$C_6H_{12}O_6 + 6H_2O \xrightarrow{\text{Obligate/facultative anaerobic bacteria}} 12H_2 + 6CO_2 \quad (1)$$

Glycolysis is the main pathway of this process which transforms a substrate into pyruvate, a central metabolic intermediate. Under anaerobic condition, the pyruvate enters into the acidogenic pathway as the terminal step of fermentation coupled with H_2 production (Chandrasekhar et al., 2015). Many acidogenic pathways can occur during bioH_2 fermentative process depending on organism types and operating conditions as shown in equation 2-6.

$$C_6H_{12}O_6 + 2H_2O \longrightarrow 2CH_3COOH + 2CO_2 + 4H_2 \text{ (acetic acid pathway)} \quad (2)$$

$$C_6H_{12}O_6 + 2H_2 \longrightarrow 2CH_3CH_2COOH + 2H_2O \text{ (propionic acid pathway)} \quad (3)$$

$$C_6H_{12}2O_6 \longrightarrow CH_3CH_2CH_2COOH + 2CO_2 + 2H_2 \text{ (butyric acid pathway)} \quad (4)$$

$$C_6H_{12}2O_6 + 2H_2 \longrightarrow COOHCH_2CH_2COOH + CO_2 \text{ (malic acid pathway)} \quad (5)$$

$$C_6H_{12}O_6 \longrightarrow CH_3CH_2OH + CO_2 \text{ (ethanol pathway)} \quad (6)$$

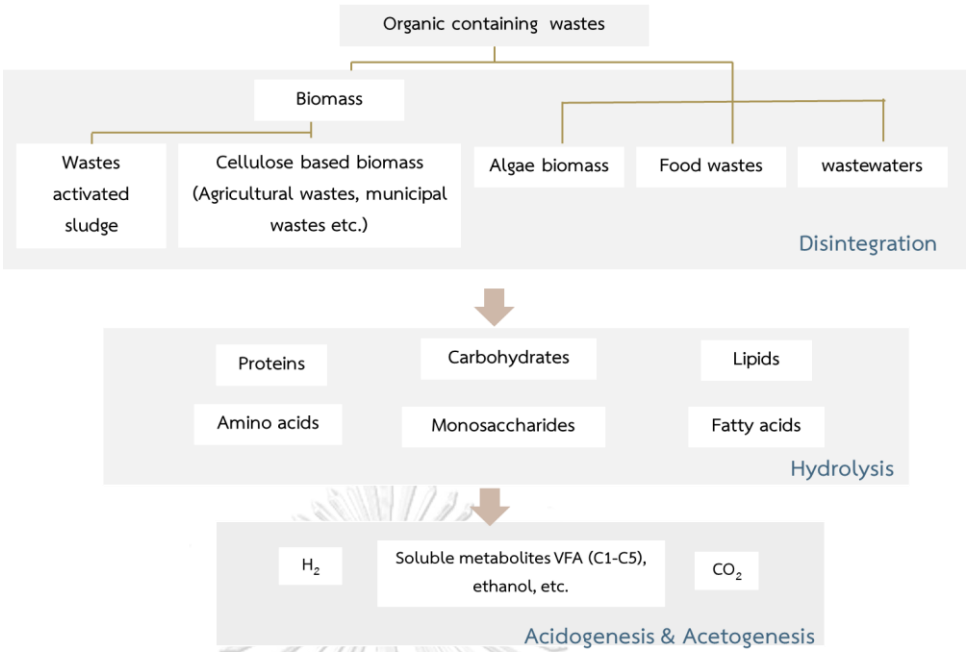

Figure II-2 Processes in biodegradation and biological processes responsible for the H_2 fermentation from materials (Wang & Yin, 2018).

2.1.2 Type of dark fermentation

Mixed acid fermentation is a general terminal step in bioH_2 fermentation in which bacteria utilizes two or more different pathways in the terminal steps. The aforementioned bacteria can be separated into two main groups including facultative anaerobic bacteria and obligate anaerobic bacteria. For facultative anaerobic bacteria such as enteric gammaproteobacteria uses aerobic respiration with the presence of oxygen which oxygen acts as an electron acceptor. Under the condition with an absence of oxygen and the suitable electron acceptors - i.e. nitrate, fumarate, the bacteria uses organic substance as electron acceptors and produce a mixture of volatile fatty acid (VFAs) including acetate, butyrate, formate, lactate, and succinate

acids (Chandrasekhar et al., 2015). Under acidogenic condition, formate will be converted to CO_2 and H_2 by formate H_2 lyase (FHL) pathway, however this process was not occurred with all *Enterobacteriaceae* family. This process is associated with hydrogenase enzyme (for *E. coli*. hydrogenase3) and formate dehydrogenase-H. (Chandrasekhar et al., 2015; Maeda et al., 2007b; Pi et al., 2016) For the other group, obligate anaerobic bacteria such as *Clostridium* species, the product from mixed acid fermentation process (acetic-butyric pathway) contains butyrate, acetate, carbon dioxide, and H_2. The H_2 production from this process is associated with the re-oxidation of NADH by ferredoxin oxidoreductase and hydrogenase (Lee et al., 2011). Moreover, ethanol can also be generated in mixed acid fermentation process. The relative amounts of each product may vary depending on growth conditions and bacterial species (Ward, 2015).

2.1.3 Hydrogenase enzymes

The enzyme which plays a critical role in H_2 production is hydrogenase (Hyd) which catalyzes the reaction $2H^+ + 2e^- \leftrightarrow H_2$ (Sybirna & Bottin, 2013). There are two main types of hydrogenase enzyme which is classified by the type of metal content at active site of the large subunit including [FeFe] and [NiFe] hydrogenase (Mei et al., 2016; Peters et al., 2015; Sybirna & Bottin, 2013). Based on nucleotide sequences reveal no sequence homology between [FeFe] and [NiFe] hydrogenase (Mishra et al., 2017); however, it has the same function in recycling reduced electron carriers which generated during anaerobic fermentation (Peters et al., 2015). [FeFe] hydrogenase are

typical monomeric which contains the catalytic unit. They are mostly found in anaerobic bacteria such as *Clostidium* sp. (Peters et al., 2015) and also found in facultative anaerobic bacteria (*Enterobacter cloacae*) (Mishra et al., 2004; J. Zhao et al., 2017). Whereas [NiFe] hydrogenase are classified into five groups, but only group 4 are defined as hydrogen evolving (Peters et al., 2015) and they are comprised of more than one subunit and their catalytic center are located in the large subunit. This enzyme can be found in facultative anaerobic bacteria such as *E. coli, Enterobacter aerogenase* (Maeda et al., 2012). Base on *E. coli* hydrogenase, they have four native hydrogenase including (Hyd1, Hyd2, Hyd3, and Hyd4) but only Hyd3 and Hyd4 are found to be associated with H_2 evolving mechanism (Matsumura et al., 2015; Mirzoyan et al., 2017). Thus, genes encoding these proteins can be used as a molecular marker for detecting H_2 producers.

These can be divided into three pathways involved in H_2 generation in microorganisms, including; (i) mixed acid fermentation pathway via the PFL, FHL, and related pathway; (ii) butyric acid fermentation pathway (Pyruvate: ferredoxin oxidoreductase and ferredoxin-dependent hydrogenase); and (iii) the NADPH regeneration pathway (Liu et al., 2017; Reischl et al., 2018; Rydzak et al., 2009; Tran et al., 2014; Zhang et al., 2020).

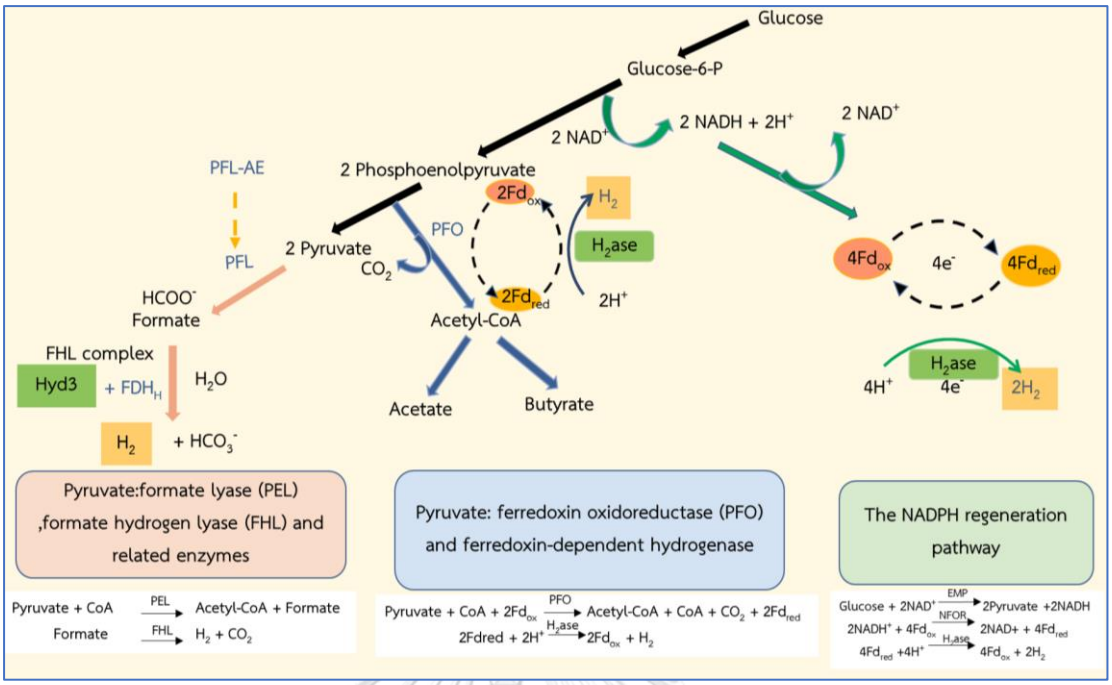

Figure II-3 General H_2 fermentation pathways and essential enzymes in the pathways.

Abbreviations: FhlA: formate H_2 lyase; FHL: formate H_2 lyase; FDHH: formate dehydrogenase-H; FDHO: formate dehydrogenase-O; Hyd3: [NiFe] hydrogenase group 3; PFL-AE: Pyruvate formate-lyase activating enzyme; PFL: pyruvate formate-lyase; Hya: [NiFe] hydrogenase, group 1; PFO: pyruvate ferredoxin oxidoreductase; Fd: ferredoxin; hydrogenase: [FeFe] hydrogenase; and ox/red: oxidation/reduction form.

2.2 Types of culture

Dark-fermentation can be operated in two different types of culture: a mixed culture and a pure culture. For the mixed culture, the process related to anaerobic digestion contains 4 steps by type of bacteria: hydrolysis, acidogenesis, acetogenesis, and metanogenesis (Khan et al., 2018). H_2 is generated during the acidogenesis. The acetogenesis not only can produce H_2 from converting volatile fatty acids (VFAs) to

acetate but also can consume H_2 by using H_2 as intermediate for producing acetate by acetogens. Moreover, methanogenesis is the reaction stage in which H_2 is consumed for methane production by methanogens. Therefore, the dark fermentation by the mixed culture needs to inhibit acetogens and methanogens from the process. Thus, it is difficult to control the bacterial community in the mixed culture. This will affect to population shifts between H_2-producers and H_2 consumers causing the metabolic shift (Khan et al., 2018). The pure culture microbial fermentation seems to be more effective for controlling H_2 productivity (Mei et al., 2014). Moreover, pure culture could provide a better understanding of metabolic pathways for H_2 production and may help to enhance H_2 productivity and yield (Yin & Wang, 2017). Furthermore, a pure culture can be employed in other ways, such as synthetic mixed culture or bioaugmentation of a natural mixed culture to increase H_2 output. Previous study has shown that bioaugmentation with *Clostridium* strains can improve the H_2 yield from lignocellulosic biomass (Öner et al., 2018; Valdez-Vazquez et al., 2019) whereas inoculation with an exogenous species can improve the stability of a mixed culture (Poirier et al., 2020).

Characteristics of pure cultures

I. High substrate selectivity

II. Easy to control of the metabolic pathway

III. Reliable H_2 yields

IV. Reproducibility of the bioprocess

V. Can be modified and altered to true genetic material

2.3 H_2 producers

Many H_2 producing bacteria (HPB) have been explored for H_2 fermentation. The H_2 yield obtained from different isolates around 2-60% of theoretical yield (Yin & Wang, 2017).

Table II-3 Comparison of different bacterial strains reported for fermentative bioH_2 production.

Microorganism	Isolation sources	Substrates	Temperature (°C)	pH	CHP (mL/L)	H_2 yield (mol/mol)	Ref.
Clostridium butyricum INET1	Digested sludge	Glucose (COD 10 g/L)	35	7	2180	2.24	(Yin & Wang, 2017)
Clostridium sp. PROH2	Submarine hydrothermal chimney	Glucose (2g/L)	37	9.5	669	2.71	(Mei et al., 2014)
Clostridium sp. 6A-5	Sludge of Funan sugar mill	Glucose (16 g/L)	43	8	2727	2.50	(Cai et al., 2013)
Clostridium butyricum CWBI 1009	Anaerobic sludge	Glucose (4.3 gCOD/L)	30	7.3	2344	0.58	(Calusinska et al., 2015)
Enterobacter sp.	Granular sludge	Glucose (2 g/L)	37	7	166	0.80	(Maintinguer et al., 2017)
Enterococcus faecium INET2 (free cells)	Gamma irradiated sludge	Glucose (15 g/L)	35	7	1300	1.16	(Yin & Wang, 2016)
Thermoanaerobacterium thermosaccharolyticum TERI S7	Oil reservoir flow pipeline	Glucose (10 g/L)	55	6.8	1900	2.50	(Singh et al., 2014)
Bacillus sp.	Banana waste	Glucose (5 g/L)	37	7	330	-	(da Silva Mazareli et al., 2019)
Vibrio tritonius strain AM2	Gut of sea hare (*A. kurodai*)	Manitol (30 g/L)	37	6		1.7	(Matsumura et al., 2014)

2.3.1 *Clostridium* spp.

Among various bacterial H_2 producing species, *Clostridium* spp. are the best candidate producing H_2 as close as theoretical yield and compatibility of various carbon source. Moreover, it is the dominant species existing in microflora of the mixed cultures which promote H_2 production in anaerobic digestion (Huang et al., 2010; Lin & Hung, 2008; Sivagurunathan et al., 2014). *Clostridium* spp. are typically obligate anaerobic bacteria which belong to the genus *Clostridium,* family *Clostridiaceae.* They are gram-positive and spore-forming bacteria. Pan et al. (2008) was isolating *C. beijerinckii* Fanp3 from sludge in an anaerobic bioreactor (Pan et al., 2008). This strain could utilize various carbon and nitrogen sources to produce H_2 such as fructose, sucrose, mannose, dextrin, and cellobiose. The maximal H_2 yield and the H_2 production rate were obtained as 2.52 $mol_{H2}/mol_{glucose}$ and 39.0 ml/g-glucose h^{-1}. In 2010, Jayasinghearachchi et al. was isolating new marine *C. amygdalinum* C9 from oil water mixtures (Jayasinghearachchi et al., 2010). This strain could produce H_2 from xylan, xylose, arabinose and starch at different optimum conditions. A novel strain *Clostidium butyricum* INET1 was isolated from gamma irradiated digested sludge. This strain was capable of utilizing various substrates for efficient H_2 production including glucose, xylose, sucrose, lactose, starch, and glycerol. The maximal H_2 yield of this strain was 2.07 mol_{H2}/mol_{hexose} (Yin & Wang, 2017). Therefore, the process optimization can improve H_2 yield. Moreover, the screening of new *Clostridium* spp. will enhance the development to find new

microorganisms which have a higher potential and is compatible with a wider range of carbon source for H_2 production.

2.4 Screening sources

Many researchers have recently reported H_2 production from fresh water using bacterial species which several are screened from domestic landfill, sewage sludge and dung. Bacteria from natural habitats have great biodiversity, however they are rarely reported.

Thailand is located in a tropical zone with an abundance of resources and biodiversity (Brown, 2014). In this study, mangrove forest and hot spring sediments in Thailand were selected for screening of HPB. These environments are quite unique, which could increase the possibility of discovering a diverse population of bacteria capable of efficiently producing H_2.

Mangrove ecosystems are a type of coastal wetland forest that plays a significant role in nutrient recycling by various microbial communities. (Sahoo & Dhal, 2009). Mangroves grow in a transition zone between marine and freshwater ecosystems. As a result, they are exposed to shifting environmental elements such as pH, salinity, and temperature, which change with the tides and seasons (Rahaman et al., 2013). This will have an impact on the local microorganisms. Additionally, the sediments of mangroves are high in nutrients, low in oxygen, and abundant in degraded vegetative matter. As a result, they have a large number of fermentable bacteria that may be efficiently used for bioH_2 production via dark fermentation

(Mullai et al., 2013; Zhu et al., 2008). In 2013, Mullai, Rene, and Sridevi evaluated H_2-producers (anaerobic bacterial consortium) from mangrove sediment and discovered that these producers can manufacture H_2 at high yields (Mullai et al., 2013). Besides, *Pantoea agglomerans* of enterobacteriaceae, which was isolated from mangrove sludge, having a H_2 producing ability (Zhu et al., 2008).

Hot springs are a habitat for a diverse spectrum of bacteria that have adapted to this rather unique extreme environment. Previous research has reported the presence of many hydrolytic bacterial groups (Grady et al., 2016; Mehetre et al., 2018), including the phylum Firmicutes that were abundant in hot spring water at 65 °C (96.10%) (Chaudhuri et al., 2017).

2.5 Genomics

With the first publication of the eponymous journal by McKusick and Ruddle in 1987, genomics, the study of the encoding, structure, and function of genetic information, can be considered to have developed as a recognized science (Gill, 2017). In recent years, Genomic studies have become increasingly relevant. The development of genomics by whole genome sequencing (WGS), followed by the invention of Next Generation Sequencing (NGS) technologies in 2004, made it feasible to discover the uncultivable microorganisms by metagenomics as well as the genetic information of an organism's whole genetic information (Caputo et al., 2019).

2.5.1 Bacteria classification by genome sequences

Current bacterial species classification is based on a combination of morphological and genotypic characteristics. The genomic G+C content composition, DNA-DNA hybridization, and, later, the 16S rRNA gene were utilized as genotypic criteria for bacterial classification. However, the above-mentioned methods for species discrimination have limitations. For example, for species discrimination, DNA-DNA hybridization uses a 70% threshold. But, as described for *Rickettsia* species, it cannot be applied for all prokaryote groups (Caputo et al., 2019). Additionally, the comparison of the 16S rRNA gene as a single gene and the low conventional divergence between the 16S rRNA genes of two different organisms result in a poor and limited description of bacteria (Ochman et al., 1999; Pei et al., 2010). Additionally, there are misidentifications of annotated species of microorganism in the NCBI database that need to be rectified using genomic data (Federhen et al., 2016; Poehlein et al., 2017). However, the criterion for taxonomic identification remains to be 16S rRNA. This is due to a number of limitations in the current microbiological taxonomies based on genomes, including insufficient phylogenetic resolution and a lack of exact numbers (Park & Won, 2018). These caused species delimitation methods based on DNA-DNA hybridization (DDH) and 16S rRNA sequences to be replaced by approaches that rely on genome sequences (complete & WGS) from type strains (Federhen et al., 2016). Moreover, methods based on culture and genetics provide diverse insights into the nature and behavior of bacteria.

With the wide availability of complete genome sequences presently, direct comparative approaches can produce results in silico that are analogous but more accurate. Despite the availability of numerous genome-wide similarity measures, average nucleotide identity (ANI) was extensively utilized and has been recommended as the best alternative for determining species boundaries and confirming identification (Schwengers et al., 2021).

ANI was defined as the pairwise average nucleotide identity of two genomes evaluated across the alignable region (Federhen et al., 2016). NCBI developed a technique for finding misidentified genomes in GenBank by combining ANI genome neighboring statistics with reference genomes from type and proxy type. The standard ANI cutoff for defining species boundaries is 96%, but this is not always acceptable. Many species range much further (or much less) than that (Federhen et al., 2016).

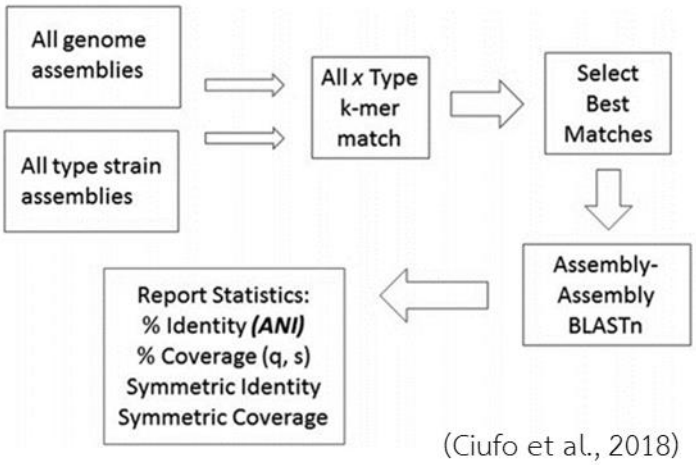

Figure II-4 ANI workflow for pre-submission genomic processing.
(Ciufo et al., 2018)

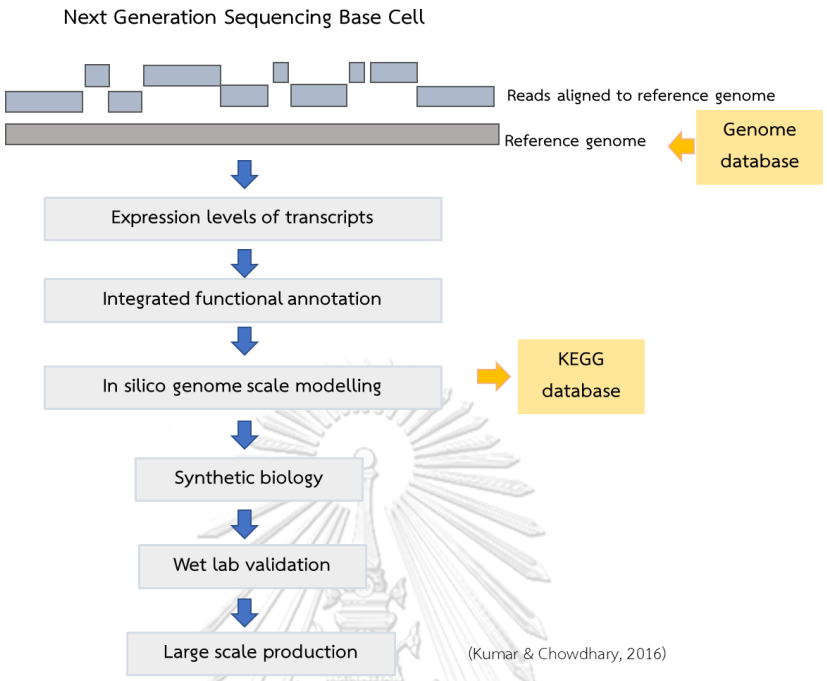

Figure II-5 Schematic depiction of numerous methods for increasing H_2 production based on NGS.
(Kumar & Chowdhary, 2016)

2.5.2 Genome annotation

It is well known that the precise arrangement of nucleotides determines the amino acid sequences crucial for the expression and functionality of proteins and biological sequences. Genome annotation, which is the process of deriving biological details from data generated by nucleotide sequencing, initially frequently concentrates on genes. The annotation adds meaning to the genome by describing the location and function of genes (i.e., protein coding region or functional RNA) and

regulatory regions from raw data using various analysis, comparison, estimation, precision, and other mining approaches (Ranganathan et al., 2018).

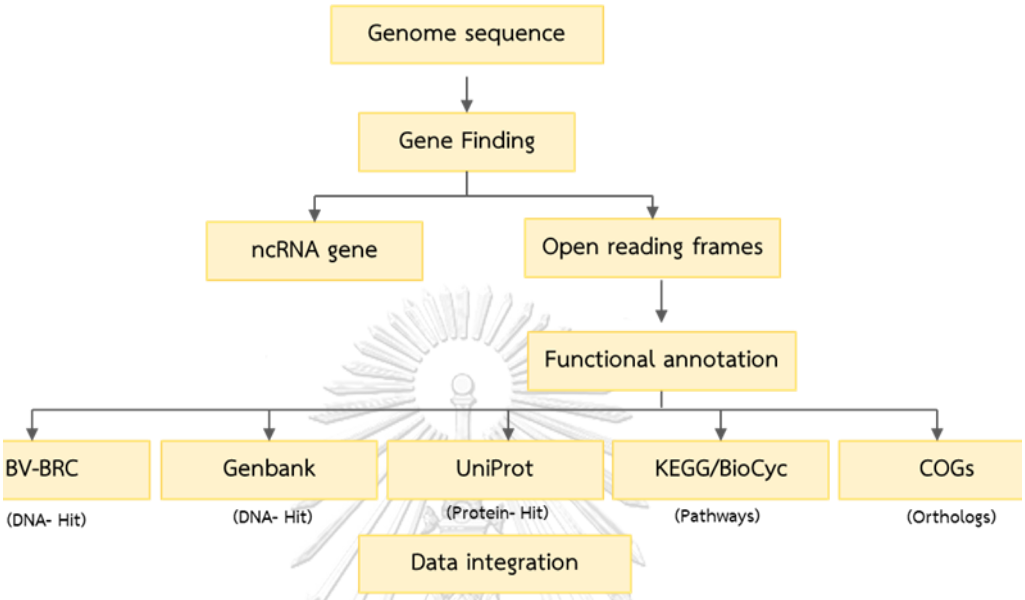

Figure II-6 Integrated genome annotation pipeline.

After we got the whole genome sequences by WGS, the prosses of genome annotation was processed by genome assembly using a reference genome-based method or novo approach. The first step in annotating the assembled genome (Fig. II-6) is to identify and mask RNA genes using RNAmmer and tRNAScanSE. Open reading frames (ORFs) in the genome sequence are discovered using tools for discovering genes, such as Prodigal, GeneMark and MetageneAnnotator. To find potential functions and protein evidence, these ORFs are BLAST searched against databases including GENBANK and UniProt (Christoffels & van Heusden, 2019).

2.6 Effect of important parameters on H_2 fermentation

Various parameters influenced not only cell development but also H_2 evolution.

2.6.1 Effect of pH

An essential factor of the microbial population and a key expression of the redox conditions for any anaerobic process was the concentration of hydronium ions or pH of the system (redox microenvironment). Therefore, pH is crucial in the regulation of metabolic pathways and in H_2 evolution. The internal pH, proton motive force, and membrane potential were a physiological characteristics that were impacted by changes in external pH levels (Chandrasekhar et al., 2015). Moreover, pH also impacts on the enzymatic function, which includes the hydrogenase enzyme. This enzyme has an important role in H_2 production (Akhlaghi & Najafpour-Darzi, 2020). It has been suggested that hydrogenase performs better in the pH range of 6 to 6.5 (Wong et al., 2014). Low pH values (below 5) could inhibit hydrogenase activity, resulting in the termination of H_2 evolution (Bao et al., 2013). Moreover, All enzymes involved in bacterial metabolic activities are active in a specific pH range, with maximum activity at the optimum pH value (Wong et al., 2014). Consequently, it impacts the HPR value in dark H_2 fermentation. As a result, the batch fermentation process enters the termination step in H_2 production due to the decreased pH driven on by the accumulation of VFAs in fermented broth. Therefore, maintaining pH at an

optimal value is crucial to maintaining H_2 production (Penniston & Gueguim Kana, 2018). The optimal pH of dark fermentation varied based on the type of bacteria and substrate (Ziara et al., 2019). Consequently, determining the optimum pH is important in dark fermentation owing to its relevance in the metabolic pathway of the specific organism, by-product accumulation, and H_2 yield. An optimum pH serves to maintain the surface charge on the cell membrane, enabling nutrient uptake and hence maintaining bacterial growth (Wong et al., 2014).

2.6.2 Effect of temperature

In the fermentation process, the operating temperature has a significant impact on the formation of metabolic products and H_2 production in addition to the microbial consumption of the substrate and the specific growth rate (Chandrasekhar et al., 2015). Several studies investigated dark fermentative H_2 production at different temperatures, including psychrophiles (0–25 °C), mesophiles (25–45 °C), thermophiles (45–65 °C), extreme thermophiles (65–80 °C) and hyperthermophiles (above 80 °C) (Łukajtis et al., 2018). The optimum temperature for mesophilic bacteria including *C. butyricum* was 30 to 45 °C (Chandrasekhar et al., 2015). The optimum temperature is dependent on the type of bacteria employed during the fermentation process and the kind of substrate used (Łukajtis et al., 2018). Higher temperatures have been found to enhance the activity of the enzymes responsible for hydrolysis (Guo et al., 2010; Shin et al., 2004). High temperatures both increase enzyme activity and accelerate substrate degradation. However, a temperature higher than the optimum

causes thermal denaturation and deactivation of the enzymes, which can suppress the activity of enzymes (Srimawong & Chulalaksananukul, 2022).

2.6.3 Effect of substrate concentration

The efficiency of the entire process is greatly influenced by the substrate load, which also affects the populations and communities of microbiota that are present during fermentation. By supplying sufficient organics for microorganisms and encouraging bacterial enzyme activity, increasing the substrate concentration helps H_2 production. However, excessive organic input has a negative effect on H_2 fermentation because it produces too many volatile fatty acids (VFAs), which lower pH and reduce system buffer capacity (Pu et al., 2019). Moreover, higher substrate concentrations impose limitations on the substrate digesting processes. High substrate concentrations have been shown to hinder mass transfer, which in turn causes cellular osmosis to become unbalanced and disrupt substrate assimilation and degradation processes (Qi et al., 2018). Additionally, the development of cells and the production of H_2 could be negatively affected by a high glucose content (Cai et al., 2019). For grown spore-forming bacteria like *Clostridium* sp., sufficient substrate is necessary to initiate germination and prevent re-sporulation (Kim et al., 2006). The appropriate initial glucose level for *Clostridium* spp. as typically 2 to 20 g/L (Mei et al., 2014). Furthermore, it has been noted that increasing the initial glucose concentration from 10 to 25 g/L clearly decreased the H_2 yield of *Clostridium* sp. 5A-1. (Cai et al., 2021). While, low substrate concentration typically leads to low HPR,

H_2 content, and biomass concentration, whereas higher substrate concentrations may cause the HPB to overproduce inhibitory compounds such as ethanol and VFAs, which lowers HPR (Lu et al., 2018). Therefore, an appropriate initial substrate concentration for a specific HPB is required.

2.6.4 Carbon sources

In dark fermentation, the substrate has a considerable impact on the H_2 production (Shin et al., 2004). Numerous studies have examined the H_2 fermentation process using a variety of substrates, including wastewater, agricultural wastes, simple sugars (such as glucose, sucrose, and lactose), and waste from the food industry (Baeyens et al., 2020; Guo et al., 2010; Hay et al., 2013; Kim et al., 2009). Each organism contains a different genetic material that is encoded for diverse hydrolytic enzymes. As a result, bacteria vary in their ability to metabolize various substances, including carbon sources. Sugar is the principal source of carbohydrates that bacteria require. Bacteria have the ability to incorporate different sugars into their cytoplasm and use them to generate bacterial components such peptidoglycan, lipoteichoic acid, and nucleic acids as well as polysaccharides and ATP via glycolysis (Kawada-Matsuo et al., 2016). Although bacteria are known to prefer some sugars to others, they can use a variety of carbon sources concurrently (Beisel & Afroz, 2016). In order to apply the bacteria to the appropriate substrate, it is essential to evaluate the ability to use various carbon sources by a specific HPB. For example, *Vibrio tritonius* strain AM2, can create H_2 by utilizing mannitol effectively; hence, brown macroalgae

(*Saccharina sculpera*), which contains 31.1% (w/w) mannitol in powdered brown macroalgae, can be used as feed stock. (Matsumura et al., 2014). While *C. pasteurianum* CH4, which has been demonstrated to have a strong ability to make H_2 from glycerol, can also produce H_2 from crude glycerol, a byproduct of biodiesel manufacturing (Lo et al., 2013). The ability to use sugar is also related to gene expression. This can also be predicted by CDS in the bacterial genome.

2.7 Generation of H_2 production

Previously, the first generation of bioH_2 production used expensive raw materials monosaccharide and alpha-link disaccharides which cause a high production cost leading to low economic performance for H_2 production. Subsequently, the second generation of H_2 production is from organic wastes which have a lower cost of potential feedstock. Dark-fermentation process by using organic wastes as feedstock can generate sustainable bioenergy at the same time, treating the wastes which can also reduce COD and BOD of organic waste resulting in the reduction of the cost of waste treatment process (Liu et al., 2016). Many wastes can be used as substrate for dark-fermentation such as food waste, agricultural waste, wastewater (Rorke & Kana, 2016). Among several organic wastes, wastewater has the beneficial criteria - i.e. low nutrient requirement, high net energy gain and conversion with high organic loading possibility (Lin et al., 2012). The process alternative for applying the wastes as substrate which is required for microbial metabolism for

growth is beneficial (Pachapur et al., 2015). However, wastes contain many inhibitors in which they can impact on microbial growth. Therefore, synthetic wastewater which is able to control some undesired factors could help to select the appropriate substrate wastes for specific bacterial species for H_2 production. Shi et al. (2010) were producing H_2 from brewery wastewater by batch fermentation using anaerobic sewage sludge as inoculum and found that this wastewater can use for H_2 production which showed a high H_2 yield and H_2 production rate (6.11 mmol H_2/g COD, 8.58 L/L/d) (Shi et al., 2010).

2.8 H_2 production from agro-industrial wastes

Interestingly, a variety of organic wastes can be used as a substrate for the fermentation process that produces H_2 and recovers clean energy by reducing the chemical oxygen demand (COD) value of the waste before it is released into the environment. Using food wastewater as the substrate for H_2 fermentation by *Acinetobacter junii*-AH4 in a batch reactor resulted in a 70% COD removal efficiency (Murugan et al., 2021). It is clear that this approach for producing and using energy fulfills the requirements of sustainable development (Boodhun et al., 2017). In order to incorporate organic waste or biomass into the fermentation process, complex components should be decomposed. Numerous investigations have been carried out to find new H_2-producing bacteria in order to improve the efficiency of H_2 generation from organic wastes. Recently, Oceguera-Contreras et al. reported on the synthesis of H_2 from agro-industrial wastes using vermihumus-associated microbes (Oceguera-

Contreras et al., 2019). While several pretreatment procedures have been developed to enable the extraction of fermentable sugars from the complex of organic waste (Zheng et al., 2021), this raises the cost and may produce toxic byproducts that impair microorganisms and H_2 production.

CHAPTER III

MATERIAL AND METHODS

3.1 Samples collection

Mangrove sediments and hot spring sediments were gathered in Songkhla, Mae Hong Son (Mea Um Long Luang), and Chiang Mai (Theppanom), respectively, while effluent sludge was obtained from food industrial waste (Theppadungporn Coconut Co., Ltd.). The samples were collected in 50 ml sterile conical bottom tube. All samples were kept in anaerobic condition and stored in an ice box and transported to the laboratory within 2 days. The samples were collected for HPB isolation until at least 20 isolates.

3.2 Isolation of H_2 producing *Clostridium* spp.

3.2.1 Growth medium

Fermentation Medium (BFM) was used for isolation and batch H_2 fermentation. The medium composition is described by Marone et al. (2012) (Marone et al., 2012). The pH was adjusted to 7.0±0.2 by adding 5M NaOH or 5M HCL. The isolation plates were prepared by adding 15 g/l agar to the medium. The medium for batch fermentation was added into serum bottles and were autoclaved (121°C for 15 min) after O_2 removal by O_2 free N_2 gas flushing. Prior to inoculation, the vitamins solution which filtering with 0.22 μm filter was added to the medium by syringe. Modified DSMZ 640 (Srimawong & Chulalaksananukul, 2022) supplemented with 0.1% (v/v) trace

element solution SL-10 (Ivanova et al., 2009) was used as a growth medium for precultured isolates before being used as an inoculum and was also used for the optimization.

3.2.2 Samples preparation

The samples were pretreated by constant heating at 80 °C for 10 min in order to stimulate spore germination of *Clostidium* spp. and eliminate the nonspore-forming bacteria such as methanogens. 1 g of samples were suspended in 9 ml sterile saline solution (0.85% NaCl) which was contained in 15 ml centrifuge tube and then mixed by vortex.

Table III-1 H_2 producing bacteria screening sources.

Natural sources			Industrial waste
Mangrove sediments	Hot spring sediments		Coconut factory wastewater
Thepha, Songkhla	Theppanom hot spring, Mae Chaem, Chiang Mai	Mae Urm Long hot spring, Mae Sariang, Mae Hong Son	Theppadungporn coconut, Sam Phran, Nakhon Pathom

Figure III-1 The sampling source used in this research A: mangrove; B: hot spring; C: wastewater tank of the coconut factory.

3.2.3 Isolation of pure cultures

3 ml of prepared sample was inoculated into serum bottles containing 27 ml of BFM and the bottles were incubated at 37°C for 72 h. After that, the culture sample was serially diluted (10^{-2}-10^{-4} dilutions) and spread on isolation plates and anaerobically incubated at 37°C. Each different colony was picked from the plate and streaked into new isolation plates. The plates were incubated at 37°C under anaerobic conditions and single colonies were re-streaked several times to obtain the pure culture. Single isolated bacterium was precultured in basal medium for 24-48 h (until cells enter the exponential phase). After that, inoculated to 1% (w/v) glucose BFM in serum bottle and incubated at 37°C for 72 h. Biogas was detected by using syringe. The isolates which have the ability to produce gas were selected for testing the H_2 producing ability by using H_2 gas detector.

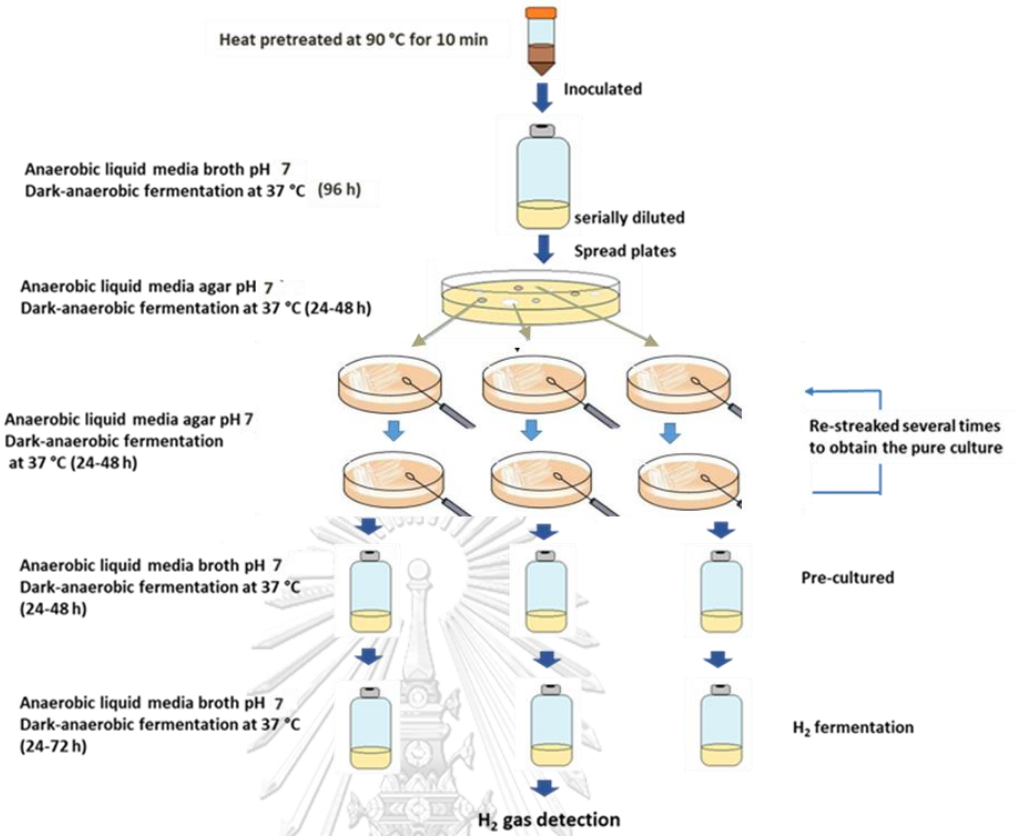

Figure III-2 H_2 producing bacteria isolation procedure.

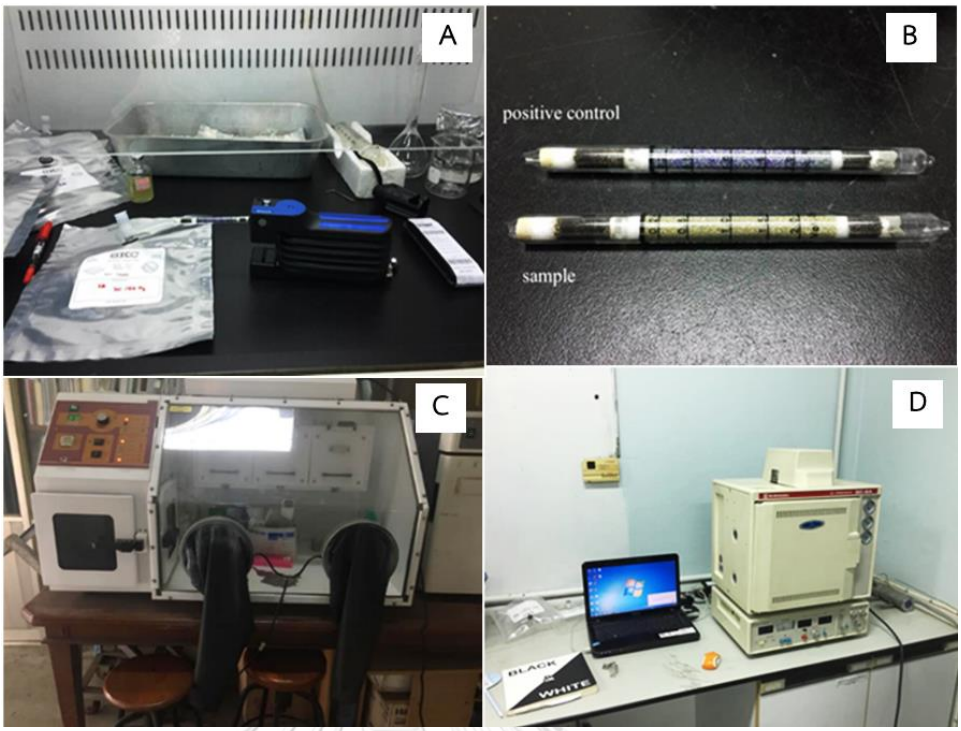

Figure III-3 H_2 analysis and anaerobic culture instrument.

A: H_2 gas detector hand pump; B: H_2 gas detector tube; C: anerobic chamber; D: GC with TCD

3.3 Identification and characterization

3.3.1 Morphological characterization

Morphological characteristics including colony morphology and cell morphology were observed.

- Colony morphology (color, shape, margin, elevation, and surface)
- Cell morphology (shape, gram reaction, spore germination, and arrangement) were observed by using light microscope.

For the appropriated *Clostridium* spp. (SW5A, SW1S)

Gram straining (Doetsch, 1981), scanning electron microscopy (SEM; JEOL JSM-IT500HR, Japan), and transmission electron microscopy (TEM; JEOL JEM-1400, Japan) were used to examine the cellular morphology of the appropriated Clostridium spp. at the Scientific and Technological Research Equipment Centre (Chulalongkorn University, Bangkok, Thailand).

3.3.2 Biochemical characterization

An API 50 CH Kit (BioMerieux, St. Louis, MO, USA), HiCarbo Kit (HiMedia, India), and traditional methods (Aslanzadeh, 2006) were also used for the biochemical tests.

3.3.3 Molecular characterization

3.3.3.1 DNA extraction and amplification of 16S rRNA gene

Genomic DNA was extracted from pure isolates by using Bacterial DNA kit (OMEGA Bio-Tek, USA), according to the manufacturer's instructions. 16sRNA gene was amplified by PCR technique using 27F/1492R primers (Dalia et al., 2017). PCR was performed in a DNA thermal cycler and the PCR protocol was as follows: initial denaturation step at 98 ^{o}C for 30 s, 30 amplification cycles of denaturation at 98 ^{o}C for 10 s, annealing at 55 ^{o}C for 30 s, extension at 72 ^{o}C for 10 s, and followed by a final extension at 72 ^{o}C for 10 min. The PCR products were purified and sequenced by Pacific Science Co., Ltd (Bangkok, Thailand). The Sequence similarity searches were performed using the BLAST network

service of the NCBI database (http://www.ncbi.nlm.nih.gov/BLAST/). Obtained sequences and reference sequences by BLAST analysis were aligned using CLUSTAL-W program (www.ebi.ac.uk/Tools/clustalw2). The resulting files were used for the construction of a phylogenetic tree using Neighbour Joining method.

3.4 Genomics of CUEA01 and CUEA03

3.4.1The WGS and genome assembly

Omics Sciences and Bioinformatics Center (Chulalongkorn University, Bangkok, Thailand) sequenced the genomic DNA with an Illumina MiSeq. The unicycler hybrid assembly (version 0.4.4) was used to assemble the sequences and contigs. Clusters of regularly interspaced short palindromic repeats (CRISPRs) were found and validated using CRISPRFinder (Grissa et al., 2007). Genome alignment (GA) (Darling et al., 2010) digital DNA-DNA hybridization (DDH) (Meier-Kolthoff et al., 2022), and average nucleotide identity (ANI) (Goris et al., 2007) have all been evaluated when comparing closely related species using the ANI calculator, genome-to-genome distance calculator (GGDC), and whole genome alignment service of the BV-BRC website, respectively.

3.4.2 Phylogenetic analysis

High-quality reference and representative genomes were chosen and categorized by the National Center for Biotechnology Information (NCBI) team. The reference and representative genomes, as well as the Comprehensive Genome Analysis report,

were given to PATRIC and employed in the phylogenetic analysis. Mash/MinHash (Ondov et al., 2016) was used to determine the closest reference and representative genomes. PATRIC global protein families (PGFams) (Davis et al., 2016) were chosen from these genomes to designate the phylogenetic placement of this genome. The protein sequences from these families were aligned using MUSCLE (Edgar, 2004), and the nucleotides for each sequence were mapped to the protein alignment. The data matrix produced by the combined set of amino acid and nucleotide alignments was evaluated using RaxML (Stamatakis, 2014), and fast bootstrapping (Stamatakis et al., 2008) was used to produce the support values in the maximum likelihood (ML) tree.

3.4.3 Enzyme prediction and pathway analysis

The comprehensive genome analysis service at PATRIC (Wattam et al., 2017) was used to annotate the assembled genome sequences of CUEA01 and CUEAO3 using the RAST tool kit (RASTtk) (Brettin et al., 2015) based on annotation data and comparison to other genomes in PATRIC belonging to the same species. For the final step of annotating genes, BlastKOALA (Kanehisa et al., 2016) and the UniProt BLAST databases were used to execute BLAST searches against the Kyoto Encyclopedia of Genes and Genomes (KEGG). CRISPRFinder (Grissa et al., 2007) was used to find and validate clusters of CRISPRs (regularly interspaced short palindromic repeats).

3.5 Batch fermentation for H_2 production

3.5.1 Evaluation of H_2 production from the isolated bacteria

Batch H_2 fermentation experiments were carried out in 120 mL serum bottles with a 50 mL working volume. The isolated bacteria were precultured in 1% (w/v) glucose modified DSMZ 640 medium with an initial pH of 7 until entering the late exponential phase (a cell density of 0.8 ± 0.1 OD600 was obtained), and then inoculated into fresh modified DSMZ 640 medium at 10% (v/v) and incubated at 37 °C at static condition. Batch experiments were performed in triplicate. Every 24 h, samples of the gas and liquid were taken.

3.5.2 Optimization of H_2 production by the appropriated *Clostridium* spp. (CUEA01, CUEA03)

The optimum condition for H_2 production of the CUEA01 and CUEA03 were investigated by batch fermentative experiments using modified DSMZ 640 media. The bacterial isolates were precultured in modified DSMZ 640 media (until achieved an exponential phase or cell density of 0.8 ± 0.1 OD_{600}). After that, the culture was used as inoculum. H_2 production testing for the isolate will be carried out in 125 ml serum bottles containing 45 ml of modified DSMZ 640. After O_2 –free N_2 gas flushed for 10 min, the bottles were capped with rubber stopper and aluminum seals and then sterilized (Yin & Wang, 2017). 5 ml of inoculum was added to the medium. The bottles were incubated at 37°C for 72 h. Each isolate was performed in triplicate

experiment. The samples including gas and liquid medium were collected for analysis every 24 h. For the gas collection, gas was collected by using syringe and transferred gas into sample bags (SKC polypropylene fitted bags).

The optimal conditions of CUEA01 and CUEA03 for H_2 fermentation were determined through sequential unilateral variation of the initial pH, temperature, NaCl concentration, and initial glucose concentration.

3.5.2.1 Effect of initial pH

The isolates were cultured in modified DSMZ 640 supplemented with 1% glucose at different pH ranging from 4 to 13 with 1 increment and then incubated at 37 ℃.

3.5.2.2 Effect of temperature

The isolates were cultured in modified DSMZ 640 supplemented with 1% glucose and then incubated at different temperatures including 15 to 45 ℃ with 5 increments.

3.5.2.3 Effect of NaCl concentration

The isolates were cultured in 1% glucose modified DSMZ 640 supplemented with different NaCl concentration including 0, 10, 20, 25, 30, 35 and 40 g/L NaCl.

3.5.2.4 Effect of the initial glucose concentration

Suitable substrate of the isolates was used for analysis. The isolates were cultured in modified DSMZ 640 supplemented with glucose. The initial concentration of the substrate was varied (5-100 g/L) with 5 increments.

3.5.3 H_2 production by the appropriated *Clostridium* spp. (CUEA01, CUEA03) from different carbon sources

Different carbon sources were used to evaluate the H_2 production by CUEA01, and CUEA03 at the optimal conditions, including mannose, fructose, galactose, arabinose, maltose, sucrose, lactose, cellobiose, xylose, xylan, starch, and microcrystalline cellulose (MCC).

3.6 H_2 fermentation from industrial by-products and agricultural residues

Sugarcane molasses (SM), cassava pulp (CP), and dried rice straw (RS), which are abundant in Thailand, were chosen as substrates for batch fermentation of H_2.

3.6.1 Sugarcane molasses (SM)

The components of the SM may be seen from (Lertsriwong & Glinwong, 2020) were derived from Lertsriwong and Glinwong. Distilled water was used to dilute the SM for this investigation, yielding a 10X (9.494 g COD/L), 50X (1.899 g COD/L), and 100X (0.949 g COD/L) dilution. Following that, the diluted solutions were sterilized in an autoclave steam sterilizer before H_2 fermentation testing. Chemical oxygen demand (COD) will be analyzed before and after cultivation according to the standard methods (APHA, 2005).

3.6.2 Cassava pulp (CP)

The CP was sourced from a Thai tapioca starch mill. The composition of CP was examined by the AOAC (1990) method (OAC, 1990). The main components were starch (58.25%), acid detergent fiber (21.73%), crude fiber (19.25%), and TS (19.5%). Before autoclave sterilization, the CP was added to modified DSMZ 640 medium at concentrations of 20 (3.9 g TS), 40 (7.8 g TS), and 51 (10 g TS) g/L.

3.6.3 Dried rice straw (RS)

RS was collected from a local Thai rice field. RS was subjected to physical preparation by mixing and filtering through 0.4 mm mesh. According to AOAC (2019) and a proprietary method based on Maynard and Loosli, 1969 (Maynard & Loosli, 1979), the composition of RS was determined. RS included 16.62% ash, 12.04% lignin, 36.53% cellulose, 17.26% hemicellulose, and 90.35% TS. In the modified DSMZ 640 medium, the blended RS was added with 10 (9 g TS) or 100 (90 g TS) g/L as a carbon source before being autoclave sterilized.

3.7 Data analysis of fermentative products

3.7.1 Biomass analysis

The cell concentration was determined by measuring the OD600 with a nanodrop spectrophotometer. The cell dry weight (CDW) was calculated by centrifuging a 3,000 mL culture sample (3000 g, 10 min), twice washing the cell pellet with distilled water, and then drying the cell pellet at 105 °C until the cell weight

remained constant. From several subsets of the same culture, a standard curve was constructed.

3.7.2 H_2 gas analysis

A gas tight syringe was used to measure the total volumetric biogas generation at each time interval at 1 atm and 25 °C (298 K). Gas chromatography (GC; GC-8A Series, Shimadzu, Japan) fitted with a thermal conductivity detector and a Porapak Q column (Agilent, USA) was used to measure the H_2 gas concentration. N_2 gas was employed as the carrier gas at a flow rate of 25 mL/min, with the injection port, column, and detector temperatures all set at 60 °C. The mass balance equation was used to compute the CHP (Aly et al., 2018; Skonieczny & Yargeau, 2009), shown in Eq. (1);

$$V_{H,i} = V_{H,i-1} + C_{H,i}(V_G - V_{G,i-1}) + V_H(C_{H,i} - C_{H,i-1}) \quad (1),$$

where $V_{H,i}$ and $V_{H,i-1}$ are the cumulative H_2 gas volume at the present and prior time interval, respectively, $C_{H,i}$ and $C_{H,i-1}$ are the H_2 gas concentration (represents x/100 fraction) at the present and prior time interval, respectively, V_G, $V_{G,i-1}$ are the total volumetric gas at the present and prior time interval, respectively, and V_H is the head space of the reactor.

According to Eq. 2, the moles of H_2 generated were computed using the ideal gas law (Charles's Law, Boyle's Law, and Gay-Lussac's Law) (Wong et al., 2014);

$$PV = nRT \quad (2),$$

where P represents the pressure [Pascal (Pa), where 1 atm = 101,325 Pa], V is the volume (L), n is the number of moles of a gas, T is the temperature (K), and R is the molar gas constant (8.314472 atm•L/mol•K).

H_2 yield was calculated according to Eq. (3).

$$H_2 \text{ yield} = \frac{\text{Produced } H_2 \text{ (mol)}}{\text{Consumed substrate (mol)}} \quad (3).$$

Volumetric production rate (HPR)

$$\text{HPR} = \frac{\text{Total amount of } H_2 \text{ produced}}{\text{Total volume of the culture x Time duration}} \quad (4)$$

3.7.3 Liquid analysis

The DNS assay (Miller, 1959) was used to determine the reducing sugar content, whereas the phenol-sulfuric acid technique was employed to determine the amounts of other carbohydrates (Masuko et al., 2005). The glycerol concentration was also determined using the modified glycerol assay (Kuhn et al., 2015). The content of volatile fatty acids (VFA) and alcohol were measured by GC (GC-2010, Shimadzu, Japan) with N_2 flowing at a rate of 175 mL/min as the carrier gas. The injection port, column, and detector temperatures were adjusted to 210 °C, 45 °C, and 220 °C, respectively.

3.8 Calculation of the important parameters

3.8.1 The SCE

The SCE by this strain for utilization of the carbon sources were calculated from Eq. 5 (Zhang et al., 2015);

$$SCE = [(C_{initial} - C_{final}) / C_{initial}] \times 100 \quad (5),$$

where $C_{initial}$ and C_{final} are the concentration of carbon source at initial and after fermentation.

3.8.2 COD removal efficiency

The COD removal efficiency (%) will be calculated according to the equation (6) (Mohan et al., 2008)

$$\text{COD removal efficiency (\%)} = \frac{C_{SO} - C_S}{C_{SO}} \times 100. \quad (6)$$

C_{SO} represents the initial COD concentration and C_S is COD concentration at the end of the operation.

3.8.3 Carbon recovery (CR) and ER

The energy content of each substrate and products were calculated based on specific enthalpy of substances. The CR and ER was calculated from Eq. 7 and Eq. 8 (Singh et al., 2019), respectively:

$$CR = (\text{Output carbon content/Input carbon content}) \times 100 \quad (7),$$

$$ER = (\text{Total HV of } H_2 / \text{HV of substrate consumed}) \times 100 \quad (8),$$

where HV is the heating value.

3.9 Statistics

Statistical analysis was performed using SPSS v.16 software. One-way ANOVA was undertaken using Post hoc comparisons with the Tukey HSD method, accepting

significance at the $p < 0.05$ level. All data were represented as mean ± standard deviation (SD).

CHAPTER IV

RESULTS AND DISCUSSION

4.1 Isolation of endospore-forming HPB

The screening and isolation of endospore forming HPB from various sources yielded a total of 40 endospore forming isolates, of which 23, 15, and 2 isolates were obtained from mangrove sediments, hot spring sediments, and coconut factory wastetwaters respectively. The colonies mophology of the isolated bacteria were shown in Fig. IV-1 – IV-3. The H_2 gas producing ability of all isolated bacteria was shown in Table IV-1. Herein, only 17 isolated strains which can produce hight H_2 gas were selected for further study and the result was shown in Table IV-2. And then the 14 isolated bacteria with a high H_2 producing ability were selected for further study by batch fermentation and the results were shown in Fig. IV-2.

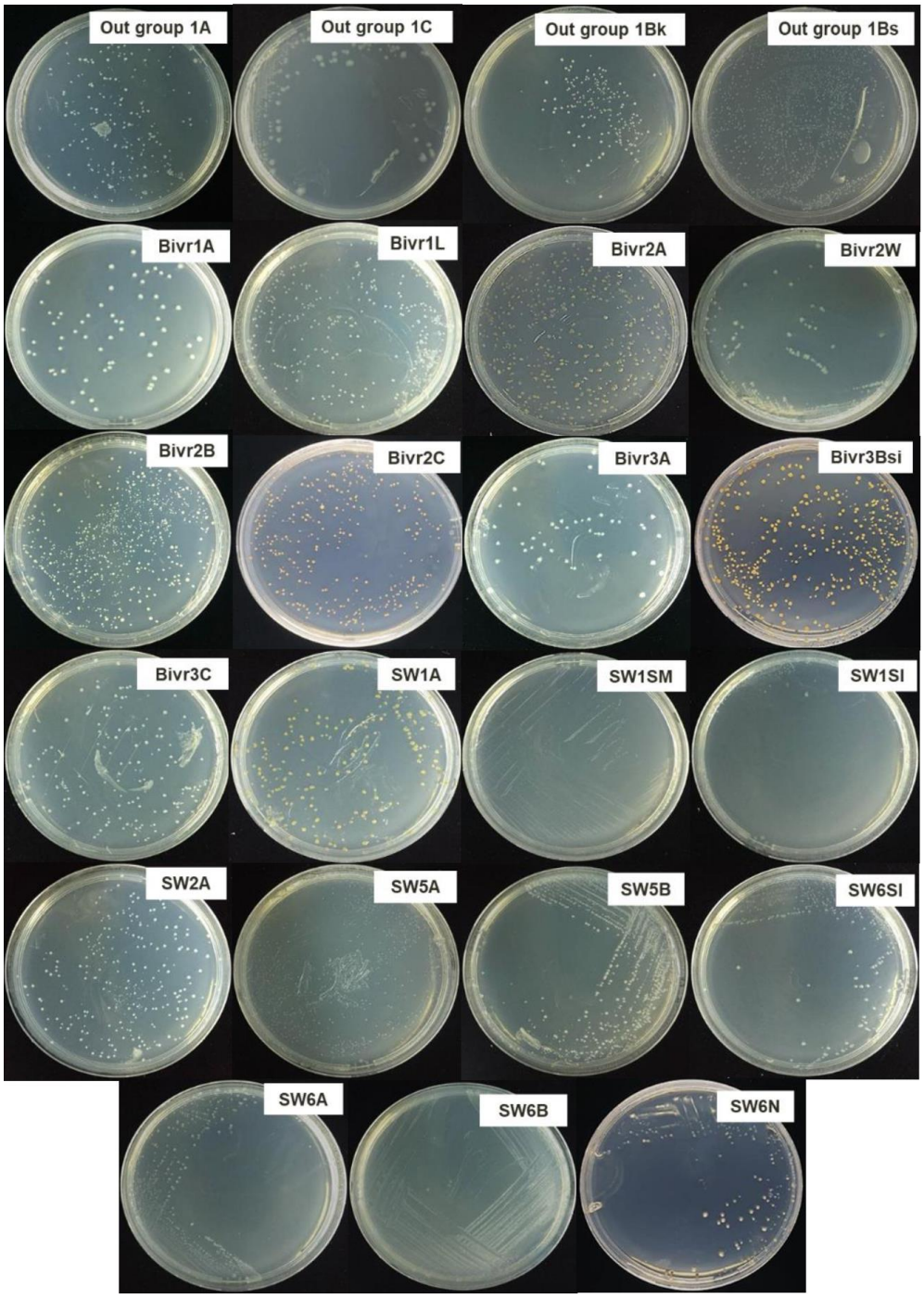

Figure IV-1 Colony morphology of endospore-forming HPB isolated from mangrove sediments.

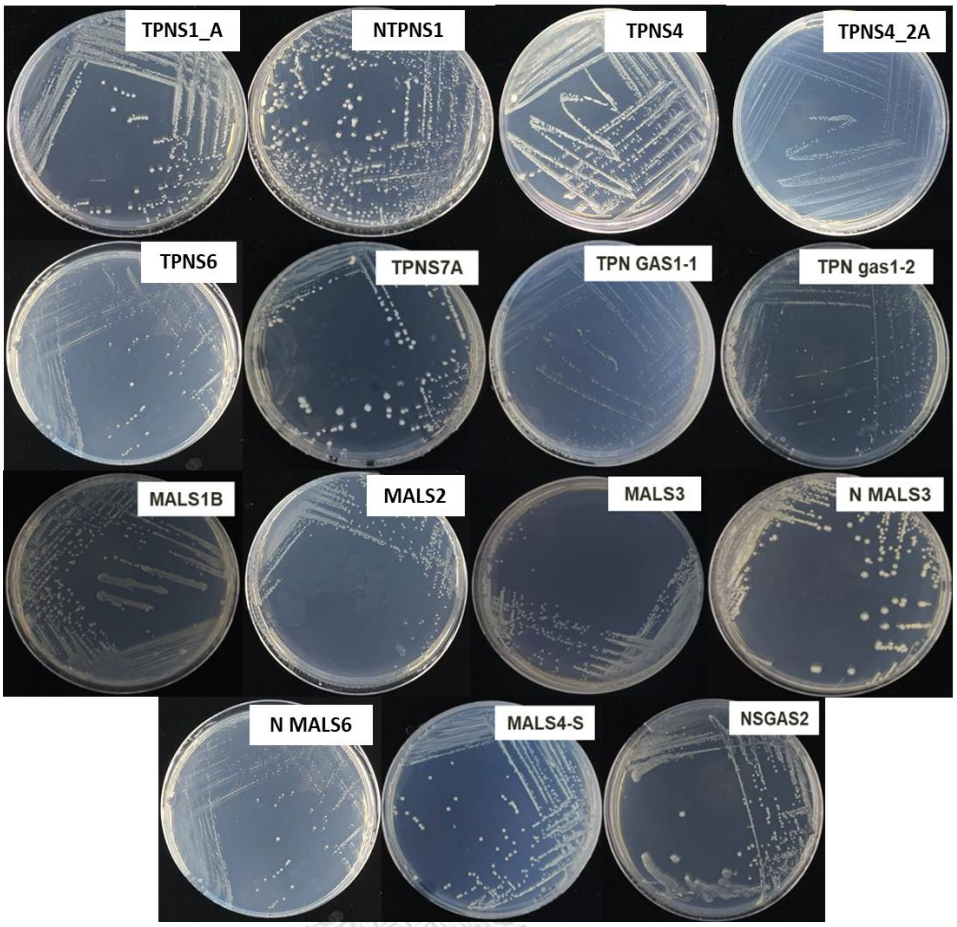

Figure IV-2 Colony morphology of endospore-forming HPB isolated from hot spring sediments.

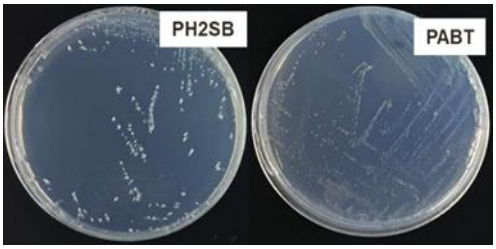

Figure IV-3 Colony morphology of endospore-forming HPB isolated from the wastewater tank of the coconut factory.

Table IV-1 H_2 detection of isolated bacteria by using Dräger tube pump with detector tube H_2.

No.	Isolates	Releasing ga (mL)	%H_2 gas	Volume of H_2 (mL)
1	Out group 1A	18	17	8.16
2	Out group 1C	14	12	5.28
3	Out group 1Bk	13	12	5.16
4	Out group 1Bs	12	14	5.88
5	Bivr1A	18	19	9.12
6	Bivr1L	17	17.5	8.225
7	Bivr2A	21	>20	10.2
8	Bivr2W	4		0
9	Bivr2B	5		0
10	Bivr2C	22	19	9.88
11	Bivr3A	3		0
12	Bivr3Bsi	20	>50	>25
13	Bivr3C	5		0
14	SW1S	19	>20	>9.8
15	SW1SM	12	12	5.04
16	SW1Si	15	10	4.5
17	SW2A	16	15	6.9
18	SW5A	26	>20	11.2
19	SW5B	28	17	9.86
20	SW6Si	10		
21	SW6A	24	17	9.18
22	SW6B	24	>20	>10.8
23	SW6N	20	>4	>2
24	TPNS1_A	15		
25	N TPNS1	10		
26	TPNS4	24	10	5.4
27	TPNS4_2A	24	>20	>10.8
28	TPNS6	17	4.6	2.162
29	TPNS7A	5		
30	TPN GAS1-1	6		
31	TPN gas1-2	4		
32	MALS1B	12		
33	MALS2	3		
34	MALS3	18	5	2.4
35	N MALS3	22	6	3.12
36	N MALS6	5		
37	MALS4-S	10		
38	NSGAS2	5		

No.	Isolates	Releasing ga (mL)	%H_2 gas	Volume of H_2 (mL)
39	PH2SB	24	17	9.18
40	PABT	14	12	5.28

4.2 Selection of the appropriate HPB for H_2 production.

4.2.1 Determination of H_2 production from the isolated bacteria by batch fermentation.

Table IV-2 H_2 detection of isolated bacteria by using GC-TCD

No.	Isolates	Releasing gas (ml)	%H_2	H_2 vol. (mL/L)
1	SW1S	19	44.90	449
2	SW5A	26	40.80	408
3	SW5B	24	27.00	270
4	PH2SB	24	17.00	170
5	Bivr3B	24	28.46	284.6
6	MALS1B	12	10.01	100.1
7	TPNS4_2A	24	48.44	484.4
8	TPNS4	26	45.15	451.5
9	SW6N	22	35.34	353.4
10	Bivr2B	26	36.24	362.4
11	SW6A	24	31.10	311
12	Bivr2A	20	38.38	383.8
13	MALS3	18	12.04	120.4
14	Out1B	13	7.60	76
15	MALS4	20	7.20	72
16	PABT	14	12.00	120
17	SW6M	24	40.00	400

4.2.2. Evaluation of H_2 production from isolated bacteria with high H_2 producing ability.

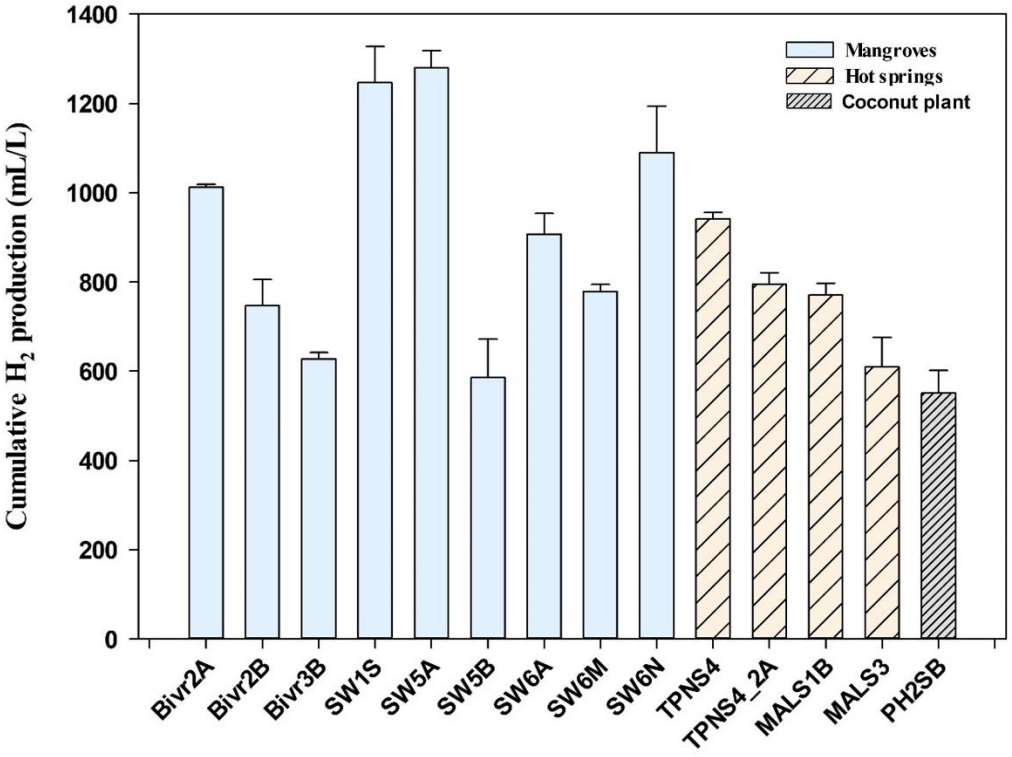

Figure IV-4 Cumulative H_2 production compared between isolated bacteria with high H_2 producing ability.

* 10 g/L glucose concentration, pH7, 37°C, 96 h incubation time

4.3 Bacterial characterization

4.3.1 Biochemical characterization

10 Isolated bacteria were selected for biochemical test using HiCarbo Kit. The results are shown in table IV 3.

Table IV-3 Biochemical characteristics of isolated bacteria

No.	Test	Bivr2B	SW5A	SW6N	Bivr3B	SW5B	Bivr2A	SW6M	KYS2A	SW1S	PH2SB
1	Lactose	+	+	+	+	w	w	-	+	+	+
2	Xylose	-	+	-	-	-	-	-	+	+	+
3	Maltose	+	+	+	-	w	-	-	+	+	+
4	Fructose	-	+	-	-	-	-	-	+	+	+
5	Dextrose	+	+	+	+	w	-	-	+	+	+
6	Galactose	-	+	+	-	-	-	-	+	+	-
7	Raffinose	+	-	+	w	-	w	-	+	+	-
8	Trehalose	+	-	+	w	-	w	-	+	-	-
9	Melibiose	-	-	+	w	+	-	-	+	-	-
10	Sucrose	+	+	+	w	+	w	-	-	-	-
11	L-Arabinose	-	+	-	-	w	-	-	-	-	-
12	Mannose	+	+	+	+	+	+	-	-	+	w
13	Inulin	+	-	+	+	+	-	-	+	+	-
14	Sodium gluconate	w	-	+	w	w	-	+	+	-	w
15	Glycerol	-	+	-	-	-	-	+	+	v	+
16	Salicin	+	-	+	w	+	w	-	+	+	w
17	Dulcitol	+	+	+	+	±	-	-	+	+	+
18	Inositol	+	-	-	w	+	-	-	+	w	+
19	Sorbitol	v	-	-	w	+	-	-	+	-	+
20	Mannitol	+	-	-	-	+	-	-	+	+	w
21	Adonitol	+	+	+	+	+	w	-	+	+	+
22	Arabitol	-	-	-	-	+	-	-	-	-	-
23	Erythritol	+	+	-	-	+	-	-	-	-	w
24	A-Methyl-D-glucoside	-	+	+	+	+	+	-	-	-	-
25	Rhamnose	+	-	+	-	+	-	-	-	-	-
26	Cellobiose	+	+	w	-	+	-	-	-	-	-
27	Metezitose	+	-	w	w	±	-	-	-	-	-
28	A-Methyl-	-	-	w	-	+	-	-	+	+	-

No.	Test	Bivr2B	SW5A	SW6N	Bivr3B	SW5B	Bivr2A	SW6M	KYS2A	SW1S	PH2SB
	D-mannoside										
29	Xylitol	+	-	+	-	w	-	-	+	-	+
30	ONPG	-	-	-	-	-	-	-	-	-	-
31	Esculin hydrolysis	w	+	+	+	w	w	+	+	-	-
32	D-Arabinose	-	-	-	-	-	-	+	+	-	+
33	Citrate utilization	-	-	-	-	+	-	-	-	-	-
34	Malonate utilization	-	-	-	-	-	-	-	-	-	-
35	Sorbose	-	-	-	w	-	-	-	-	-	-

+, positive; -, negative; w, weak; v, variable.

For 4 isolated bacteria which have a gram negative were tested the biochemical characterization using API 50 CH Kit and bacillus identification kit the result show in table IV 4.

Table IV-4 Biochemical characteristics of isolated bacteria by API 50 CH Kit

Tube	Test	Active ingredients	TPNS4_2A	MALS3	MALS1B	TPNS4
0		CONTROL	-	-	-	-
1	GLY	Glycerol	-	+	+	+
2	ERY	Erythritol	-	-	-	-
3	DARA	D-arabinose.	-	-	-	-
4	LARA	L-arabinose	+	+	+	+
5	RIB	D-ribose	-	+	+	+
6	DXYL	D-xylose	+	+	+	+
7	LXYL	L-xylose	-	-	-	-
8	ADO	D-xylose	-	-	-	-
9	MDX	Methyl-beta-D-xylopyranoside	+	-	-	-
10	GAL	D-galactose	+	+	+	+
11	GLU	D-glucose	+	+	+	+
12	FRU	D-fructose	+	+	+	+
13	MNE	D-mannose	+	+	+	+
14	SBE	L-sorbose	-	-	-	-

Tube	Test	Active ingredients	TPNS4_2A	MALS3	MALS1B	TPNS4
15	RHA	L-rhamnose	+	-	-	-
16	DUL	Dulcitol	-	-	-	-
17	INO	Inositol	-	-	-	-
18	MAN	D-mannitol	+	+	+	+
19	SOR	D-sorbitol	-	-	-	-
20	MDM	Methyl-alpha-D-mannopyranoside	-	-	-	+
21	MDG	Methyl-alpha-D-glucopyranoside	+	-	+	+
22	NAG	N-acetylglucosamine	-	+	-	-
23	AMY	Amygdalin	+	-	-	+
24	ARB	Arbutin	+	+	-	+
25	ESC	Esculin ferric citrate	+	+	+	+
26	SAL	Salicin	+	+	+	+
27	CEL	D-cellobiose	+	+	+	+
28	MAL	D-maltose	+	+	+	+
29	LAC	D-lactose (bovine origin)	+	+	+	+
30	MEL	D-melibiose	+	+	+	+
31	SAC	D-saccharose (sucrose)	+	+	+	+
32	TRE	D-trehalose	+	+	+	+
33	INU	Inulin	-	-	-	+
34	MLZ	D-melezitose	+	-	-	-
35	RAF	D-raffinose	+	-	+	+
36	AMD	Amidon (starch)	+	+	+	+
37	GLYG	Glycogen	+	+	+	+
38	XLT	Xylitol	-	-	-	-
39	GEN	Gentiobiose	+	-	-	-
40	TUR	D-turanose	+	+	+	+
41	LYX	D-lyxose	-	-	-	-
42	TAG	D-tagatose	-	-	-	-
43	DFUC	D-fucose	-	-	-	-
44	LFUC	L-fucose	-	-	-	-
45	DARL	D-arabitol	+	-	-	-
46	LARL	L-arabitol	-	-	-	-
47	GNT	Potassium gluconate	-	-	-	-
48	2KG	Potassium 2-ketogluconate	-	-	-	-
49	5KG	Potassium 5-ketogluconate	-	-	-	-

+, positive; -, negative.

4.3.2 Molecular characterization

4.3.2.1 16S rDNA gene sequencing and phylogenetic analyses

Table IV-5 H_2 producing isolated bacteria and the results from sequence alignment of 16s rRNA gene.

Isolates	Sources	Related species	% Identity	Accession numbers
Natural source screening				
Out1A	mangrove	*Clostridium* sp. BL22	98.57	DQ196626.2
Bivr1A	mangrove	*C. guangxiense* strain ZGM211	99.45	NR_156155.1
Bivr1B	mangrove	*Clostridium* sp. 44a-T5zd	99.69	AY082483.1
Bivr2A	Mangrove (721196E, 757948N)	*C. aurantibutyricum* CBA7522	99.78	MN646985.1
Bivr2B	Mangrove (721196E, 757948N)	*C. aurantibutyricum* CBA7522	99.52	MN646985.1
Bivr3B	Mangrove (722803E, 757445N)	*C. felsineum* JCM1399	99.79	LC036316.1
SW1S	Mangrove (717582E, 759835N)	*C. felsineum* JCMN1399	99.89	LC036316.1
SW5A	Mangrove (725719E, 757702N)	*Clostridium* sp. strain WN9	99.79	MF148496.1
SW5B	Mangrove (725719E, 757702N)	*Clostridium sp.* strain WN9	99.78	MF148496.1
SW6A	Mangrove (725719E, 757702N)	*C. neuense* G1	99.54	NR_156156.1
SW6M	Mangrove (725719E, 757702N)	*C. neuense* G1	99.80	NR_156156.1
SW6N	Mangrove (725719E, 757702N)	*Clostridium sp.* strain WN9	99.78	MF148496.1
TPNS4	Thepphanom hot spring (394291E, 2013413N)	*P. polymyxa* SN-22	99.63	KR010176.1
		P. polymyxa	97.4	
TPNS4_2A	Thepphanom hot spring (394291E, 2013413N)	*P. macerans* IAM1243	99.54	LC127104.1
		P. macerans	73.1	
MALS1B	Mea Um Long Luang hot spring (394263E, 2013359N)	*P. jamilae* KCTC 13919	99.65	HE981805.1
		Bacillus subtilis/amyloliquefaciens	69.1	
MALS3	Mea Um Long Luang hot spring (394291E, 2013413N)	*P. jamilae* IIF5SW-B4	99.90	KY218874.1
		P. polymyxa	64.9	
Unnatural source screening				
PABT	Coconut plant (aeration tank) (643385.02E, 1520563.02N)	*C. guangxiense* strain ZGM211	99.35	NR_156155.1
PH2SB	Coconut plant (anerobic tank) (643385.02E, 1520563.02N)	*C. guangxiense* strain ZGM211	96.43	NR_156155.1

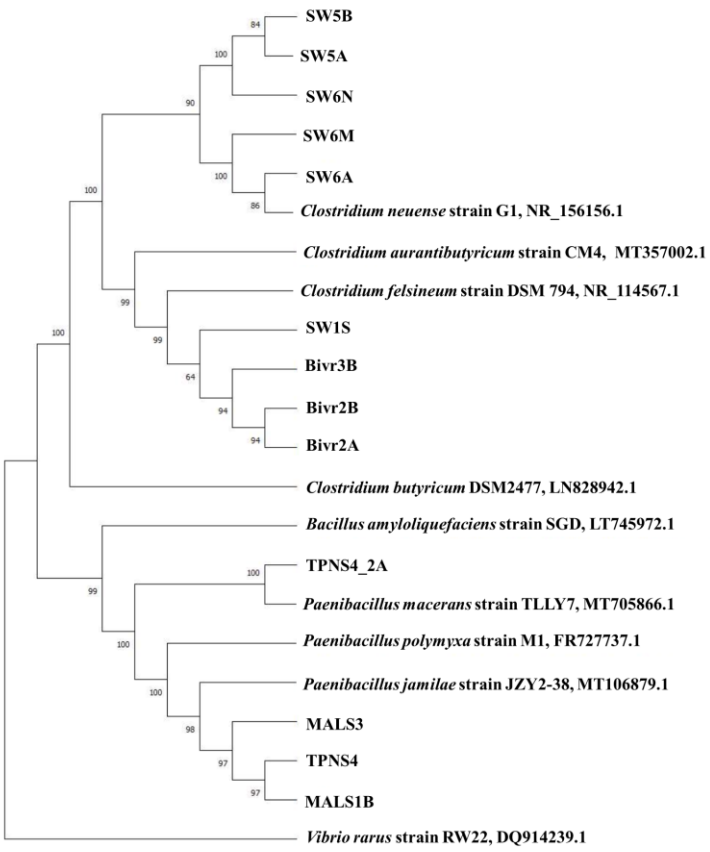

Figure IV-5 Phylogenetic tree (NJ) showing the evolution relationships among isolated endospore-forming HPB, and closely related species based on 16s rRNA gene sequence.

The colony morphology of the isolated bacteria can be observed in Fig. IV-(1-3). For the 16s rRNA gene sequence analysis, all of the bacteria isolated from mangrove sediments and wastewater tank of the coconut factory were classified as *Clostridium* spp., obligate anaerobic bacteria, whereas all of the bacteria isolated from the hot spring sediments were classified as *Paenibacillus* spp., facultative anaerobic bacteria. This is most likely due to the different environments encouraging the growth of distinct organisms. However, both genera share similarities in that they are members

of the same phylum, Firmicutes, and are endospore-forming Gram-positive bacteria (Figueiredo et al., 2020; Patowary & Deka, 2020). These genera can be found in a wide variety of environments. For instance, agricultural soil, mountains, grassland, biogas digesters, cow manure, lakes, food, plant roots, landfills, and estuarine wetlands (Bae et al., 2010; Bardají et al., 2019; Berezina et al., 2009; Berge et al., 2002; He et al., 2007; Li et al., 2015; Wu et al., 2010; Youn et al., 2016; Zhang et al., 2018; X. Zhao et al., 2017; Zhu et al., 2018). This finding was consistent with other reports that isolated *Clostridium* spp. from mangroves (Chang et al., 2008; Gao et al., 2014; Hong et al., 2020; Shanmugam et al., 2018) and *Paenibacillus* spp. from hot springs (Brown, 2014; Cai et al., 2019; Masset et al., 2012; Mehetre et al., 2018).

The presence of *Clostridium* has been attributed to organic matter degradation and nutrient cycling, and a specific relationship with plant roots (Gomes et al., 2014). This genus is well known to have a high H_2 production from a various of carbon sources (Wang & Yin, 2021). Conversely, *Paenibacillus* have been reported to produce bio-flocculants capable of secreting exo-polysaccharide and a variety of hydrolytic enzymes (Kanso et al., 2011; Morillo Pérez et al., 2008). Therefore, this genus is well known as hydrolytic bacteria that can hydrolyze various carbon sources, such as lignocellulose, glycerol, and starch (Adlakha et al., 2015; Villanueva-Galindo & Moreno-Andrade, 2021). Additionally, this genus was discovered in a H_2-producing bioreactor and was found to express the *hydA* gene, which encodes for an Fe hydrogenase, throughout the fermentation process (Huang et al., 2010). Besides, the

genus is relevant in terms of the biodegradation of phenol (Chandra et al., 2011), decolorization (Nho et al., 2021; Sompark et al., 2021), and heavy metals (Gaur et al., 2021; Morillo Pérez et al., 2008). This indicates that this genus possesses both hydrolytic and H_2 fermentation capabilities. The hydrolytic property refers to the ability to use carbon sources and resistance to unfavorable environmental conditions.

The chemical characteristics of the isolated bacteria are presented in Table IV-3, IV-4. These bacteria were capable of utilizing a variety of carbon sources. For instance, most of them could utilize D-xylose, glycerol, D-mannose, L-alabinose, and starch. Taxonomic classification of the isolated bacteria by alignment of 16s rRNA gene sequence with related sequences in the NCBI database identified the species of each isolate, as represented in Table IV-5, and allowed exploration of the evolutionary relationships with other closely related species (Fig. IV-5). The *Clostridium* spp., which were isolated from mangrove sediments, were assigned to *C. felsineum, C. aurantibutyricum,* and *C. neuense.* All four species have previously been reported to be capable of producing H_2 (Baghchehsaraee et al., 2010; Li et al., 2015; Youn et al., 2016; Zhu et al., 2018). However, there is not much research on these species, and only a limited number of strains have been examined. This was, therefore, an opportunity to obtain new HPB capable of producing H_2 from a broader variety of carbon sources.

Whereas the isolated bacteria from hot springs were all classified as *Paenibacillus* spp., and specifically *P. polymyxa, P. macerans,* and *P. jamilae.* These species have been rarely reported before for biofuel production (Adlakha et al., 2015; Baghchehsaraee et al., 2010; Gupta et al., 2009), including H_2 production by *P. polymyxa* (Maintinguer et al., 2017; Watanapokasin et al., 2009) and *P. macerans* (Łukajtis et al., 2018).

Batch fermentation for H_2 production was performed to evaluate the H_2 production ability of the different isolates, with the results shown in Fig. IV-4. Under identical conditions (BFM medium, initial pH 7, incubation temperature of 37 °C, and 10 g/L glucose concentration), the CHP from SW1S and SW5A were significantly higher than the other isolates. Therefore, SW1S and SW5A were chosen for further investigation and identified as strains CUEA03 and CUEA01. However, all of these microbes have the ability to produce H_2, which might be useful in the future. For example, developing synthetic microbial consortia that promote H_2 production from organic waste. This will rely on the cooperation of various types of bacteria to digest a variety of substrates in order to produce H_2 and reduce organic waste. Previous studies have shown that co-fermenting with three species of *Enterococcus* enhanced the generation of H_2 from wheat straw (Valdez-Vazquez et al., 2015). Therefore, as suggested by Wang et al., it is likely that the combination of several bacterial species might result in syntrophic interactions (Wang et al., 2019).

4.4 SW5A: *Clostridium hydrogenum* sp. nov. strain CUEA01

4.4.1 Characteristics of *C. hydrogenum* CUEA01

We selected the *C. hydrogenum* sp. *nov.* strain CUEA01 for additional study because of its outstanding ability to generate H_2. According to Fig. IV-6, CUEA01 is an obligate anaerobic, Gram-positive, endospore-forming, and mobile bacteria with peritrichous flagella. CUEA01 displayed a colony morphology on the modified DSMZ 640 medium agar that was colorless, circular in shape, with a convex elevation, and an entire edge (Fig. IV-6A), while the bacterial cells were rod-shaped, with 3-5 m for length and 0.5-0.8 m for diameter (Fig. IV-6C). They were able to grow in the modified DSMZ 640 medium with a NaCl concentration of 0-1% (w/v), pH ranges of 4-12, and temperatures ranging from 15 to 43 °C. Fermentation releases primarily a gas mixture of CO_2 and H_2, with a high H_2 content ranging from 30-73% depending on growing circumstances, and it also produces butyric and acetic acid in fermented broth. Table IV-6 summarizes the biochemical properties suggested for the CUEA01, which include a wide range of carbon sources such as glycerol, starch, and xylose.

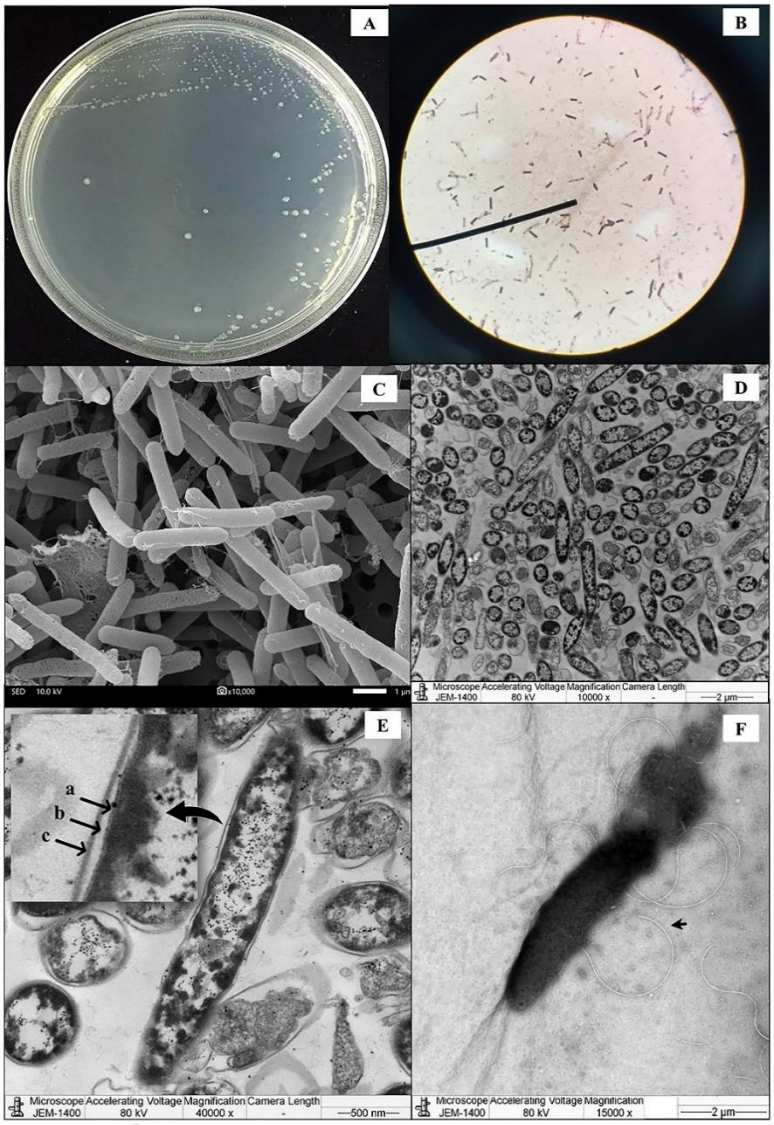

(Srimawong & Chulalaksananukul, 2022)

Figure IV-6 CUEA01 colony morphology image on basal agar medium.

(A), The Gram stained of CUEA01 (B), SEM image of bacterial cells with 10,000x magnification (C), Cell morphology of CUEA01 using TEM technique (D-F); thin section of bacterial cells at 10,000x (D), 40,000x magnification (E) with the features of Gram-positive bacteria's cell wall (a: plasma membrane, b: periplasmic space, and c: peptidoglycan), and The negatively strained cell (15,000x magnification) of CUEA01

vegetative cells grown in basal broth medium. Arrowhead points at the bacterial flagellum (F).

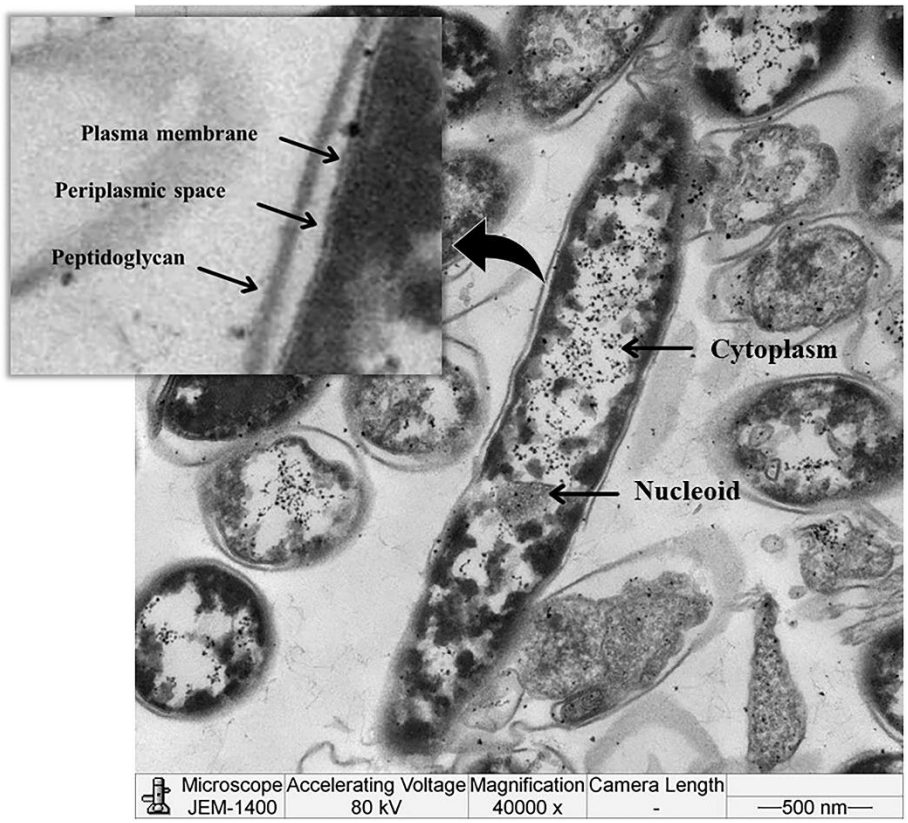

(Srimawong & Chulalaksananukul, 2022)

Figure IV-7 TEM image of a thin segment of bacterial cells magnified by 40,000x from CUEA01 cells cultured in basal broth medium.

Table IV-6 *C. hydrogenum* sp. *nov*. strain CUEA01 characteristics under various conditions.

Characteristics	Results	Characteristics	Results
Morphology:		**Carbon source**	
Shape	Rod-shaped	Glucose	+
Width	0.5–0.8	Maltose	+
Length (μm)	3–5	Fructose	+
Spore formation	+	Dextrose	+
Gram stain	+	Galactose	+
Anaerobic growth:	+	Lactose	+
Catalase	-	Sucrose	+
Oxidase	-	L-Arabinose	+
Methyl red test	+	Mannose	+
NaCl concentration (w/v):		Glycerol	+
0.09%	+	Starch	+
0.5%	+	Esculin hydrolysis	+
1%	+	Cellobiose	+
1.5%	-	Xylose	+
Growth pH	4–12	Xylan	+
Growth temperature (°C)	15–43	CMC	-
Glucose concentration (g/L)	5–100	Avicel	+

(Srimawong & Chulalaksananukul, 2022)

4.4.2 The WGS and genome assembly

WGS, genome assembly, and genome annotation were conducted for the purpose of investigating the CUEA01 genome. The assembled genome, which was obtained from five contigs with an average G+C content of 30.34% and a total length of 5,501,482 bp and submitted to the Comprehensive Genome Analysis Service.

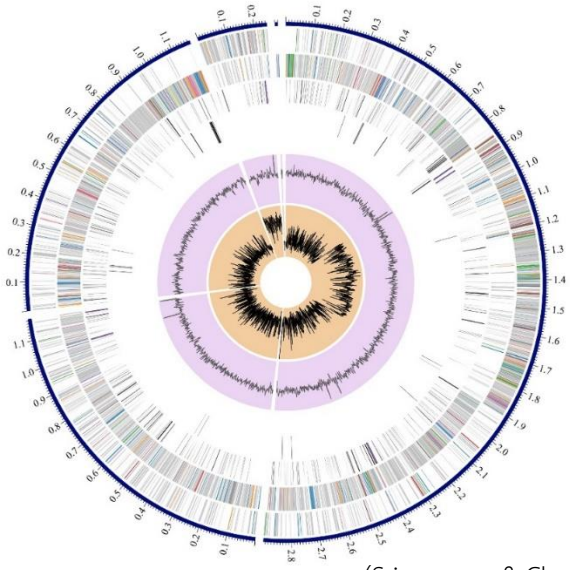

(Srimawong & Chulalaksananukul, 2022)

Figure IV-8 Circular graphical representation of the CUEA01 chromosome's genome annotation distribution.

Contigs, CDS on the forward strand, CDS on the reverse strand, RNA genes, CDS with homology to known antimicrobial resistance genes, CDS with homology to known virulence factors, GC content, and GC skew are all included. The forward and reverse strand CDS colors illustrate the subsystem to which these genes belong.

4.4.3 Genome annotation

The genome of CUEA01 was annotated, and the number 1485.374 was assigned as a unique genome identifier. This Whole Genome Shotgun project has been deposited at DDBJ/ENA/GenBank under the accession number of JAEACT000000000. The version described in this paper is JAEACT010000000, with the classification of the superkingdom and annotation using genetic code 11, giving a taxonomic position of: cellular organisms > Bacteria > Terrabacteria group > Firmicutes > Clostridia > Clostridiales > Clostridiaceae > *Clostridium.*

Table IV-7 Assembly details of CUEA01

Assembly features	
Contigs	5
GC Content	30.34
Plasmids	0
Contig L50	1
Genome Length	5,501,482 bp
Contig N50	2,898,020
Chromosomes	0
CDS	4,957
Repeat Regions	793
tRNA	86
rRNA	17
Partial CDS	0
Miscellaneous RNA	0
Job ID	Annotation_403967
Job started	July 1st 2020, 10:01:02pm
Job Completed	July 1st 2020, 10:06:52pm
Total Time	5 minutes and 50 seconds

(Srimawong & Chulalaksananukul, 2022)

Table IV-7 and Fig. IV-8 provide a summary of the annotated features. There are 4,957 protein-coding sequences (CDS), 86 transfer RNA (tRNA) genes, and 17 ribosomal RNA (rRNA) genes in this genome. The [FeFe] hydrogenase (EC 1.12.7.2) and a complex form of the [NiFe] hydrogenase gene were found to be highly duplicated in the genome of CUEA01, according to the annotation of its genes using RASTtk. Although the [NiFe] hydrogenases are typically present in facultative anaerobic bacteria and are more oxygen-tolerant than [FeFe] hydrogenase (Kim et al., 2010), the function of [NiFe] hydrogenase on H_2 production in strictly anaerobic bacteria has received little attention. Interestingly, this genome also contained pyruvate formate-lyase (EC 2.3.1.54) and PFL activating enzyme (EC 1.97.1.4). These enzymes have been associated to H_2 generation via the formate H_2 lyase (FHL) pathway, which converts formate to CO_2 and H_2. The Enterobacteriaceae family discovered this mechanism, which was related to the [NiFe] hydrogenase enzyme. The interaction of formate dehydrogenase-H with hydrogenase 3 ([NiFe] hydrogenase group 4) in the FHL pathway for H_2 evolution in *E. coli* has been discovered (Kim et al., 2010; Maeda et al., 2007a). Even though the [NiFe] hydrogenase found in this strain was categorized as belonging to group 1, it also has been reported that it participates in the formate-driven H_2 generation in the FHL pathway (Kim et al., 2010). Therefore, it is possible that three different pathways will be used to produce H_2 in this strain: I the mixed acid fermentation pathway using the PFL, FHL, and related pathway; (ii) the butyric acid fermentation pathway using pyruvate: ferredoxin oxidoreductase and

ferredoxin-dependent hydrogenanase; and (iii) the NADPH regeneration pathway (Liu et al., 2017; Reischl et al., 2018; Rydzak et al., 2009; Tran et al., 2014; Zhang et al., 2020). Fig. IV-9 shows the encoding enzymes in the genomic DNA of CUEA01 that were related to the evolution of H_2 by these routes. However, the expression of related genes and the regulation of metabolic processes remain equivocal and need to be investigated further. Annotation of the genomic DNA revealed a substantial number of potentially encoded hydrolytic enzymes related to substrate utilization capabilities in CUEA01. The number copy of these enzymes is shown in Table IV-8.

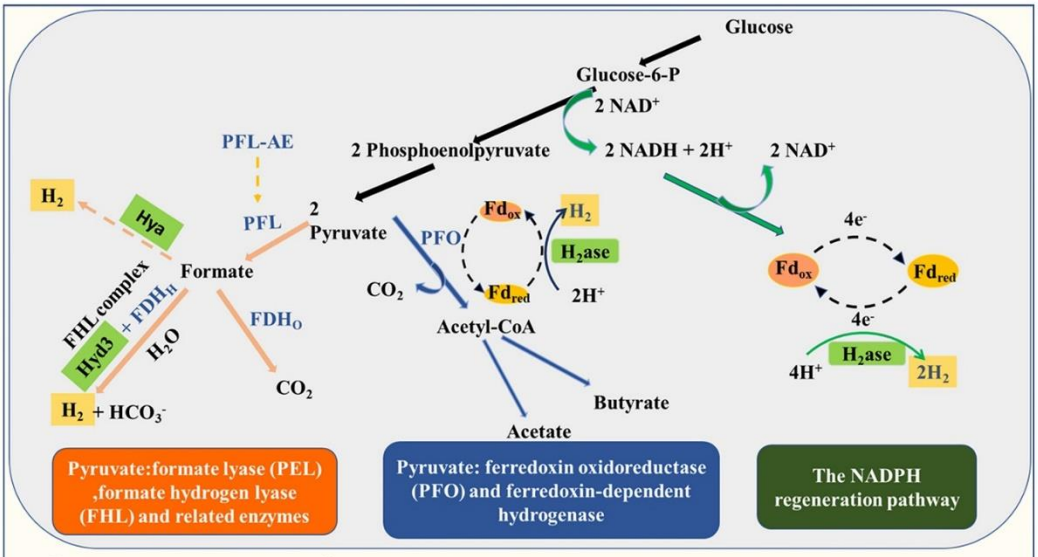

Enzymes	copy number
[NiFe] hydrogenase, group 1, large subunit	1
[NiFe] hydrogenase, group 1, small subunit	1
[NiFe] hydrogenase HypE	1
[NiFe] hydrogenase HypD	1
[NiFe] hydrogenase HypC	1
[NiFe] hydrogenase HypF	1
Pyruvate formate-lyase activating enzyme (EC 1.97.1.4)	3
Pyruvate formate-lyase (EC 2.3.1.54)	4
Formate dehydrogenase-O, major subunit (EC 1.2.1.2)	1

Enzymes	copy number
[FeFe] hydrogenase (EC 1.12.7.2)	2
[FeFe]-hydrogenase maturation protein HydE	1
[FeFe]-hydrogenase maturation protein HydF	1
[FeFe]-hydrogenase maturation protein HydG	1
[FeFe] hydrogenase, cytoplasmic, one subunit form (EC 1.12.7.2)	1
NAD(FAD)-utilizing dehydrogenases	1
NAD(P)H dehydrogenase (quinone) (EC 1.6.5.2)	1
Fe-S oxidoreductase	6
Oxidoreductase, short-chain dehydrogenase/reductase family	7
Dihydroorotate dehydrogenase (NAD(+)), catalytic subunit (EC 1.3.1.14)	1
Ferredoxin	9
Pyruvate-flavodoxin oxidoreductase	2
Tungsten-containing aldehyde ferredoxin oxidoreductase cofactor modifying protein	1
Electron bifurcating butyryl-CoA dehydrogenase (NAD+, ferredoxin)	2
NADH-dependent reduced ferredoxin:NADP+ oxidoreductase subunit B related protein CAC0764	1
Electron bifurcating butyryl-CoA dehydrogenase (NAD+, ferredoxin)	2
Electron bifurcating butyryl-CoA dehydrogenase, electron transfer flavoprotein alpha	1
Electron bifurcating butyryl-CoA dehydrogenase, electron transfer flavoprotein beta	1

(Srimawong & Chulalaksananukul, 2022)

Figure IV-9 Fundamental H_2 fermentation routes, and the CUEA01-encoding enzymes that probably serve an important role in the pathways.

Abbreviations: FhlA: formate H_2 lyase; FHL: formate H_2 lyase; FDH_H: formate dehydrogenase-H; FDH_O: formate dehydrogenase-O; Hyd3: [NiFe] hydrogenase group 3; PFL-AE: Pyruvate formate-lyase activating enzyme; PFL: pyruvate formate-lyase; Hya: [NiFe] hydrogenase, group 1; PFO: pyruvate ferredoxin oxidoreductase; Fd: ferredoxin; hydrogenase: [FeFe] hydrogenase; and ox/red: oxidation/reduction form.

Table IV-8 Predicted carbon source utilization enzymes of *C. hydrogenum* strain CUEA01.

EC code	Enzymes	Number encoded in genome
EC 3.2.1.86	6-phospho-beta-glucosidase	10
EC 3.2.1.23	beta-galactosidase	5
EC 3.2.1.22	alpha-galactosidase	3
EC 3.2.1.4	Endoglucanase M	1
EC 3.2.1.73	Endo-beta-1,3-1,4 glucanase (licheninase)	1
EC 3.2.1.37	Xylan 1,4-beta-xylosidase	3
EC 3.2.1.26	beta-fructofuranosidase	1
EC 3.2.1.21	beta-glucosidase	2
EC 3.1.1	Esterase/lipase	3
EC 3.2.1.15	Polygalacturonase	2
EC 3.2.1.4	Endoglucanase E precursor (EgE) (Endo-1,4-beta-glucanase E) (Cellulase E)	2
EC 3.2.1.55	alpha-L-arabinofuranosidase II	1
EC 3.2.1.55	alpha-L-arabinofuranosidase	2
EC 3.2.1.177	alpha-xylosidase	3
EC 3.2.1.176	Cellulose 1,4-beta-cellobiosidase (reducing end)	1
EC 3.2.1.8	Endo-1,4-beta-xylanase	2
EC 3.2.1.4	beta-1,4-glucanase (cellulase)	2
EC 3.2.1.20	Alpha-glucosidase	1
EC 3.2.1.82	Exo-poly-alpha-D-galacturonosidase	3
EC 3.2.1.41	putative alpha-dextrin endo-1, 6-alpha-glucosidase	1
EC 3.2.1.89	Arabinogalactan endo-1,4-beta-galactanase	1
EC 3.2.1.25	Beta-mannosidase	1
EC 3.2.1.26	Sucrose-6-phosphate hydrolase	2
EC 3.2.1.131	Xylan alpha-1,2-glucuronosidase	1
EC 3.2.1.10	Oligo-1,6-glucosidase	2
	Putative xylanase	1
EC 3.2.1.135	Neopullulanase	2
EC 1.1.1.6	Glycerol dehydrogenase	2

(Srimawong & Chulalaksananukul, 2022)

4.4.3.1 Phylogenetic analysis

The phylogenetic analysis (Fig. IV-10) revealed that CUEA01's genome was most closely related to *Clostridium* sp. DMHC 10, a strain capable of producing a high H_2 yield (3.35 $mol_{H2}/mol_{glucose}$) under acidic conditions (pH 5). In comparison, CUEA01 in this investigation appeared to prefer an environment that was moderately alkaline (pH 8) (Kamalaskar et al., 2010). However, the average nucleotide identity between the two species was only 80.67% (Goris et al., 2007). Additionally, CUEA01 is related to the species *C. pasteurinum* DSM 525, which has been shown to produce H_2 from glycerol (Sarma et al., 2016).

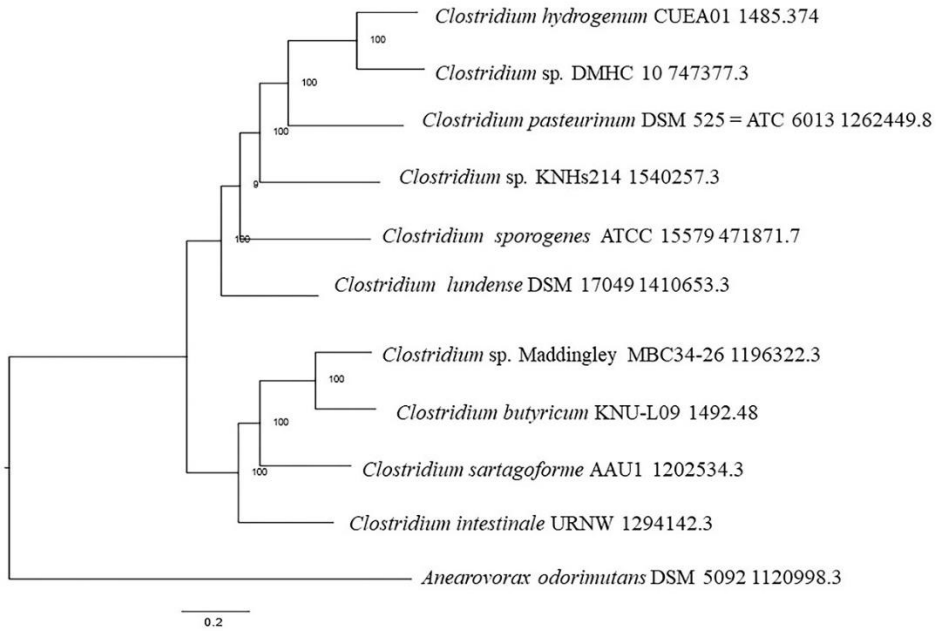

(Srimawong & Chulalaksananukul, 2022)

Figure IV-10 A phylogenetic tree of CUEA01 and the closest reference based on genomic data.

4.4.4 Characteristics of H_2 production

By using sequential univariate analysis, the optimum culture conditions for H_2 production by CUEA01 through batch fermentation were assessed in terms of culture temperature, initial pH, and initial glucose concentration. The effect of incubation temperature on H_2 production at pH 7 and an initial glucose content of 10 g/L is illustrated in Fig. IV-11, where CUEA01 grew and produced H_2 at temperatures ranging from 10 to 45 °C. It was assumed that H_2 production was associated to cell growth since the H_2 yields were related to culture growth. This assumption was in accordance with a previous study that discovered *C. beijerinckii* Fanp3 produced more H_2 during the exponential growth phase (Pan et al., 2008).

In this investigation, CUEA01 was cultivated at temperatures ranging from 15 to 40 °C, with the highest CHP achieved at 37 °C. This resulted in a CHP of 1790 to 2896 mL/L. This proved categorically that CUEA01 is mesophile, wherein cells could develop, or enzymes may function at ambient temperature. Evidently, the temperature had a significant impact on the HPR as well, which followed the same trend as the temperature increased from 15 °C to the optimum temperature. That is, the growth rate and HPR were both increased as the temperature was raised from 15 °C, the lowest temperature at which the cells generated H_2, to 37 °C. This was most likely caused by the temperature increase accelerating enzymatic activities (Daniel & Danson, 2013). Cell growth and H_2 yield declined with rising temperature above the optimal temperature (37 °C), and both were entirely

repressed at 43 °C, which was attributed to thermal denaturation and deactivation of the enzymes (Chittibabu et al., 2006; Saratale et al., 2018).

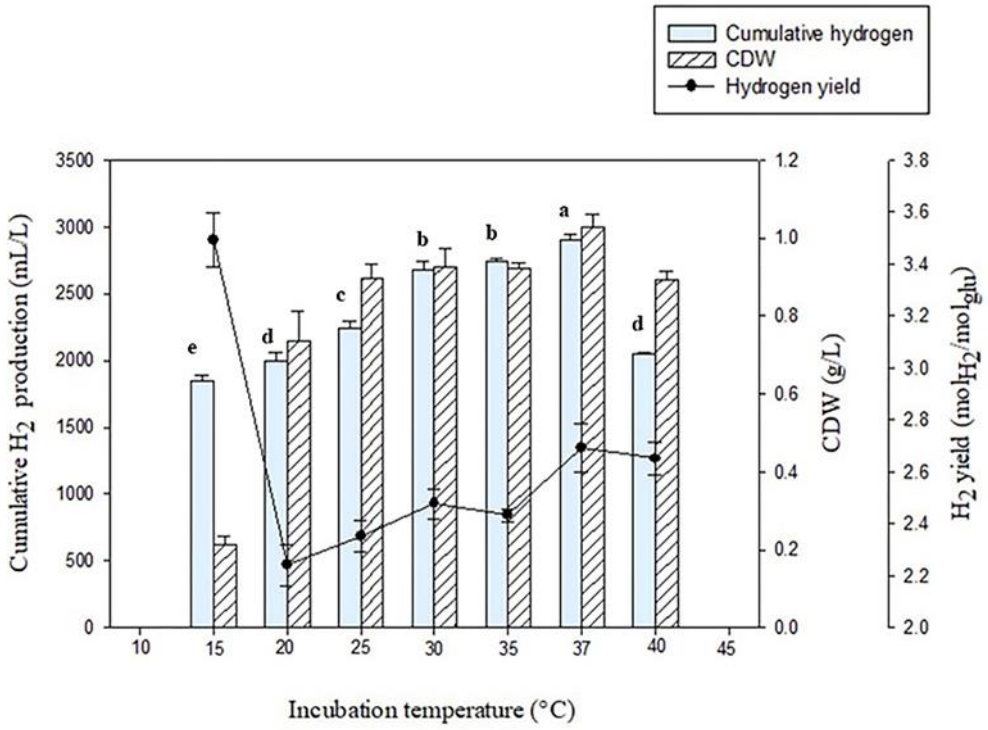

(Srimawong & Chulalaksananukul, 2022)

Figure IV-11 Characteristic of H_2 production by *C. hydogenum* strain CUEA01 under different incubation temperature.

*Initial pH and glucose concentration of 7 and 10 g/L, respectively. All data are represented as the mean ± SD. Means of the CHP with a different letter are significantly different ($P < 0.05$; Tukey HSD test).

CUEA01 developed and produced H_2 throughout a wide pH range of 4-12 at 37 °C and an initial glucose concentration of 10 g/L with regard to the impact of pH on cell growth and H_2 production (Fig. IV-12). The maximum CHP (3125 mL/L) was obtained at pH 8, the same pH as the highest cell growth, demonstrating that H_2

fermentation is dependent on the acidogenesis stage, which also produces VFA. As a result, the pH of the cultures gradually decreased as VFA accumulated in the broth. It is probable that decreasing pH influenced enzyme function, whereas raising VFA concentration inhibited enzyme performance and cell development. A higher initial pH may help maintain the pH level in the ferment medium for longer and support enzymatic function as the end pH of all the fermentation media was generally around 4. A higher initial pH (pH 10) is believed to have a stronger buffer capacity, which encourages the bacterial community to generate more VFA than at a lower initial pH (pH 8) (Atasoy et al., 2019). Additionally, it has been documented that when the pH was lower than 4, acid-producing bacteria, such as *Clostridium* spp., were suppressed (da Silva Mazareli et al., 2021).

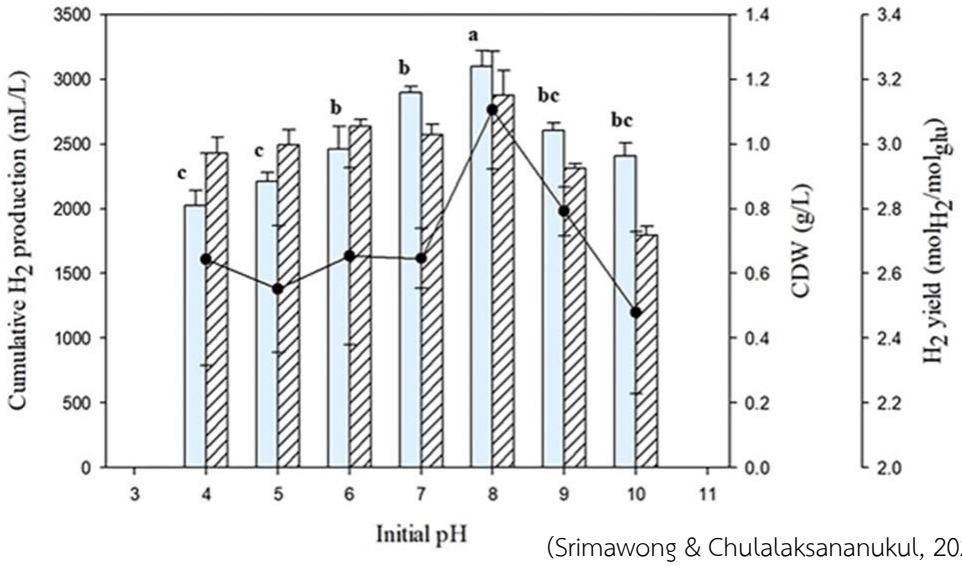

(Srimawong & Chulalaksananukul, 2022)

Figure IV-12 Characteristic of H_2 production by *C. hydogenum* strain CUEA01 under different initial pH concentration.

*Incubation temperature and glucose concentration of 37 °C and 10 g/L, respectively. All data are represented as the mean ± SD. Means of the CHP with a different letter are significantly different ($P < 0.05$; Tukey HSD test).

CUEA01 generated H_2 with a maximum CHP of 3264 mL/L (H_2 yield of 3.11 $mol_{H2}/mol_{glucose}$) at an initial glucose concentration of 10 g/L as it grew under initial glucose concentrations ranging from 5 to 60 g/L at 37 °C and pH 8 (Fig. IV-13) The initial glucose concentration was increased from 20 to 45 g/L with no noticeable effect on cell growth or H_2 production. Increasing the initial glucose concentration above 45 g/L lowered CHP and cell development gradually. This was most likely owing to substrate inhibition and substrate uptake restrictions. Furthermore, a high glucose content may have a negative feedback effect on cell development and H_2 generation, which is consistent with a recent finding (Cai et al., 2019). Furthermore, it has been noted that raising the initial glucose concentration from 10 to 25 g/L clearly decreased the H_2 yield of *Clostridium* sp. 5A-1 (Cai et al., 2021). The optimal initial glucose concentration for *Clostridium* spp. is typically between 2 and 20 g/L (Cai et al., 2013; Mei et al., 2014), which was comparable to the values seen on the CUEA01. On the other hand, CUEA01 has the advantage of being able to withstand high initial glucose concentrations, which means it might potentially be employed with organic waste that usually has a high COD value.

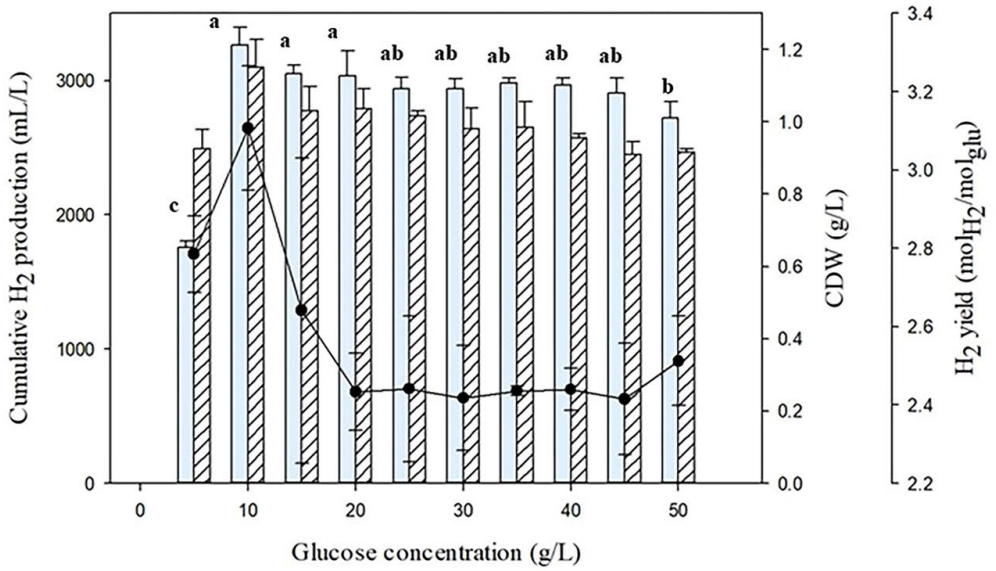

(Srimawong & Chulalaksananukul, 2022)

Figure IV-13 Characteristic of H_2 production by *C. hydogenum* strain CUEA01 under different glucose concentration.

*Incubation temperature and initial pH concentration of 37 °C and 8, respectively. All data are represented as the mean ± SD. Means of the CHP with a different letter are significantly different ($P < 0.05$; Tukey HSD test).

4.4.5 H_2 production from different substrates

The genomic sequence analysis revealed that CUEA01 comprised several genes encoding enzymes involved in a wide range of carbon utilization abilities (Table IV-9). Fig. IV-14 depicts the capability of CUEA01 producing H_2 from glucose, xylose, fructose, galactose, L-arabinose, mannose, maltose, cellobiose, avicel, and sucrose, soluble starch, insoluble starch (cassava starch), xylan and glycerol. Sugar alcohols and C6 and C5 sugars in the form of monosaccharides, disaccharides, and

polysaccharides linked by **α** or **β** -glycosidic linkages were also considered as carbon sources.

The result shows that all those carbon sources could be used as substrates by CUEA01. Additionally, at the same initial concentration of carbon sources, CUEA01 produced H_2 from glucose, soluble starch, insoluble starch (cassava starch), glycerol, and cellobiose at high CHPs of 3100, 2976, 3057, 2815, and 3212 mL/L, respectively

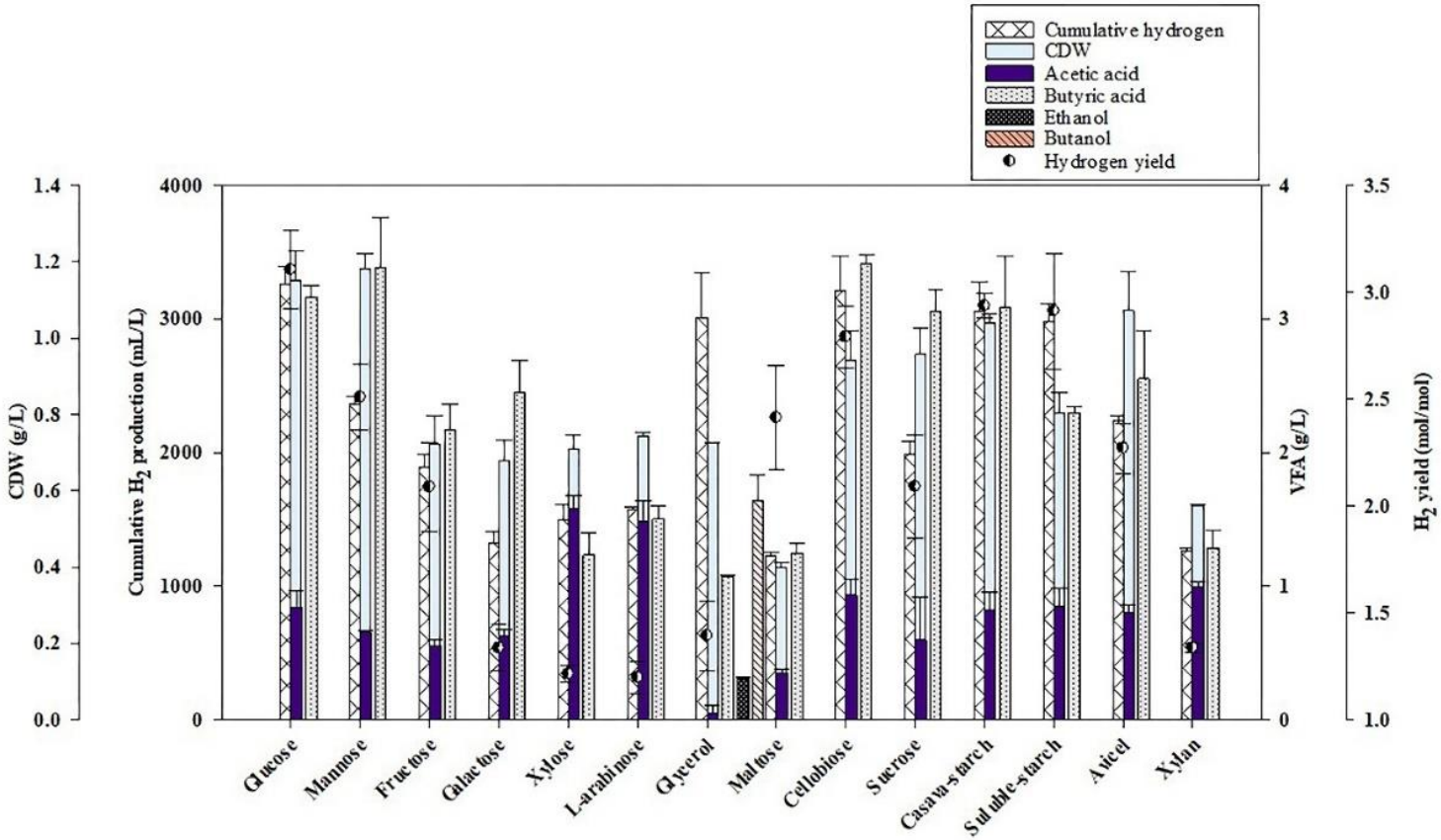

(Srimawong & Chulalaksananukul, 2022)

Figure IV-14 Characteristic of H_2 production by *C. hydogenum* strain CUEA01 utilizing different carbon sources. Data are shown as the mean ± SD

Table IV-9 Kinetic features related to H_2 production by *C. hydrogenum* CUEA01 from different carbon sources.

Substrate	SCE (%)	CR (%)	ER (%)	Energy yield of H_2 (kJ/g VS)	CHP (mL/L)	HPR (mL/L/h)	Metabolites (g/L)					H_2 yield (mol/mol)
							Acetic acid	Butyric acid	Ethanol	butanol	Total	
Glucose	77.77	100	31.85	4.97	3264	129	0.844	3.167	ND	ND	4.011	3.11
Mannose	69.71	100	25.71	4.01	2363	49	0.654	3.382	ND	ND	4.036	2.51
Fructose	67.09	75	21.42	3.34	1891	39	0.550	2.170	ND	ND	2.720	2.09
Galactose	73.36	67	12.62	2.14	1325	28	0.623	2.450	ND	ND	3.073	1.34
xylose	75.81	62	14.93	2.33	1496	31	1.580	1.234	ND	ND	2.814	1.21
L-arabinose	80.82	62	14.74	2.30	1569	33	1.486	1.502	ND	ND	2.988	1.20
Glycerol	76.28	81	27.96	4.36	3009	63	0.046	1.075	0.312	1.643	3.076	1.39
Maltose	37.68	70	24.75	3.86	1225	26	0.346	1.249	ND	ND	1.595	2.41
Cellobiose	84.95	88	28.63	4.46	3213	134	0.934	3.416	ND	ND	4.316	2.79
Sucrose	70.54	80	21.45	3.34	1989	41	0.596	2.211	ND	ND	2.807	2.09
Casava-starch	74.56	100	30.12	3.13	3057	127	0.820	3.084	ND	ND	3.904	2.94
Soluble starch	72.19	85	31.47	4.91	2976	124	0.846	2.295	ND	ND	3.141	2.91
Avicel	65.67	100	25.89	4.04	2240	47	0.802	2.888	ND	ND	3.680	2.27
Xylan	57.33	66	16.44	2.57	1265	26	0.993	1.284	ND	ND	2.277	1.36

ND* not detected. (Srimawong & Chulalaksananukul, 2022)

H_2 yield was calculated from $mol_{H2}/mol_{monosaccharide}$

The glycolysis pathway, a key metabolic pathway that results in the production of numerous reducing chemicals (NADH, protons), was employed to produce H_2 during cell development. As seen from the generated VFA, the acetate-butyrate pathway was the final stage in this process. Only acetic acid and butyric acid were found in the large proportion of the carbon fermented broths, with butyric acid being the most abundant. Butanol, on the other hand, was detected in a considerable proportion of the products in the glycerol fermented broth, while butyric acid and acetate acid were only found in a minor proportion. This indicated

that the routes used for glycerol fermentation to produce H_2 were distinct from those employed for other carbon sources. This is most likely owing to the fact that using glycerol as a substrate raises NADPH levels, which can disrupt the redox balance and cause the metabolic flux to shift from acetate generation to butanol generation (Johnson & Rehmann, 2020; Kaushal et al., 2018). Furthermore, H_2 fermentation from glycerol differed from other carbon sources that use two metabolic stages, acidogenesis and solventogenesis. H_2 and VFA were generated during cell development in the first stage. Following that, the acetic acid and butyric acid created were utilized to manufacture ethanol and butanol in the second stage, resulting in a reduced amount of them (Arslan et al., 2021; Fonseca et al., 2020). It should be emphasized that, unlike other *Clostridium*, which typically produce acetone-butanol-ethanol (ABE) in the solventogenesis stage, CUEA01 does not produce ABE from other carbon sources, including glucose (Abd-Alla et al., 2015). CUEA01 had an ABE in a glycerol-supplemented broth at a 0:8:2 ratio, which differed from the common ABE ratio (3:6:1). This is most likely owing to the previously mentioned redox balance in cells. It was discovered that CUEA01 secreted lignocellulolytic enzymes accompanied with exoglucarnase, beta-glucosidase, beta-mannosidase, xylanase, β-glucosidase, and L-arabinofuranosidase to degrade lignocellulose and retrieve energy and create H_2 from these substrates (Table IV-8) These could successfully hydrolyze avicel, cellobiose, manose, xylan, xylose, and L-

arabinose. As a result, strain CUEA01 can be employed to ferment H_2 from a lignocellulosic cellulose mostly consisting of cellulose and hemicellulose.

Despite the fact that CUEA01 may directly use xylan as a carbon source for H_2 fermentation, it only achieved a maximum CHP of 1265 mL/L. (Table IV-9). In comparison to previous findings, the yield from CUEA01 in this investigation was comparable to that produced from enzymatically hydrolyzed xylan by *C. butyricum* CGS5 (CHP of 1288 mL/L), a xylose-utilizing bacteria. It should be highlighted that the direct H_2 fermentation from xylan in CUEA01 is advantageous. By eliminating the pretreatment procedure, it might also be possible to potentially manufacture H_2 from agricultural wastes including xylan while lowering the production cost and substrate damage by the acid pretreatment. Lower sugar levels of substrates were reported as a result of the acid pretreatment of rice straw, which also caused hemicellulose components to be lost (Lo et al., 2010).

The range of the ER value for the H_2 produced by CUEA01 from different carbon sources was 12.62 to 31.85%, which was correlated with the CR value. Starch and glucose both had maximal ERs of 31.47% and 31.85%, respectively. The acquired ER values were close to the theoretical ER of H_2 from dark fermentation, which is approximately 33.5% ($C_6H_{12}O_6 + 2H_2O \longrightarrow 4H_2 + 2CO_2 + 2CH_3COOH$) (Xie et al., 2008). In this experiment, we achieved an energy yield of 4.97 and 4.91 kJ/g VS from glucose and starch, respectively, in this study, which was greater than the usually obtained energy yield of H_2 (2.54-4.45 kJ/g glucose) in previous research (Xia et al.,

2016). Galactose had a comparatively low ER (12.62%) compared to the other carbon sources, providing only 2.14 kJ/g VS of H_2 energy despite having a high SCE (73.36%). This was most likely owing to the carbon source's employment of different fermentation routes, which may have been employed to produce other products, resulting in a lower H_2 production.

Nevertheless, an integrated H_2 manufacturing process might improve the ER. Cogeneration of H_2 and methane (CH_4) utilizing the effluent of dark fermentation as the substrate for CH_4 synthesis enhanced the ER in biomass fermentation from 4.3% to 22.28% (Zhang et al., 2017), and from 23% to 82% (Xie et al., 2008). Additionally, the ER was improved by the combination of dark and photo-fermentation (Su et al., 2009). These strategies could be used in the future to improve the ER from H_2 fermentation by CUEA01.

Table IV-10 Comparison of batch fermentation H_2 generation by *C. hydrogenum* CUEA01 and other *Clostridium* species.

Microorganism	Substrate	Temperature (°C)	pH	Cumulative H_2 yield	H_2 yield (mol/mol)	HPR (mL/L/h)	Ref.
C. butyricum DSM 10702	Glucose (10g/L)	37	7.0		3.47		(Yin & Wang, 2017)
Clostridium sp. YM1	Glucose (20g/L)	37	6.5	3821 mL/L	1.7		(Abdeshahian et al., 2014)
C.butyricum INET1	Glucose (COD 10 g/L)	35	7	2159 mL/L	2.24	302	(Yin & Wang, 2017)
Clostridium sp. 6A-5	Glucose (16g/L)	43	8	2727 mL/L	2.50		(Cai et al., 2013)
C. butyricum CWBI1009	Glucose	30	5.2	211 ml/ g	1.7	126	(Masset et al., 2010)
C. hydrogenum CUEA01	Glucose (10g/L)	37	8	3264 mL/L, 420 mL/g	3.11	136	This study
C. butyricum INET1	Xylose (COD 10 g/L)	35	7	1033mL/L	1.23	75	(Yin & Wang, 2017)
C. beijerinckii YA001	Xylose (10g/L)	40	8		2.31	311.3	(An et al., 2014)
C. amygdalinum C9	Xylose	40	8.5	3631 mL/L	2.5		(Jayasinghearachchi et al., 2010)
C. butyricum CGS5	Hydrolysed xylan (xylose)	37	7.5	1288 mL/L	0.7		(Lo et al., 2010)
C. hydrogenum CUEA01	Xylose (10g/L)	37	8	1496 mL/L, 197 mL/g	1.21	62	This study
C. butyricum INET1	Starch (COD=10 g/L)	35	7	1126 mL/L	2.17	61	(Yin & Wang, 2017)
C. amygdalinum C9	starch	37	7.5	3481 mL/L, 390 mL/g			(Jayasinghearachchi et al., 2010)
C. butyricum CWBI1009	Soluble starch	30	5.6		2.0		(Masset et al., 2010)
C. saccharoperbutylacetonicum DSM14923	Starch (10g/L)	37	6.5	2772 mL/L ,264.3 mL/g,			(Singh et al., 2019)
C. hydrogenum CUEA01	Starch (10g/L)	37	8	3057 mL/L, 398 mL/g	2.94	127	This study

Microorganism	Substrate	Temperature (°C)	pH	Cumulative H_2 yield	H_2 yield (mol/mol)	HPR (mL/L/h)	Ref.
Clostridium sp. strain X53	Xylan (10 g/L)	40	6	1,254 mL/L		240	(Taguchi et al., 1996)
Clostridium strain BOH3	Xylan (30 g/L) in RCM	35	6.8	980 mL/L			(Rajagopalan et al., 2014)
C. saccharoperbutylacetonicum DSM 14923	Xylan (15g/L)	37	6.5	216 mL/ g xylan			(Singh et al., 2019)
C. beijerinckii YA001	Xylan (10 g/L)	40	8	83.5 mL/g xylan		47.8	(An et al., 2014)
C. hydrogenum CUEA01	Xylan (10g/L)	37	8	1265 mL/L, 217 mL/g	1.34	53	This study
C. pasteurianum MTCC 116 (ATCC6013)	Glycerol (crude 7.4 g/L)	36	6.7	790 mL/L	0.627		(Sarma et al., 2016)
C. pasteurianum MTCC 116 (ATCC6013)	Glycerol (crude 7.4 g/L)	36 (Ultrasound assisted)	6.7		0.89		(Sarma et al., 2017)
C. beijerinckii DSM791	Glycerol (110 mM)	37	7.5		1.21		(Sarma et al., 2016)
C. butyricum INET1	Glycerol (COD=10 g/L)	35	7	678 mL/L	0.67	47	(Yin & Wang, 2017)
C. butyricum (NRRL B-41122)	Glycerol (crude 17.5 g/L)	36	6.5	377 mL/L			(Pachapur et al., 2016)
C. pasteurianum CH4	Glycerol (10 g/L)	35	7		0.41	257	(Lo et al., 2013)
C. hydrogenum CUEA01	Glycerol (10 g/L)	37	8	3009 mL/L, 394 mL/g	1.39	63	This study

(Srimawong & Chulalaksananukul, 2022)

Table IV-10 compares the H_2 production by CUEA01 from various carbon sources used in this study to that observed in batch fermentation by other *Clostridium* species. The pH range for the H_2-producing *Clostridium* species was 5-8.5, with most of them preferring pH values between 5.0 and 7.0 and being intolerant of high pH (Yin & Wang, 2017). The optimum pH for CUEA01 in this report was 8 and it

produced H_2 in alkaline broth up to pH 12. This implies that it ought to be possible to use CUEA01 to produce H_2 from a waste with a relatively high pH. A high pH feedstock would eliminate the need for substrate pretreatment and the risk of contamination by alkali-intolerant species.

The normal optimum temperature for *Clostridium* spp. incubation is 37 ℃, which is also the temperature for CUEA01. Nonetheless, CUEA01 exhibited promising H_2 production performance at room temperature (15-40 ℃), indicating that it could be used without a temperature control unit. CUEA01 had a relatively high H_2 yield and HPR when compared to other *Clostridium* spp. that used the same carbon source for H_2 fermentation. Although the CHP and H_2 yield from xylose and xylan fermentation were significantly lower than the obtained value from other H_2-producing *Clostridium* spp., the CHP could be improved further by optimizing additional factors such as the type of nitrogen source, headspace ratio, fermentation media, inoculation ratio, or shaker incubator rpm.

For instance, Rajagopalan improved the culture media for xylan derived H_2 production by *Clostridium* sp. strain BOH3. They stated that the CHP increased from 980 mL/L to 1780 mL/L when an optimized culture medium (OCM) was used in place of Reinforced Clostridial Medium (RCM). Additionally, there was an increase in xylanase activity in the OCM (Rajagopalan et al., 2014). The optimal conditions for a specific substrate need to be determined for effective expression of the xylanase gene and xylanase activity.

4.4.6 H_2 fermentation from industrial by-products and agricultural residues

To assess the capacity of CUEA01 to generate H_2 from agro-industrial wastes, SM, CP, and RS were chosen for use as substrates. The achievements were shown in Fig. IV-15 The CUEA01 could produce H_2 from SM with a high COD value (up to 94,940 mg/L) and gave the highest CHP, H_2 yield, and COD removal efficiency (%) from SM50X, with values of 4639 mL/L (190 mmol H_2/L), 2443 mL/g COD, and 33.6%, respectively. The value was found to be remarkably considerable when compared to the previous study, which found that batch fermentation of SM with *C. butyricum* W5 could produce 73 mmol H_2/L of the gas (Wang et al., 2008). Unexpectedly, despite having a low HPR value, this species can produce more H_2 from complex organic waste than simple sugar. The accessibility of bacteria to digest substrate is impacted by the complexity of substrate forms, which also promote a longer exponential growth phase during which more H_2 is produced and, ultimately, results in a slower product inhibition. Additionally, a variety of cell-based enzymes' ability to work together synergistically to digest the substrates is altered by their complex composition. This offers a variety of nutrients that support H_2 evolution and cell growth.

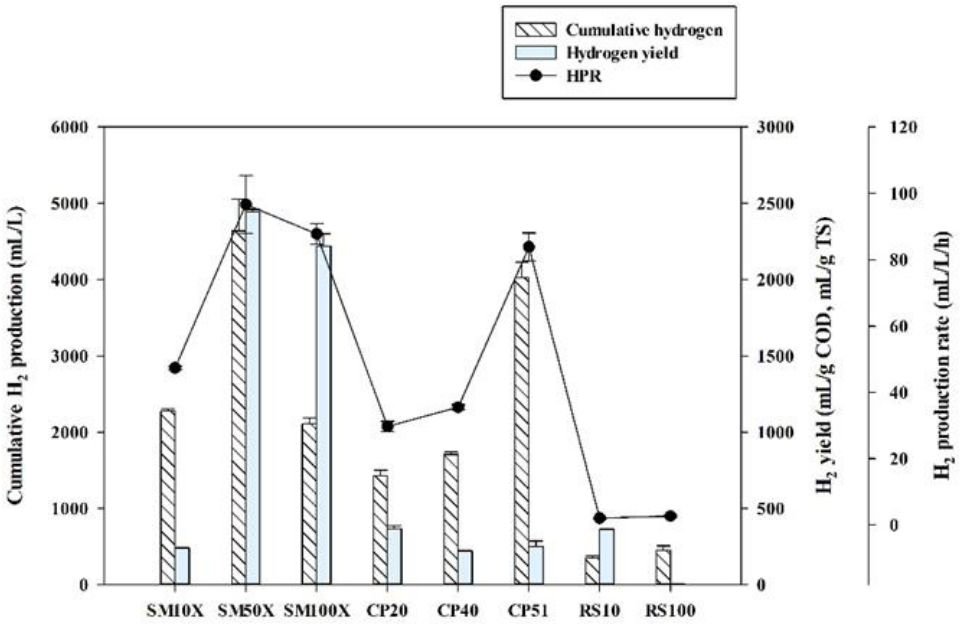

(Srimawong & Chulalaksananukul, 2022)

Figure IV-15 Characteristic of H_2 production by *C. hydogenum* strain CUEA01 utilizing different industrial by-products and agricultural residues.

Data are shown as the mean ± SD. *H_2 yield were calculated from mL H_2/g TS_{added} or g COD_{added}.

Additionally, CUEA01 was able to utilize CP and generate H_2 from CP51 with a maximum CHP and H_2 yield of 4024 mL/L and 402 mL/g TS, respectively. This is comparable to the CHP of 760 mL/L produced by a thermophilic consortium of different types of H_2-producing and hydrolytic bacteria (Pason et al., 2020). Thus, it can be seen that CUEA01 can digest complex materials at least as efficiently as a mixed culture. Nevertheless, only 453 mL/L and 38.47 mL/g TS from RS100 and RS10 were produced from RS using CUEA01, which was most likely because CUEA01's carboxymethyl cellulase (CMCase) or endoglucanase (EC 3.2.1.4) function was insufficient. The CMCase helped break down a large unit of cellulose into smaller

units before other enzymes could access and digest it (Olukunle et al., 2021). Co-culturing CUEA01 with a CMCase-producing strain can help with this, as can pretreating the substrate before being used. However, as mentioned by Survase et al. (Survase et al., 2020), some RS components, like lignin, may be toxic to cells.

4.5 SW1S: *Clostridium felsineum* strain CUEA03

4.5.1 Characteristics of *C. felsineum* strain CUEA03

4.5.1.1 Morphological characteristics

Light microscopy and SEM were used to investigate the cellular morphology of strain CUEA03. The strain was observed to be Gram-positive, rod-shaped bacteria with dimensions of 0.5–1, and 3–4 m, respectively (Fig. IV-16). A raised elevation, an undulating margin, and an orange color were all features of the colonies that were grown on BFM (Srimawong & Chulalaksananukul, 2023).

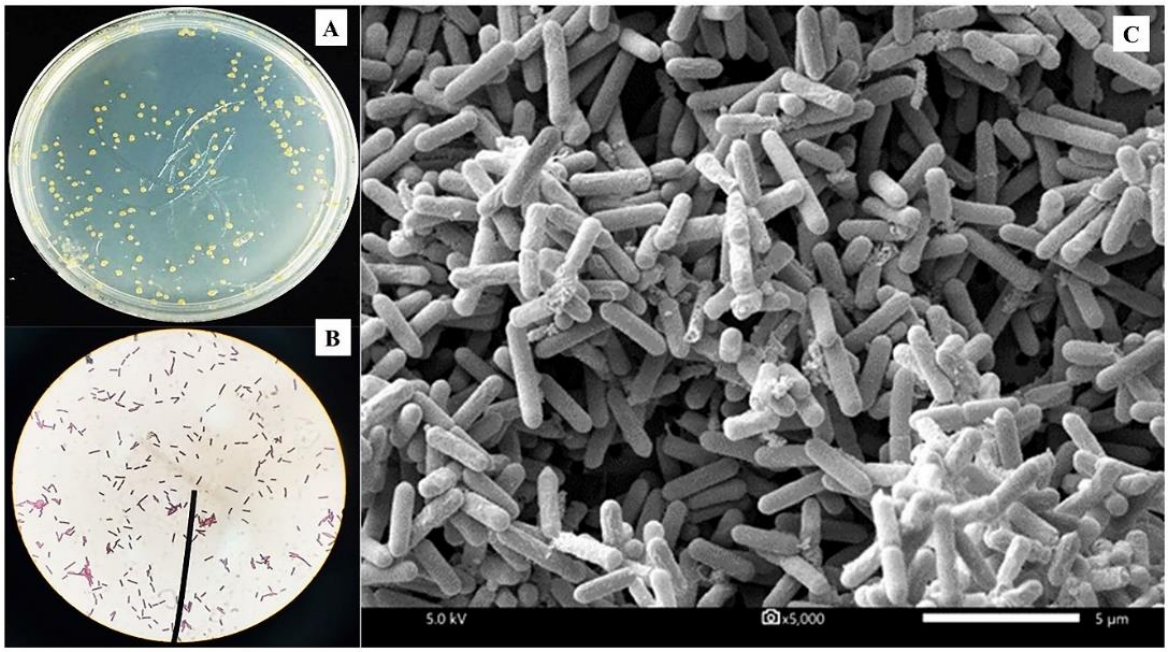

(Srimawong & Chulalaksananukul, 2023)

Figure IV-16 *C. felsineum* strain CUEA03 morphology (A) colonies, (B) Gram staining under light microscopy, and (C) SEM micrograph at 5,000X after growth on basal medium.

4.5.1.2 Chemical characteristics

Table IV-12 illustrates the findings of comparing the chemical properties of stain CUEA03 with those of related species. This strain could utilize glycerol, D-mannose, L-arabinose, starch, and a number of other carbon sources.

4.5.1.3 Genotypic characteristics

CUEA03 was found to be more than 98% similar to three species based on 16S rRNA gene sequence analysis*: C. felsineum, C. roseum, and C. aurantibutyricum*. As a consequence, WGS was used to assess all of CUEA03's nucleotide sequences and compare them to other species, as well as to analyze CUEA03's genotypic

characteristics. This WGS project was submitted to DDBJ/ENA/GenBank with the accession JAHWDM000000000. Version JAHWDM010000000 is described in this paper.

4.5.2 The WGS and genome assembly

This assembled genome had 147 contigs comprising 5,081,113 bp and a GC content of 29.76%. Table IV-11 and Table IV-13 summarize the assembly details and annotated genome features. According to the WGS, CUEA03 has closed to three species: *C. felsineum, C. roseum, and C. aurantibutyricum* with an ANI of over 97%. Additionally, a comparison of the DDH, GC content, and biochemical characterization reveals that these three nominate species are actually the same species, with a high DDH percentage (more than 80%) and a similar percentage of GC (as indicated in Table IV-11 and Table IV-12). The results of genome alignment between CUEA03 and the nearest species also clearly demonstrated the similarity between CUEA03 and three of those species, as shown in Fig. IV-17. There are several locally collinear blocks (LCB) that clearly separate CUEA03 from *C. acetobutyricum*, while CUEA03 and three other species share a large number of homologous LCBs (shown in the same color in Fig. IV-17). In acknowledgment of the discoverers, we assigned the CUEA03 species *C. felsineum* a name following the first announcement. Four strains of three different species were compared using ANI, and the results showed 98–100% identity, confirming that all three are the same species (Poehlein et al., 2017). It has been noted that some strains of this species can produce H_2. But only a small number of strains have been studied.

Table IV-11 A comparison of genotypic features of CUEA03 with its relative species.

Microorganism	ANI (%)	Aligned (%)	Size (bp)	DDH (%)	Contigs	GC (%)	Accession Number
Clostridium sp. CUEA03	-	-	5,081,113	-	147	29.76	JAHWDM010000000
Clostridium felsineum DSM 794	98.03	84.83	5,178,654	84.00	100	29.92	LZYT00000000.1
Clostridium roseum DSM 7320	98.11	84.65	5,067,725	85.70	124	29.80	LZYV00000000.1
Clostridium aurantibutyricum DSM 793	97.89	79.04	4,922,827	87.65	221	29.87	LZYW00000000.1
Clostridium acetobutylicum GXAS18-1	80.98	51.19	3,796,049	32.00	64	-	JRWL00000000.1

(Srimawong & Chulalaksananukul, 2023)

Table IV-12 Comparison of CUEA03 biochemical characteristics and its relative species

Bacteria	CUEA03	*C. felsineum* (3 strains) (Lund et al., 1981)	*C. roseum* C (Avcı et al., 2014)	*C. aurantibutyricum* NCIB 10659 (Lund et al., 1981)	*C. acetobutyricum* ATCC 824 (X. Zhao et al., 2017)
Colony color	Yellow/orange	Yellow/brown	Yellow/orange	Pink/orange	White
NaCl (g/L)	0–30	nd	nd	nd	nd
pH	4–13	nd	nd	nd	nd
Temperature (°C)	20–40	19–41	nd	14-43.5	nd
Cell size (µm)	0.5–1, 3–4	nd	nd	nd	nd
Glucose	+	+	+	+	+
Lactose	+	+	+	+	-
Sucrose	+	+	+	+	-
Fructose	+	+	+	+	nd
Maltose	+	w	nd	+	nd
Galactose	+	+	+	+	nd
Arabinose	+	+	+	+	nd
Xylose	+	+	+	+	nd
Mannose	+	+	nd	+	+
Starch	+	+	+	+	nd
Raffinose	+	w	-	+	nd
Rhamnose	-	+	+	-	-
Salicin	+	+	nd	+	+

Bacteria	CUEA03	*C. felsineum* (3 strains) (Lund et al., 1981)	*C. roseum* C (Avcı et al., 2014)	*C. aurantibutyricum* NCIB 10659 (Lund et al., 1981)	*C. acetobutyricum* ATCC 824 (X. Zhao et al., 2017)
Glycogen	nd	nd	nd	+	nd
Inositol	w	-	nd	-	nd
Inulin	+	w	nd	-	nd
Mannitol	+	-	+	-	+
Melezitose	-	-	nd	-	nd
Melibiose	nd	-	-	+	nd
Ribose	nd	-	nd	+	nd
Trehalose	nd	-	nd	-	-
Dextrin	nd	nd	+	nd	nd
Cellulose	w	nd	-	nd	nd
Esculin	-	nd	nd	+	nd
Amygdalin	nd	-	nd	-	nd
Glycerol	W	-	nd	-	nd
Sorbitol	-	-	nd	-	+
Cellobiose	+	+	+	+	+
Gelatin liquefaction	nd	+	nd	+	nd

(Srimawong & Chulalaksananukul, 2023)

+, Positive or present; W, weakly positive; –, negative or absent; nd, no data

C. felsineum strains were NCIB 10690, NCIB 9539 and NCIB 9540

Table IV-13 Assembly details and annotated genome features of *C. felsineum* strain CUEA03

Parameters	Number
Contigs	147
GC Content	29.76
Plasmids	0
Contig L50	16
Genome length	5,081,113 bp
Contig N50	95,115
Chromosomes	0
CDS	4,797
tRNA	67
Repeat regions	47
rRNA	1
Partial CDS	0
Miscellaneous RNA	0
CRISPR spacer	40
CRISPR repeat	47
CRISPR region with repeat	7
CRISPR-associated protein, Cas6	1
Transposase	14

CDS: Coding sequence

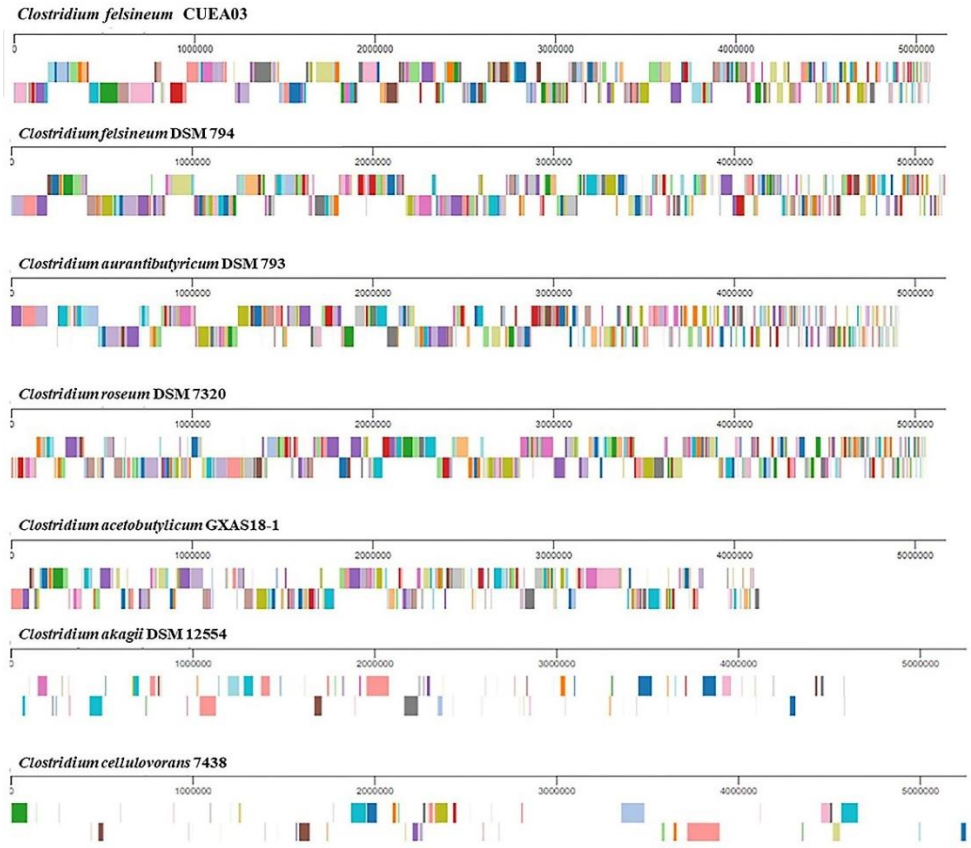

(Srimawong & Chulalaksananukul, 2023)

Figure IV-17 A comparison of the genomes of *C. felsineum* strain CUEA03 and related species reveals 248 locally collinear blocks (LCB) of CUEA03 that show homologous areas shared by all seven species. Each chromosome was drawn horizontally, and homologous LCBs in each genome were colored the same. The white areas within each LCB represent locations with low similarity.

4.5.2.1. Phylogenetic analysis

According to phylogenetic analysis, *C. acetobutylicum* was the most closely related species (Fig. IV-18). According to reports, this species is employed to generate large

amounts of H_2 from a variety of carbon sources (El-Dalatony et al., 2022; Morales-Martínez et al., 2020).

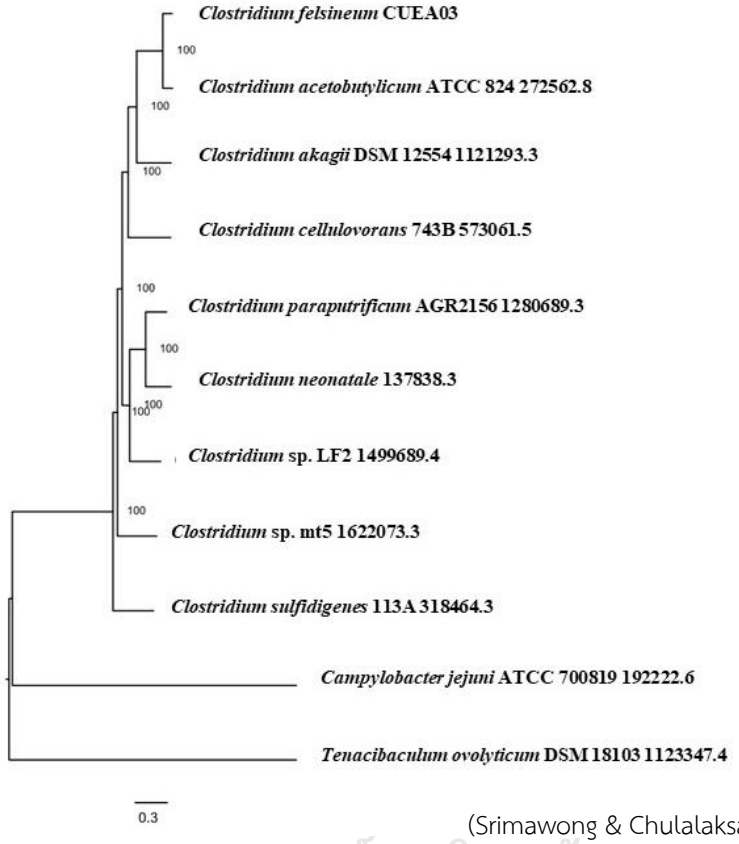

(Srimawong & Chulalaksananukul, 2023)

Figure IV-18 A maximum likelihood phylogenetic tree based on genomic data combining alignments of amino acid and nucleotide coding sequences using RAxML shows the relationship between CUEA03 and other species.

4.5.3 Genome annotation

Fig. IV-19 depicts the findings of an annotated gene. The genome of CUEA03 contains a wide variety of synergistic genes in each subsystem that carry out various cellular functions.

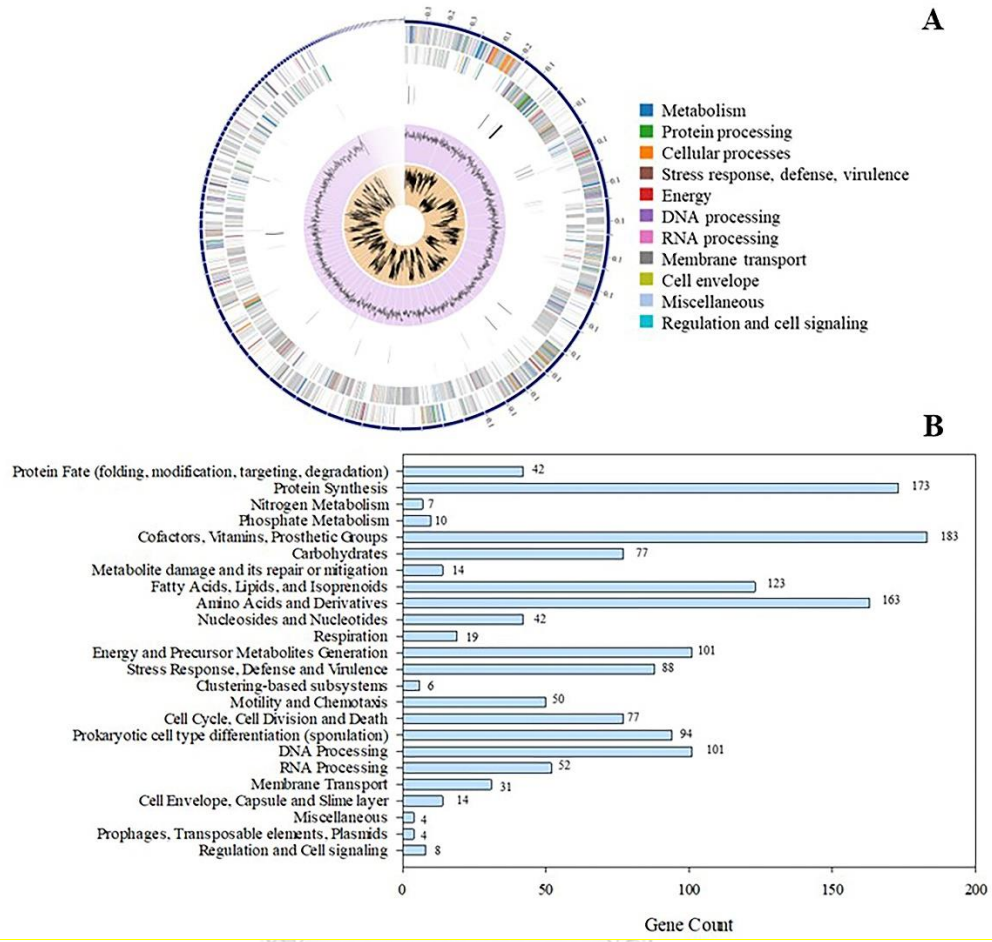

(Srimawong & Chulalaksananukul, 2023)

Figure IV-19 Genomics features of CUEA03.

A: Circular schematic illustration of the distribution of the genome annotations of the CUEA03 chromosome. Contigs, the coding sequence (CDS) on the forward strand, the CDS on the reverse strand, RNA genes, CDS with homology to known antimicrobial resistance genes, CDS with homology to known virulence factors, GC content, and GC skew have been part of this, listed from outer to inner rings. Each subsystem's CDS are color coded on the forward and reverse strands; B: The genes count of CUEA03 genome in each subsystem.

4.5.3.1 Predicted enzymes in intermediary metabolism pathways for carbon utilization.

Patrick's annotation of a gene Combining KEGG and SwissProt gene analyses revealed that this strain has a large number of genes involved in carbon utilization (Table IV-14), as shown and discussed in Fig. IV-20. Numerous genes were clearly involved in the utilization pathways of various carbon sources, such as pectin, starch, lactose, arabinogalactan, arabinan, arabinoxylan, cellulose, glycerol, rhamnose, fructan, and sucrose, and many others. This clearly shows that when combined with a variety of substrates, including industrial, food, and agricultural wastes, CUEA03 can be used as a potential H_2 producer.

Table IV-14 Predicted enzymes in the metabolic pathways of *C. felsineum* strain CUEA03 for carbon source utilization.

EC code	Gene symbol	Enzymes	Number encoded in genome
EC 3.2.1.55	CA_C3436	alpha-L-arabinofuranosidase	1
EC 3.2.1.55	CA_C1529	alpha-L-arabinofuranosidase II	1
EC 3.2.1.55	CA_P0120	Arabinoxylan arabinofuranohydrolase	1
EC 3.2.1.23	CA_C2514	beta-galactosidase	4
EC 3.2.1.99	CA_C0577	Arabinan endo-1,5-alpha-L-arabinosidase	1
EC 3.2.1.85	CEA_G2970	6-phospho-beta-galactosidase	1
EC 3.2.1.22	Tmath_1705	alpha-galactosidase	1
	CUB90_14755	Arabinogalactan endo-1,4-beta-galactosidase	2
	CA_C3032	Galactose mutarotase related enzyme	2
	CA_C0836	probably beta-D-galactosidase	1
EC 3.2.1.40	CLPUN_12250	alpha-L-rhamnosidase	4
EC:3.2.1.78	CEA_G0343	Beta-mannanase (Mannan endo-1,4-beta-mannosidase)	1
EC 3.2.1.176	CA_C0561	Cellulose 1,4-beta-cellobiosidase (reducing end)	1
EC 3.2.1.91	CA_C0911	Cellulose 1,4-beta-cellobiosidase (non-reducing end)	1
EC 3.2.1.4	CA_C0913	beta-1,4-glucanase (cellulase)	6
EC 3.2.1.4	CA_C2556	Endoglucanase D precursor	1
EC 3.2.1.21	FHS18_003002	beta-glucosidase	2
EC 3.2.1.86	CA_C1084	6-phospho-beta-glucosidase	10
EC 3.2.1.1	CEA_P0166	Alpha-amylase	1
	CUB90_18740	alpha-glucosidase	4
EC 3.2.1.4	CEA_G0220	Endoglucanase M	1
EC 3.2.1.20	Cspa_c48820	Alpha-glucosidase	3
EC 3.2.1.21	Tlet_1036	beta-glucosidase	2
EC 4.2.2.2	CEA_G3390	Pectate lyase	4
	CEA_P0055	Pectate lyase, secreted, polysaccharide lyase family	2
EC 3.1.1.11	BCS7_15440	Pectinesterase	2
	CA_C0359	Rhamnogalacturonides degradation protein RhiN	1
EC 3.2.1.15	CA_C0355	Polygalacturonase (Pectinase)	1
	SMB_G3413	Possible pectin degradation protein (sugar phosphate isomerase family)	1
EC 3.2.1.82	CA_C3684	Exo-poly-alpha-D-galacturonosidase	3
EC 3.2.1.41	CEA_G2688	Pullulanase	1
EC 3.2.1.135	CEA_G2695	Neopullulanase, pullulanase II	1
EC 3.2.1.177	CA_C1085	alpha-xylosidase	1
	CA_P0114	Possible beta-xylosidase, family 43 of glycosyl hydrolases	1
	CA_P0117	Possible beta-xylosidase diverged, family 5/39 of glycosyl	1

EC code	Gene symbol	Enzymes	Number encoded in genome
		hydrolases and alpha-amylase C (Greek key) C-terminal domain	
EC 3.2.1.37	CEA_G3456	Xylan 1,4-beta-xylosidase	3
EC 3.2.1.8	CEA_P0070	Endo-1,4-beta-xylanase	3
	CTDIVETGP_2135	Putative xylanase	1
EC 3.2.1.8	CUB90_05905	Endo-1,4-beta-xylanase A precursor	2
EC:3.2.1.8	CEA_P0115	Xylanase, glycosyl hydrolase family 10	2
EC 3.2.1.136	SMB_P116	Glucuronoarabinoxylan endo-1,4-beta-xylanase	1
	CEA_P0118	Possible xylan degradation enzyme (glycosyl hydrolase family 30-like domain and Ricin B-like domain)	1
	CEA_G0368	Predicted xylanase/chitin deacetylase	1
EC 3.2.1.14		Chitinase	1
EC 3.2.1.80	FruA	Fructanase	
EC 3.1.1.3	CA_C1028	Lipase precursor	1
	CLC_2129	Esterase/lipase	1
	CA_C3024	Lipase/Acylhydrolase with GDSL-like motif	1
EC 3.1.1.3	Cspa_c56810	Triacylglycerol lipase	1
	CA_C0816	Lipase-esterase related protein	1

(Srimawong & Chulalaksananukul, 2023)

*Gene symbol obtained from amino acid blast on databases

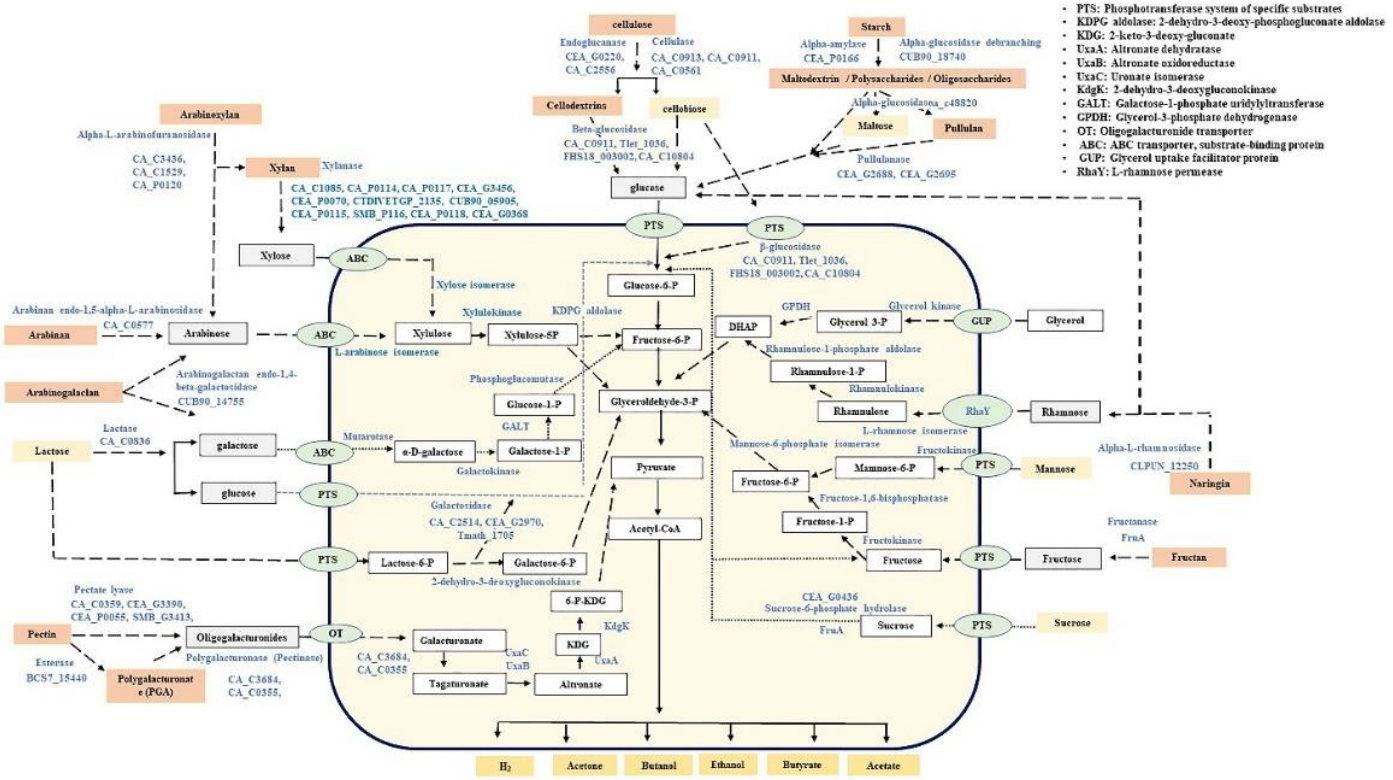

(Srimawong & Chulalaksananukul, 2023)

Figure IV-20 Predicted enzymes for carbon source utilization pathways in the CUEA03 genome depicts the expected enzyme encoded from CDS genes in pathways that convert various carbon sources into fermentation products.

4.5.3.2 Predicted enzymes involved in H_2 production and stress response.

As shown in Table IV-15, strain CUEA03 contains genes involved in H_2, including [NiFe] hydrogenase, formate dehydrogenase H (EC 1.2.1.2), [FeFe] hydrogenase (EC 1.12.7.2), periplasmic [FeFe] hydrogenase (EC 1.12.7.2), electron bifurcating butyryl-CoA dehydrogenase (EC 2.3.1. (EC 1.97.1.4). This indicates that this strain has three possible ways to produce H_2: (i) pyruvate: formate lyase (PEL), pyruvate: ferredoxin oxidoreductase (PFO), (ii) ferredoxin-dependent hydrogenase, and (iii) NADPH regeneration (Srimawong & Chulalaksananukul, 2022; Zhang et al., 2020). As previously documented, *Clostridium* spp. are often only found in [FeFe] hydrogenase, including *C. butyricum* DSM 10702 (Accession Number GCA 000409755.1), which is known to produce a substantial quantity of H_2 yield (Calusinska et al., 2010). This species is deficient in [NiFe] hydrogenase and formate dehydrogenase H, two essential enzymes involved in the production of H_2 in facultative anaerobic bacteria like *E. coli.* These enzymes are involved in the pyruvate: ferredoxin oxidoreductase (PFO) and pyruvate: formate lyase (PEL) pathways (Trchounian et al., 2021). As a result, it would almost certainly contribute to encouraging a high level of H_2 evolution. However, more research is required to investigate the specific process. It was discovered that CUEA03 contains genes for alkaline shock protein, 2-haloalkanoic acid dehalogenase (EC 3.8.1.2), Cof-like hydrolase, heat shock protein, cold shock protein, and other stress response-related

genes that help the organism withstand and adapt to unfavorable environmental conditions like high pH and salinity. Furthermore, the spores can withstand extreme environments.

Table IV-15 Predicted crucial enzymes in the H_2 and butanol production of *C. felsineum* strain CUEA03.

EC code	Enzymes	Number encoded in genome
H_2 producing related enzymes		
EC 1.12.7.2	[FeFe] hydrogenase	1
	[FeFe]-hydrogenase maturation protein HydF	1
	[FeFe]-hydrogenase maturation protein HydE	2
	[FeFe]-hydrogenase maturation protein HydG	1
EC 1.12.7.2	[FeFe] hydrogenase, cytoplasmic, one subunit form	1
EC 1.12.7.2	Periplasmic [FeFe] H2ase large subunit	2
	[NiFe] hydrogenase metallocenter assembly protein HypF	1
EC 1.2.1.2	Formate dehydrogenase H	1
EC 2.3.1.54	Pyruvate formate-lyase	1
	Pyruvate formate-lyase activating enzyme	1
Butanol production related enzymes		
EC 1.1.1.-	NADH-dependent butanol dehydrogenase	4
EC 1.2.1.10/EC 1.1.1.1	Acetaldehyde dehydrogenase / Alcohol dehydrogenase	2
	Electron bifurcating butyryl-CoA dehydrogenase (NAD+, ferredoxin)	2
	Electron bifurcating butyryl-CoA dehydrogenase, electron transfer flavoprotein alpha	2
EC 1.3.99.2	Butyryl-CoA dehydrogenase	1

(Srimawong & Chulalaksananukul, 2023)

4.5.4 Optimization of H_2 production from *C. felsineum* strain CUEA03

The development conditions/medium were optimized for H_2 production to assess CUEA03's ability to produce more H_2. The various kinetic parameters were observed on modified DSM640 media under various growth conditions.

4.5.4.1 Effect of initial pH

At pH 9, the highest CHP (2449 mL/L), HPR, and cell growth were obtained (Fig. IV-23). As a consequence, CUEA03 was classified as a facultative alkaliphile, which differs from the other H_2 producers, which are typically slightly acidophile-neutrophile, favoring a pH range of 5.2–7.4 (Lertsriwong & Glinwong, 2020; Lo et al., 2010). Ntaikou suggests that H_2 evolution happens throughout acidogenesis pathways to dispose of the electrons released during glycolysis (Ntaikou, 2021). A lower pH after the fermentation period is the result of an acidic buildup in the broth. It is reasonable to assume that a high initial pH would contribute to a longer period of time until the pH drops to a level where H_2 production is prevented (pH less than 4), as previously mentioned (da Silva Mazareli et al., 2021). When the initial pH was raised above the optimum, cell growth and H_2 evolution were substantially reduced, which was attributed to protein breakdown. Furthermore, the influence of OH^-, which consumes H^+, and the inactivation of enzymes were addressed to reduce H_2 production yield and cell death (Tan et al., 2018).

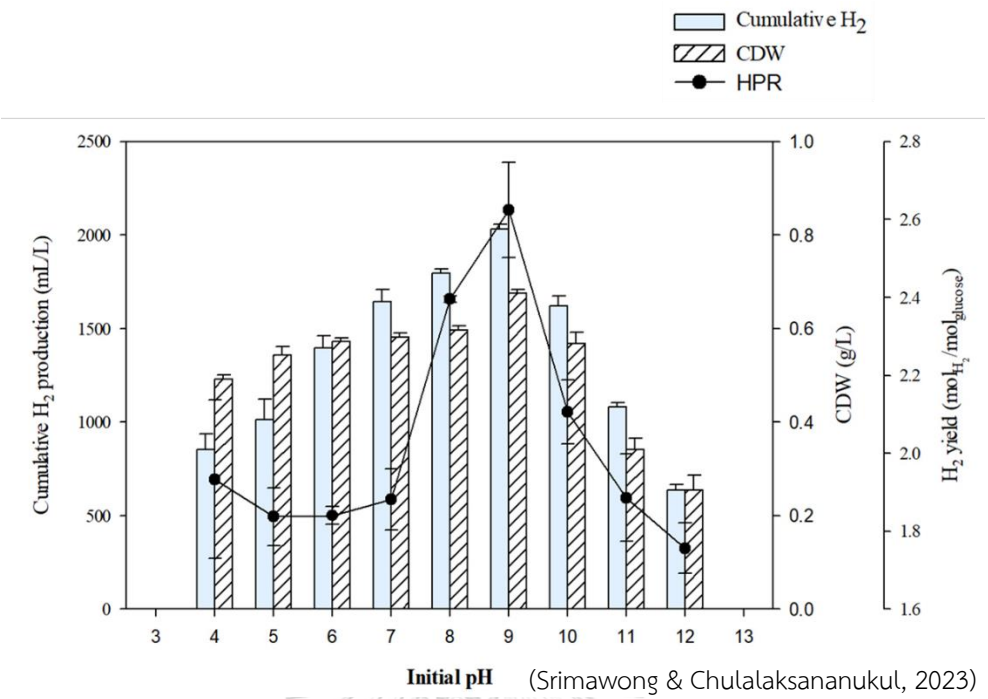

(Srimawong & Chulalaksananukul, 2023)

Figure IV-21 H_2 production characteristics of *C. felsineum* strain CUEA03 under different initial pH.

*37 °C, NaCl concentration of 0.9 g/L, and initial glucose concentration of 10 g/L. Data are shown as the mean ± SD.

4.5.4.2 Effect of incubation temperature

CUEA03 was capable of growing strongly and produce H_2 at temperatures ranging from 20-40 °C within the evaluated cultivation temperature range of 15-45 °C Fig. IV-24, with a maximum CHP of 2993 mL/L and robust cell growth at 30 °C. In contrast, reduced H_2 yield and cell development were observed at 15 °C and 45 °C.

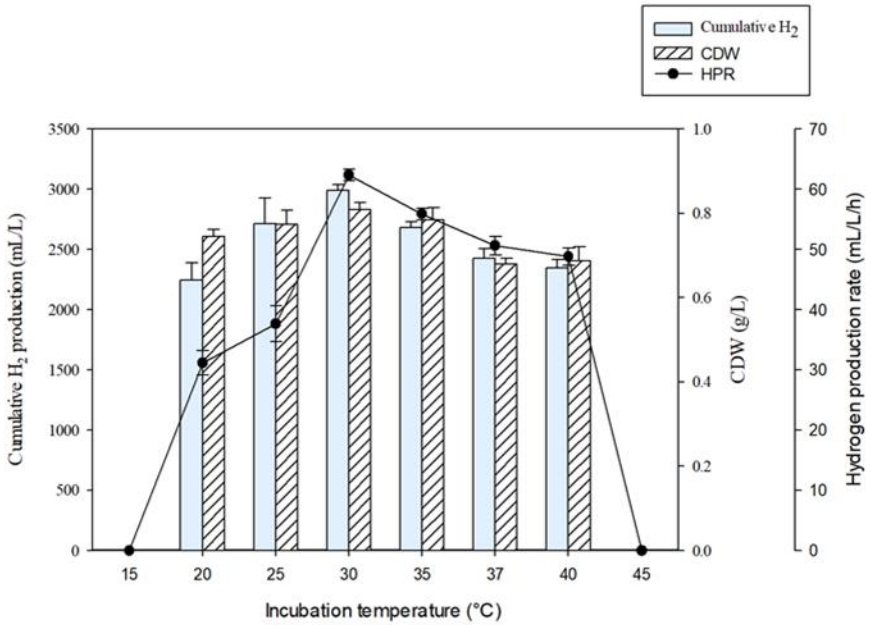

(Srimawong & Chulalaksananukul, 2023)

Figure IV-22 H_2 production characteristics of *C. felsineum* strain CUEA03 under different incubation temperature.

*Initial pH of 9, NaCl concentration of 0.9 g/L, and initial glucose concentration of 10 g/L. Data are shown as the mean ± SD.

4.5.4.3 Effect of NaCl concentration

CUEA03 was isolated from mangrove sediments which were subjected to various NaCl concentrations. As a result, the impact of NaCl content was studied. The HPR definitely dropped as the NaCl content increased, supporting the CHP (Fig. IV-25). CUEA03, on the other hand, thrived up to a NaCl concentration of 25 g/L but not higher than 30 g/L. It's interesting to note that the cell growth was not significantly correlated with the H_2 production, in contrast to the effects of pH and incubation temperature. This was addressed by implying that increasing NaCl concentrations would damage hydrogenase enzymes. The metalloenzymes [NiFe] hydrogenase and

[FeFe] hydrogenase, which contained metal ions at active sites, were recognized to be important in the formation of H_2 (Peters et al., 2015). Excess salt increased ionic strength and so hindered the action of the metalloenzymes. However, the mechanism of NaCl inhibition of H_2 evolution remains unknown and must be researched further. Furthermore, most endospore forming HPB are unable to withstand high NaCl concentrations. As a result of its relative salt tolerance, CUEA03 can be applied to wastes with a high NaCl concentration or substrates derived from marine sources. A recent study revealed that *C. butyricum* TM-9A, a sea isolate, could grow and produce H_2 at NaCl concentrations as high as 20 g/L but that 0 g/L was the optimum concentration (Junghare et al., 2012).

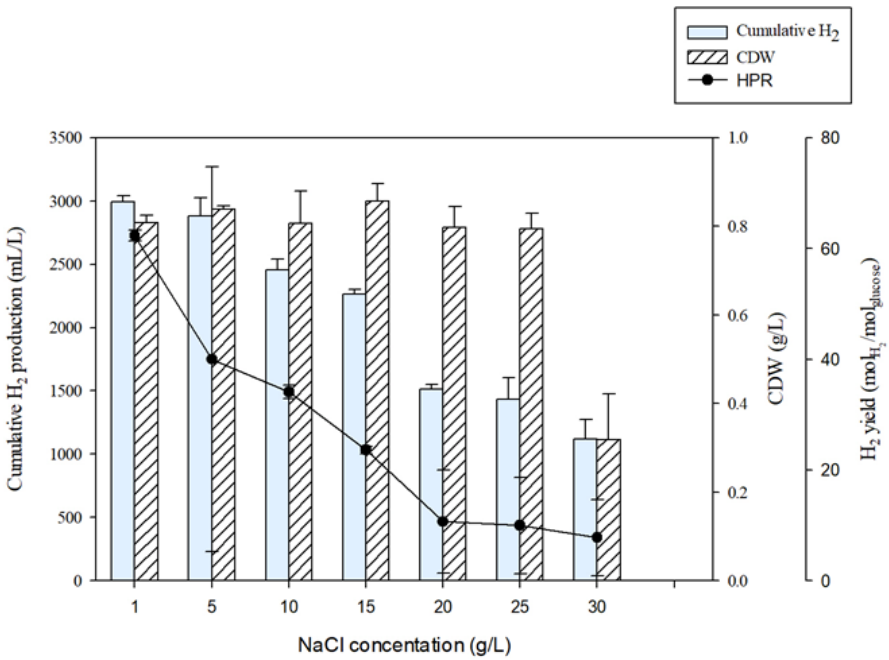

(Srimawong & Chulalaksananukul, 2023)

Figure IV-23 H_2 production characteristics of *C. felsineum* strain CUEA03 under different NaCl concentration.

*Initial pH of 9, incubation temperature of 30°C, and initial glucose concentration of 10 g/L. Data are shown as the mean ± SD.

4.5.4.4 The effect of initial glucose concentration

The ideal glucose concentration for H_2 generation was evaluated over the range of 5–100 g/L. Strain CUEA03 was able to grow and produce H_2 at glucose concentrations across the studied range as shown in Fig. IV-26. 35 g/L of initial glucose was found to be the optimal concentration for H_2 production and cell development, and this resulted in maximum CHP and HPR of 5425 mL/L and 75 mL/L/h, respectively. The lag period was extended when the initial glucose concentration was higher than 10 g/L, resulting in a lower HPR. Increasing the glucose concentration, meanwhile, allows the cells to access glucose and enhances the H_2 generation output. On the other hand, increased glucose concentrations beyond the optimum caused a progressive decline in CHP and cell growth, which was most likely caused by this strain's restricted substrate uptake or substrate inhibition (Cai et al., 2019). Nguyen et al. (2008) discovered that *Thermotoga* spp. had an optimal CHP at an initial glucose concentration of less than 12.5 g/L (Nguyen et al., 2008), Moreover, the most of HPB can survive at low initial glucose concentrations, and previous studies revealed that COD stress had a serious effect on H_2 producer by fermentation (Cai et al., 2021). This shown that CUEA03 can resist high sugar concentrations, assuming large osmotic pressures. Therefore, this strain has

the potential to greatly decrease organic waste, notably COD, by producing H_2 from organic waste.

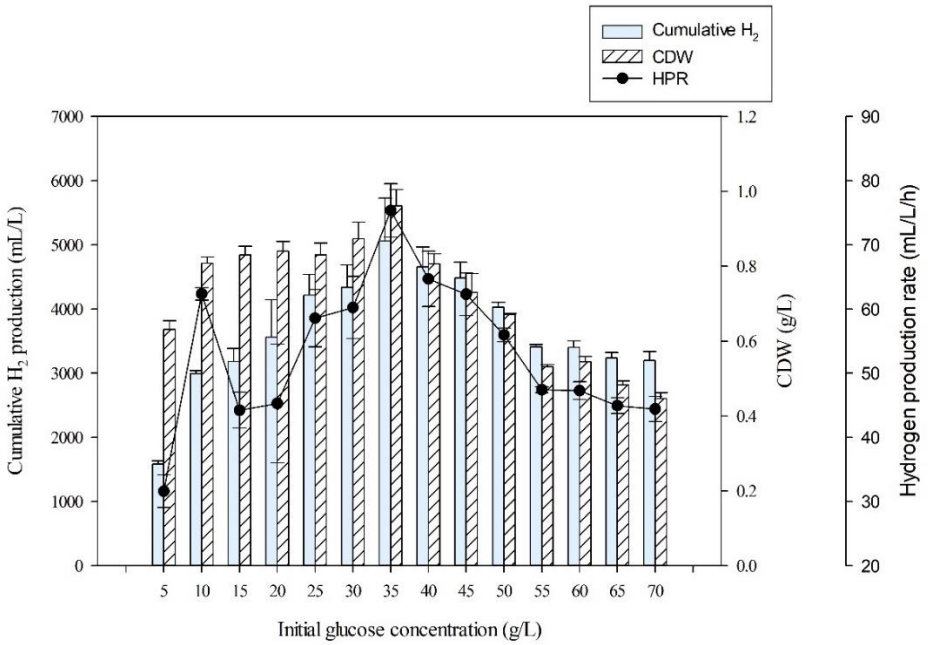

(Srimawong & Chulalaksananukul, 2023)

Figure IV-24 H_2 production characteristics of *C. felsineum* strain CUEA03 under different initial glucose concentration.

*Initial pH of 9, incubation temperature of 30°C, and NaCl concentration of 0.9 g/L. Data are shown as the mean ± SD.

4.5.5 H_2 production from various carbon sources by *C. felsineum* strain CUEA03

CUEA03 was able to generate H2 from a variety of carbon sources with a CHP close to the maximum CHP from glucose (5425 mL/L). Fig. IV-27 and Table IV-16 depict the characteristics and kinetics associated with H2 fermentation from various carbon sources. This strain successfully metabolized mannose, lactose, and

cellobiose, which involves cleavage of aldohexose, β–(1,4′) glycosidic linkage of galactose and glucose, and β–(1,4′) glycosidic linkage of two molecules of glucose (Berg et al., 2002).

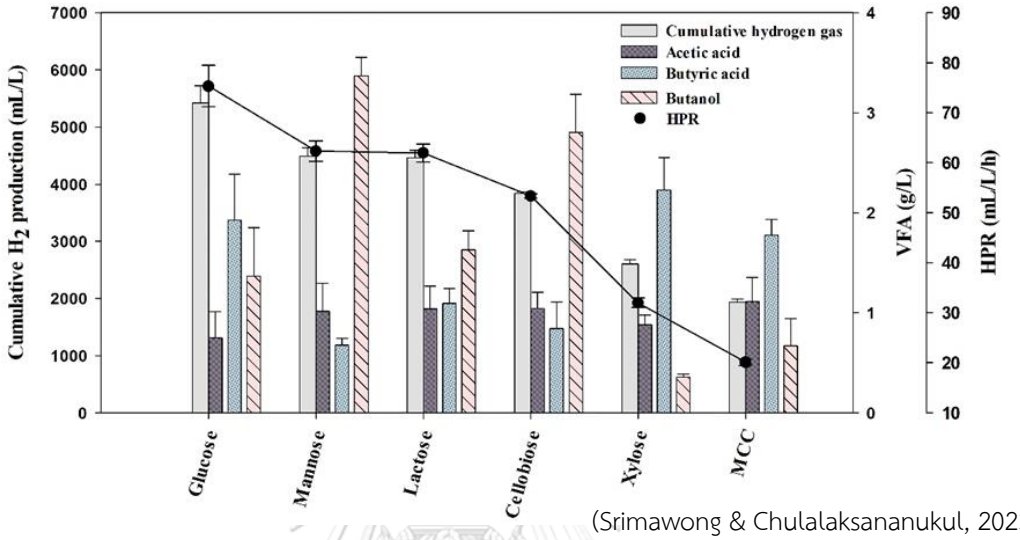

(Srimawong & Chulalaksananukul, 2023)

Figure IV-25 Characteristics of H_2 production by *C. felsineum* strain CUEA03 from various carbon sources.

*At the optimum condition (pH 9, 30 °C, 0.95 g/L NaCl, and 35 g/L initial carbon source concentration). Data are shown as the mean ± SD.

Table IV-16 Kinetic characteristics of H_2 generation by *C. felsineum* strain CUEA03 from various carbon sources.

Carbon sources	CHP (mL/L)	H_2 yield (mol/mol)	HPR (mL/L/h)	Acetic acid (g/L)	Butyric acid (g/L)	Butanol (g/L)	Total VFA (g/L)
Glucose	5425	1.70	75	0.75	1.93	1.37	4.05
Mannose	4490	1.87	62	1.02	0.68	3.37	5.06
Lactose	4463	1.51	62	1.04	1.10	1.63	3.76
Cellobiose	3842	1.40	53	1.04	0.84	2.80	4.69
Xylose	2604	2.48	32	0.88	2.23	0.36	3.47
MCC	1932	2.94	20	1.11	1.78	0.67	3.56

(Srimawong & Chulalaksananukul, 2023)

Butyric acid, acetic acid, and butanol were the main components of the volatile carbonyls generated by CUEA03. However, the fermented products differed depending on the substrate. For example, butyric acid was found to be mainly the liquid product output of glucose fermentation, whereas butanol was mostly produced by mannose, lactose, and cellobiose fermentation. A low butyric content was obtained when mannose, lactose, and cellobiose were used to produce butanol via solventogenesis. Butyric acid produced by the acidogenesis pathway is used in this process (Fonseca et al., 2020). n accordance with previous studies, butanol was produced using a two-stage fermentation method that first produced butyric acid and H_2 through acidogenesis fermentation, subsequently butanol via acetone butanol ethanol (ABE) fermentation (Li et al., 2018). Butyric acid has been shown to play a role in the ABE process (González-Tenorio et al., 2020), and its accumulation could be a result of the longer fermentation time on these substrates (seen with a lower HPR than glucose fermentation, resulting in butanol formation through solventogenesis). However, previous investigations demonstrated that the specific type of substrate had an impact on the fermentation pathway and, consequently, on the fermented products (Yin & Wang, 2017). The poor HPR and production yields of H_2 fermentation from xylose and MCC were caused by the difficulty that organisms face when producing H_2 from these pentose sugars and β–(1,4′) glycosidic linkages of glucose. However, the obtained yields were comparable to those obtained from the fermentation of MCC by a mixed culture of *Clostridia* spp. from a cellulose

enrichment sludge (Zagrodnik et al., 2021). It would be desirable if we could enhance the production technique to extend the H_2 fermentation period, such as by using a fed-batch operation, continuous process, pH control system, or removing the volatile fatty acids.

4.5.6 H_2 production from organic waste by *C. felsineum* strain CUEA03

Through the use of 50x diluted sugarcane molasses as the substrate for the H_2 fermentation, it was shown that CUEA03 could thrive in a high COD medium (sugarcane molasses). Furthermore, it was clear that CUEA03 could utilize the molasses without the addition of a supplementary buffer, nitrogen sources, or trace elements. The maximum CHP was achieved (5187 mL/L; 893 mL/g COD added), indicated that CUEA03 had a good potential for bio- H_2 production by fermentation. However, COD removal efficiency was only 18 %.

4.5.7 Comparison of H_2 production by *C. felsineum* strain CUEA03 with other species.

Batch H_2 production by *C. felsineum* CUEA03 from glucose was compared to that of other producers in the literature (Table IV-17). Depending on the strain or species, the optimum pH and temperature ranged from 6–9.5 and 30–80 °C. The majority of producers employed a substrate with a concentration of 2-10 g/L (da Silva Mazareli et al., 2019; Maintinguer et al., 2017; Mei et al., 2014; Nguyen et al., 2008; Singh et al., 2014; Srimawong & Chulalaksananukul, 2022; Yin & Wang, 2017; Youn et al., 2016) and were inhibited by higher glucose concentrations. Simultaneously, strain CUEA03

exhibited a higher optimal initial glucose concentration (35 g/L) and could generate H_2 with a high CHP over a 5-50 g/L initial glucose concentration range. Nonetheless, the obvious benefit of this strain over other producers was its high CHP yield. Where media quantities were equivalent, CUEA03 clearly generated more H_2 than other strains. Although the yield (with 1.70 $mol_{H2}/mol_{Glucose}$) was relatively small compared to other producers, it proved that the bacteria were effective at utilizing the substrate and could lower the total sugar content in the medium. As a result, it is an excellent option for applying to organic wastes that must have their COD level lowered before being discharged into the environment, as well as for integrating this with the generation of clean energy.

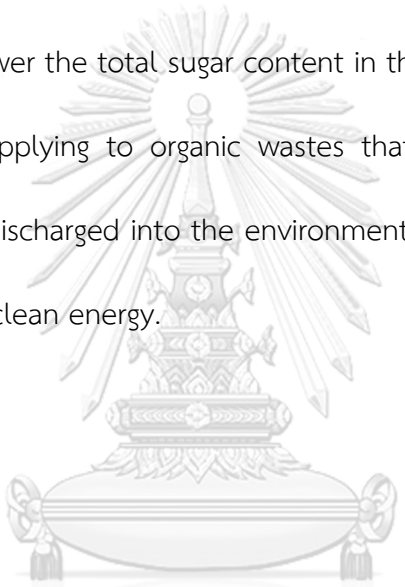

Table IV-17 Comparison of batch fermentation H_2 production between *C. felsineum* strain CUEA03 and other H_2 producing species.

Microorganism	Isolation sources	Substrates	Temperature (°C)	pH	CHP (mL/L)	H_2 yield (mol/mol)	Ref.
Clostridium butyricum INET1	Digested sludge	Glucose (COD 10 g/L)	35	7	2180	2.24	(Yin & Wang, 2017)
Clostridium sp. PROH2	Submarine hydrothermal chimney	Glucose (2g/L)	37	9.5	669	2.71	(Mei et al., 2014)
Clostridium sp. 6A-5	Sludge of Funan sugar mill	Glucose (16 g/L)	43	8	2727	2.50	(Cai et al., 2013)
Clostridium butyricum CWBI 1009	Anaerobic sludge	Glucose (4.3 gCOD/L)	30	7.3	2344	0.58	(Beckers et al., 2010; Calusinska et al., 2015)
Clostridium hydrogenum CUEA01	Mangrove sediment	Glucose (10 g/L)	37	8	3264	3.11	(Srimawong & Chulalaksananukul, 2022)
Enterobacter sp.	Granular sludge	Glucose (2 g/L)	37	7	166	0.80	(Maintinguer et al., 2017)
Enterococcus faecium INET2 (free cells)	Gamma irradiated sludge	Glucose (15 g/L)	35	7	1300	1.16	(Yin & Wang, 2016)
Thermoanaerobacterium thermosaccharolyticum TERI S7	Oil reservoir flow pipeline	Glucose (10 g/L)	55	6.8	1900	2.50	(Singh et al., 2014)
Thermotoga maritima DSM 3109	Geothermally heated sea floors.	Glucose 7.5 g/L)	80	6.5–7.0	883	1.67	(Huber et al., 1986; Nguyen et al., 2008)
Bacillus sp.	Banana waste	Glucose (5 g/L)	37	7	330	-	(da Silva Mazareli et al., 2019)
Klebsiella pneumoniae ECU-15	Anaerobic sewage sludge	Glucose (14g/L)	37	6	1100	1.25	(Niu et al., 2010)
C. felsineum strain CUEA03	Mangrove sediment	Glucose (35 g/L)	30	9	5425	1.70	**This study**

(Srimawong & Chulalaksananukul, 2023)

CHAPTER V

CONCLUSION AND FUTURE PROSPECTS

Endospore-forming HPB were isolated from three different environments: natural environments which including mangroves and hot springs, and industrial wastes from coconut factory. The ability of isolated bacteria to produce H_2 was screened and evaluated. 14 isolated bacteria with a high H_2 producing potential were chosen from a total of 40 isolates for batch H_2 fermentation testing. According to 16S RNA sequences, these isolated bacteria contained ten *Clostridium* species from mangrove sediments and coconut factory waste, along with four *Paenibacillus* species from hot spring sediments. CUEA01 (SW5A) and CUEA03 (SW1S) strains were chosen for further investigation due to a larger relative H_2 production yield than other strains. The genomic data of two species were analyzed using whole genome sequencing, and it was discovered that CUEA01 is a novel species with named as "*C. hydrogenum*" whereas CUEA03 is "*C. felsineum*," which is the same species as "*C. roseum*" and "*C. aurantibutyricum*," and has an ANI of over 97%. Additionally, genomics reveals a predicted enzymes in the metabolic pathways for H_2 production and carbon source utilization which including xylose, xylan, starch, maltose, fructose, galactose, L-arabinose, mannose, glycerol, cellobiose, avicel, and sucrose. Moreover, these two species' genomes also contain a variety of H_2 production-related enzymes including NiFe hydrogenase, and FeFe hydrogenase. These two species can thrive in a variety

of environments (board rang of pH and temperature), according to their biochemical characteristics. Following optimization of the H_2 production conditions for the two species, it was discovered that CUEA01 produced the highest cumulative H_2 yield of 3264 mL/L (3.11 $mol_{H2}/mol_{glucose}$) at 37 °C, pH 8, and 10 g/L of the initial carbon source, while CUEA03 is 5425 mL/L (1.70 $mol_{H2}/mol_{glucose}$) at 72 h of incubation (HPR of 75 mL/L/h) was obtained from an initial glucose concentration of 35 g/L, pH 9, and an incubation temperature of 30 °C. Furthermore, various carbon sources were used as substrate for evaluation of their feasibility to utilize it, which confirmed the presentation of related enzymes in organisms and the results showing that these species can secrete an effective enzyme that can digest various carbon sources to obtain H_2 gas. In addition, industrial by-products and agricultural residues were also employed as pure substrate for them to produce H_2 including sugarcane molasses (SM), cassava pulp (CP), and dried rice straw (RS) and the results show that these species have effective enzymes contrail that help to digest complex forms of substrate. Interestingly, CUEA01 and CUEA03 can directly employ a 50x dilution of sugarcane molasses and yield a CHP of 4639 mL/L and 5187 mL/L, respectively. This suggests that these species have the potential to be used as robust H_2 producers with agro-industrial wastes for the consolidation of the bioprocess of H_2 production. This revealed the potential of employing organic waste for green energy production, which not only reduced the COD of organic wastes but also generated bio-H_2 fuel, which can help fulfill future fuel generation goals.

REFERENCES

Abd-Alla, M. H., Zohri, A.-N. A., El-Enany, A.-W. E., & Ali, S. M. (2015). Acetone–butanol–ethanol production from substandard and surplus dates by Egyptian native *Clostridium* strains. *Anaerobe*, *32*, 77-86.

Abdeshahian, P., Al-Shorgani, N. K. N., Salih, N. K., Shukor, H., Kadier, A., Hamid, A. A., & Kalil, M. S. (2014). The production of biohydrogen by a novel strain *Clostridium* sp. YM1 in dark fermentation process. *international journal of hydrogen energy*, *39*(24), 12524-12531.

Adlakha, N., Pfau, T., Ebenhöh, O., & Yazdani, S. S. (2015). Insight into metabolic pathways of the potential biofuel producer, *Paenibacillus polymyxa* ICGEB2008. *Biotechnology for biofuels*, *8*, 1-10.

Akhlaghi, N., & Najafpour-Darzi, G. (2020). A comprehensive review on biological hydrogen production. *international journal of hydrogen energy*, *45*(43), 22492-22512.

Aly, S. S., Imai, T., Hassouna, M. S., Nguyen, D.-M. K., Higuchi, T., Kanno, A., Yamamoto, K., Akada, R., & Sekine, M. (2018). Identification of factors that accelerate hydrogen production by *Clostridium butyricum* RAK25832 using casamino acids as a nitrogen source. *international journal of hydrogen energy*, *43*(10), 5300-5313.

An, D., Li, Q., Wang, X., Yang, H., & Guo, L. (2014). Characterization on hydrogen production performance of a newly isolated *Clostridium beijerinckii* YA001 using xylose. *international journal of hydrogen energy*, *39*(35), 19928-19936.

Arslan, K., Veiga, M. C., & Kennes, C. (2021). Autotrophic (C1-gas) versus heterotrophic (fructose) accumulation of acetic acid and ethanol in *Clostridium aceticum*. *Bioresource technology*, *337*, 125485.

Aslanzadeh, J. (2006). Biochemical profile-based microbial identification systems. In *Advanced techniques in diagnostic microbiology* (pp. 84-116). Springer.

Atasoy, M., Eyice, O., Schnürer, A., & Cetecioglu, Z. (2019). Volatile fatty acids production via mixed culture fermentation: Revealing the link between pH,

inoculum type and bacterial composition. *Bioresource technology*, *292*, 121889.

Avcı, A., Kılıç, N. K., Dönmez, G., & Dönmez, S. (2014). Evaluation of hydrogen production by *Clostridium* strains on beet molasses. *Environmental technology*, *35*(3), 278-285.

Bae, J.-Y., Kim, K.-Y., Kim, J.-H., Lee, K., Cho, J.-C., & Cha, C.-J. (2010). *Paenibacillus aestuarii* sp. nov., isolated from an estuarine wetland. *International journal of systematic and evolutionary microbiology*, *60*(3), 644-647.

Baeyens, J., Zhang, H., Nie, J., Appels, L., Dewil, R., Ansart, R., & Deng, Y. (2020). Reviewing the potential of bio-hydrogen production by fermentation. *Renewable and sustainable energy reviews*, *131*, 110023.

Baghchehsaraee, B., Nakhla, G., Karamanev, D., & Margaritis, A. (2010). Fermentative hydrogen production by diverse microflora. *international journal of hydrogen energy*, *35*(10), 5021-5027.

Bao, M., Su, H., & Tan, T. (2013). Dark fermentative bio-hydrogen production: Effects of substrate pre-treatment and addition of metal ions or L-cysteine. *Fuel*, *112*, 38-44.

Bardají, D. K. R., Furlan, J. P. R., & Stehling, E. G. (2019). Isolation of a polyethylene degrading *Paenibacillus* sp. from a landfill in Brazil. *Archives of Microbiology*, *201*, 699-704.

Beckers, L., Hiligsmann, S., Hamilton, C., Masset, J., & Thonart, P. (2010). Fermentative hydrogen production by *Clostridium butyricum* CWBI1009 and *Citrobacter freundii* CWBI952 in pure and mixed cultures. *Biotechnologie, agronomie, société et environnement*, *14*(S2).

Beisel, C. L., & Afroz, T. (2016). Rethinking the hierarchy of sugar utilization in bacteria. *Journal of Bacteriology*, *198*(3), 374-376.

Berezina, O. V., Brandt, A., Yarotsky, S., Schwarz, W. H., & Zverlov, V. V. (2009). Isolation of a new butanol-producing *Clostridium* strain: high level of hemicellulosic activity and structure of solventogenesis genes of a new *Clostridium saccharobutylicum* isolate. *Systematic and Applied Microbiology*, *32*(7), 449-459.

Berg, J., Tymoczko, J., & Stryer, L. (2002). Complex carbohydrates are formed by linkage

of monosaccharides. *Biochemistry*.

Berge, O., Guinebretière, M.-H., Achouak, W., Normand, P., & Heulin, T. (2002). *Paenibacillus graminis* sp. nov. and *Paenibacillus odorifer* sp. nov., isolated from plant roots, soil and food. *International journal of systematic and evolutionary microbiology*, *52*(2), 607-616.

Bhutto, A. W., Bazmi, A. A., Kardar, M. N., & Yaseen, M. (2011). Developments in hydrogen production through microbial processes; Pakistan's prospective. *International Journal*, *2*(3).

Boodhun, B. S. F., Mudhoo, A., Kumar, G., Kim, S.-H., & Lin, C.-Y. (2017). Research perspectives on constraints, prospects and opportunities in biohydrogen production. *international journal of hydrogen energy*, *42*(45), 27471-27481.

Brettin, T., Davis, J. J., Disz, T., Edwards, R. A., Gerdes, S., Olsen, G. J., Olson, R., Overbeek, R., Parrello, B., & Pusch, G. D. (2015). RASTtk: a modular and extensible implementation of the RAST algorithm for building custom annotation pipelines and annotating batches of genomes. *Scientific reports*, *5*(1), 1-6.

Brown, J. H. (2014). Why are there so many species in the tropics? *Journal of biogeography*, *41*(1), 8-22.

Cai, J., Wang, R., Wu, Q., Wang, G., & Deng, C. (2021). Characterization of a hydrogen-producing bacterium *Clostridium* sp. 5A-1. *International Journal of Green Energy*, *18*(6), 624-633.

Cai, J., Wu, Q., Wang, G., & Deng, C. (2013). Fermentative hydrogen production by a new mesophilic bacterium *Clostridium* sp. 6A-5 isolated from the sludge of a sugar mill. *Renewable Energy*, *59*, 202-209.

Cai, J., Zhao, Y., Fan, J., Li, F., Feng, C., Guan, Y., Wang, R., & Tang, N. (2019). Photosynthetic bacteria improved hydrogen yield of combined dark-and photo-fermentation. *Journal of Biotechnology*, *302*, 18-25.

Calusinska, M., Hamilton, C., Monsieurs, P., Mathy, G., Leys, N., Franck, F., Joris, B., Thonart, P., Hiligsmann, S., & Wilmotte, A. (2015). Genome-wide transcriptional analysis suggests hydrogenase-and nitrogenase-mediated hydrogen production in *Clostridium butyricum* CWBI 1009. *Biotechnology for biofuels*, *8*(1), 1-16.

Calusinska, M., Happe, T., Joris, B., & Wilmotte, A. (2010). The surprising diversity of clostridial hydrogenases: a comparative genomic perspective. *Microbiology*, *156*(6), 1575-1588.

Caputo, A., Fournier, P.-E., & Raoult, D. (2019). Genome and pan-genome analysis to classify emerging bacteria. *Biology direct*, *14*(1), 1-9.

Chandra, R., Yadav, S., Bharagava, R. N., & Rai, V. (2011). Phenol degradation by *Paenibacillus thiaminolyticus* and *Bacillus cereus* in axenic and mixed conditions. *World Journal of Microbiology and Biotechnology*, *27*, 2939-2947.

Chandrasekhar, K., Lee, Y.-J., & Lee, D.-W. (2015). Biohydrogen production: strategies to improve process efficiency through microbial routes. *International journal of molecular sciences*, *16*(4), 8266-8293.

Chang, B.-V., Chang, I.-T., & Yuan, S. Y. (2008). Anaerobic degradation of phenanthrene and pyrene in mangrove sediment. *Bulletin of environmental contamination and toxicology*, *80*, 145-149.

Chaudhuri, B., Chowdhury, T., & Chattopadhyay, B. (2017). Comparative analysis of microbial diversity in two hot springs of Bakreshwar, West Bengal, India. *Genomics data*, *12*, 122-129.

Cheng, C.-L., Lo, Y.-C., Lee, K.-S., Lee, D.-J., Lin, C.-Y., & Chang, J.-S. (2011). Biohydrogen production from lignocellulosic feedstock. *Bioresource technology*, *102*(18), 8514-8523.

Chittibabu, G., Nath, K., & Das, D. (2006). Feasibility studies on the fermentative hydrogen production by recombinant *Escherichia coli* BL-21. *Process Biochemistry*, *41*(3), 682-688.

Christoffels, A., & van Heusden, P. (2019). Genome annotation: perspective from bacterial genomes.

Ciufo, S., Kannan, S., Sharma, S., Badretdin, A., Clark, K., Turner, S., Brover, S., Schoch, C. L., Kimchi, A., & DiCuccio, M. (2018). Using average nucleotide identity to improve taxonomic assignments in prokaryotic genomes at the NCBI. *International journal of systematic and evolutionary microbiology*, *68*(7), 2386.

da Silva Mazareli, R. C., Montoya, A. C. V., Delforno, T. P., Centurion, V. B., de Oliveira, V. M., Silva, E. L., & Varesche, M. B. A. (2021). Enzymatic routes to hydrogen and

organic acids production from banana waste fermentation by autochthonous bacteria: optimization of pH and temperature. *international journal of hydrogen energy*, *46*(12), 8454-8468.

da Silva Mazareli, R. C., Sakamoto, I. K., Silva, E. L., & Varesche, M. B. A. (2019). *Bacillus* sp. isolated from banana waste and analysis of metabolic pathways in acidogenic systems in hydrogen production. *Journal of environmental management*, *247*, 178-186.

Dalia, A., Loh, T., Sazili, A., Jahromi, M., & Samsudin, A. (2017). Characterization and identification of organic selenium-enriched bacteria isolated from rumen fluid and hot spring water. *Microbiology and Biotechnology Letters*, *45*(4), 343-353.

Daniel, R. M., & Danson, M. J. (2013). Temperature and the catalytic activity of enzymes: A fresh understanding. *FEBS letters*, *587*(17), 2738-2743.

Darling, A. E., Mau, B., & Perna, N. T. (2010). progressiveMauve: multiple genome alignment with gene gain, loss and rearrangement. *PloS one*, *5*(6), e11147.

Davis, J. J., Gerdes, S., Olsen, G. J., Olson, R., Pusch, G. D., Shukla, M., Vonstein, V., Wattam, A. R., & Yoo, H. (2016). PATtyFams: protein families for the microbial genomes in the PATRIC database. *Frontiers in microbiology*, *7*, 118.

Doetsch, R. (1981). Determinative methods of light microscopy. *Manual of methods for general bacteriology*, 21-33.

Edgar, R. C. (2004). MUSCLE: multiple sequence alignment with high accuracy and high throughput. *Nucleic acids research*, *32*(5), 1792-1797.

El-Dalatony, M. M., Basak, B., Kurade, M. B., Roh, H.-S., Jang, M., & Jeon, B.-H. (2022). Effect of sonication pretreatment on hydrogen and acetone-butanol-ethanol coproduction from *Chlamydomonas mexicana* biomass using *Clostridium acetobutylicum*. *Journal of Environmental Chemical Engineering*, *10*(3), 107600.

Elbeshbishy, E., Dhar, B. R., Nakhla, G., & Lee, H.-S. (2017). A critical review on inhibition of dark biohydrogen fermentation. *Renewable and sustainable energy reviews*, *79*, 656-668.

Federhen, S., Rossello-Mora, R., Klenk, H.-P., Tindall, B. J., Konstantinidis, K. T., Whitman, W. B., Brown, D., Labeda, D., Ussery, D., & Garrity, G. M. (2016). Meeting report: GenBank microbial genomic taxonomy workshop (12–13 May, 2015). In: Springer.

Figueiredo, G. G. O., Lopes, V. R., Romano, T., & Camara, M. C. (2020). Clostridium. In *Beneficial Microbes in Agro-Ecology* (pp. 477-491). Elsevier.

Fonseca, B. C., Bortolucci, J., da Silva, T. M., dos Passos, V. F., de Gouvêa, P. F., Dinamarco, T. M., & Reginatto, V. (2020). Butyric acid as sole product from xylose fermentation by a non-solventogenic Clostridium beijerinckii strain under controlled pH and nutritional conditions. *Bioresource Technology Reports*, *10*, 100426.

Gao, Z.-M., Xu, X., & Ruan, L.-W. (2014). Enrichment and characterization of an anaerobic cellulolytic microbial consortium SQD-1.1 from mangrove soil. *Applied microbiology and biotechnology*, *98*, 465-474.

Gaur, V. K., Sharma, P., Gaur, P., Varjani, S., Ngo, H. H., Guo, W., Chaturvedi, P., & Singhania, R. R. (2021). Sustainable mitigation of heavy metals from effluents: toxicity and fate with recent technological advancements. *Bioengineered*, *12*(1), 7297-7313.

Gill, A. (2017). The importance of bacterial culture to food microbiology in the age of genomics. *Frontiers in microbiology*, *8*, 777.

Gomes, N. C., Cleary, D. F., Pires, A. C., Almeida, A., Cunha, A., Mendonça-Hagler, L. C., & Smalla, K. (2014). Assessing variation in bacterial composition between the rhizospheres of two mangrove tree species. *Estuarine, Coastal and Shelf Science*, *139*, 40-45.

González-Tenorio, D., Muñoz-Páez, K. M., & Valdez-Vazquez, I. (2020). Butanol production coupled with acidogenesis and CO2 conversion for improved carbon utilization. *Biomass Conversion and Biorefinery*, 1-11.

Goris, J., Konstantinidis, K. T., Klappenbach, J. A., Coenye, T., Vandamme, P., & Tiedje, J. M. (2007). DNA–DNA hybridization values and their relationship to whole-genome sequence similarities. *International journal of systematic and evolutionary microbiology*, *57*(1), 81-91.

Grady, E. N., MacDonald, J., Liu, L., Richman, A., & Yuan, Z.-C. (2016). Current knowledge and perspectives of *Paenibacillus*: a review. *Microbial Cell Factories*, *15*(1), 1-18.

Grissa, I., Vergnaud, G., & Pourcel, C. (2007). CRISPRFinder: a web tool to identify clustered regularly interspaced short palindromic repeats. *Nucleic acids*

research, *35*(suppl_2), W52-W57.

Guo, X. M., Trably, E., Latrille, E., Carrère, H., & Steyer, J.-P. (2010). Hydrogen production from agricultural waste by dark fermentation: a review. *international journal of hydrogen energy*, *35*(19), 10660-10673.

Gupta, A., Murarka, A., Campbell, P., & Gonzalez, R. (2009). Anaerobic fermentation of glycerol in Paenibacillus macerans: metabolic pathways and environmental determinants. *Applied and Environmental Microbiology*, *75*(18), 5871-5883.

Hay, J. X. W., Wu, T. Y., Juan, J. C., & Md. Jahim, J. (2013). Biohydrogen production through photo fermentation or dark fermentation using waste as a substrate: overview, economics, and future prospects of hydrogen usage. *Biofuels, Bioproducts and Biorefining*, *7*(3), 334-352.

He, Z., Kisla, D., Zhang, L., Yuan, C., Green-Church, K. B., & Yousef, A. E. (2007). Isolation and identification of a *Paenibacillus polymyxa* strain that coproduces a novel lantibiotic and polymyxin. *Applied and Environmental Microbiology*, *73*(1), 168-178.

Hong, Y., Chen, C., & Wu, Y. R. (2020). Biobutanol production from sulfuric acid‐pretreated red algal biomass by a newly isolated Clostridium sp. strain WK. *Biotechnology and applied biochemistry*, *67*(5), 738-743.

Huang, Y., Zong, W., Yan, X., Wang, R., Hemme, C. L., Zhou, J., & Zhou, Z. (2010). Succession of the bacterial community and dynamics of hydrogen producers in a hydrogen-producing bioreactor. *Applied and Environmental Microbiology*, *76*(10), 3387-3390.

Huber, R., Langworthy, T. A., König, H., Thomm, M., Woese, C. R., Sleytr, U. B., & Stetter, K. O. (1986). *Thermotoga maritima* sp. *nov*. represents a new genus of unique extremely thermophilic eubacteria growing up to 90 C. *Archives of Microbiology*, *144*(4), 324-333.

Ivanova, G., Rákhely, G., & Kovács, K. L. (2009). Thermophilic biohydrogen production from energy plants by *Caldicellulosiruptor saccharolyticus* and comparison with related studies. *international journal of hydrogen energy*, *34*(9), 3659-3670.

Jayasinghearachchi, H., Singh, S., Sarma, P. M., Aginihotri, A., & Lal, B. (2010).

Fermentative hydrogen production by new marine *Clostridium amygdalinum* strain C9 isolated from offshore crude oil pipeline. *international journal of hydrogen energy*, *35*(13), 6665-6673.

Johnson, E. E., & Rehmann, L. (2020). Self-synchronized oscillatory metabolism of *Clostridium pasteurianum* in continuous culture. *Processes*, *8*(2), 137.

Junghare, M., Subudhi, S., & Lal, B. (2012). Improvement of hydrogen production under decreased partial pressure by newly isolated alkaline tolerant anaerobe, *Clostridium butyricum* TM-9A: Optimization of process parameters. *international journal of hydrogen energy*, *37*(4), 3160-3168.

Kamalaskar, L. B., Dhakephalkar, P., Meher, K., & Ranade, D. (2010). High biohydrogen yielding *Clostridium* sp. DMHC-10 isolated from sludge of distillery waste treatment plant. *international journal of hydrogen energy*, *35*(19), 10639-10644.

Kanehisa, M., Sato, Y., & Morishima, K. (2016). BlastKOALA and GhostKOALA: KEGG tools for functional characterization of genome and metagenome sequences. *Journal of molecular biology*, *428*(4), 726-731.

Kanso, S., Dasri, K., Tingthong, S., & Watanapokasin, R. Y. (2011). Diversity of cultivable hydrogen-producing bacteria isolated from agricultural soils, waste water sludge and cow dung. *international journal of hydrogen energy*, *36*(14), 8735-8742.

Kaushal, M., Chary, K. V. N., Ahlawat, S., Palabhanvi, B., Goswami, G., & Das, D. (2018). Understanding regulation in substrate dependent modulation of growth and production of alcohols in *Clostridium sporogenes* NCIM 2918 through metabolic network reconstruction and flux balance analysis. *Bioresource technology*, *249*, 767-776.

Kawada-Matsuo, M., Oogai, Y., & Komatsuzawa, H. (2016). Sugar allocation to metabolic pathways is tightly regulated and affects the virulence of *Streptococcus mutans*. *Genes*, *8*(1), 11.

Khan, M. A., Ngo, H. H., Guo, W., Liu, Y., Zhang, X., Guo, J., Chang, S. W., Nguyen, D. D., & Wang, J. (2018). Biohydrogen production from anaerobic digestion and its potential as renewable energy. *Renewable Energy*, *129*, 754-768.

Kim, D.-H., Kim, S.-H., & Shin, H.-S. (2009). Hydrogen fermentation of food waste without inoculum addition. *Enzyme and Microbial Technology*, *45*(3), 181-187.

Kim, J. Y., Jo, B. H., & Cha, H. J. (2010). Production of biohydrogen by recombinant expression of [NiFe]-hydrogenase 1 in *Escherichia coli*. *Microbial Cell Factories*, *9*(1), 1-10.

Kim, S.-H., Han, S.-K., & Shin, H.-S. (2006). Effect of substrate concentration on hydrogen production and 16S rDNA-based analysis of the microbial community in a continuous fermenter. *Process Biochemistry*, *41*(1), 199-207.

Kuhn, J., Müller, H., Salzig, D., & Czermak, P. (2015). A rapid method for an offline glycerol determination during microbial fermentation. *Electronic Journal of Biotechnology*, *18*(3), 252-255.

Kumar, G. R., & Chowdhary, N. (2016). Biotechnological and bioinformatics approaches for augmentation of biohydrogen production: A review. *Renewable and sustainable energy reviews*, *56*, 1194-1206.

Lee, D.-J., Show, K.-Y., & Su, A. (2011). Dark fermentation on biohydrogen production: pure culture. *Bioresource technology*, *102*(18), 8393-8402.

Lertsriwong, S., & Glinwong, C. (2020). Newly-isolated hydrogen-producing bacteria and biohydrogen production by *Bacillus coagulans* MO11 and *Clostridium beijerinckii* CN on molasses and agricultural wastewater. *international journal of hydrogen energy*, *45*(51), 26812-26821.

Li, J., Chi, X., Zhang, Y., & Wang, X. (2018). Enhanced coproduction of hydrogen and butanol from rice straw by a novel two-stage fermentation process. *International Biodeterioration & Biodegradation*, *127*, 62-68.

Li, S., Guo, Y., Lu, F., Huang, J., & Pang, Z. (2015). High-level butanol production from cassava starch by a newly isolated *Clostridium acetobutylicum*. *Applied biochemistry and biotechnology*, *177*, 831-841.

Lin, C.-Y., & Hung, W.-C. (2008). Enhancement of fermentative hydrogen/ethanol production from cellulose using mixed anaerobic cultures. *international journal of hydrogen energy*, *33*(14), 3660-3667.

Lin, C.-Y., Lay, C.-H., Sen, B., Chu, C.-Y., Kumar, G., Chen, C.-C., & Chang, J.-S. (2012). Fermentative hydrogen production from wastewaters: a review and prognosis. *international journal of hydrogen energy*, *37*(20), 15632-15642.

Liu, C.-M., Zheng, J.-L., Wu, S.-Y., & Chu, C.-Y. (2016). Fermentative hydrogen production

potential from washing wastewater of beverage production process. *international journal of hydrogen energy*, *41*(7), 4466-4473.

Liu, D., Sun, Y., Li, Y., & Lu, Y. (2017). Perturbation of formate pathway and NADH pathway acting on the biohydrogen production. *Scientific reports*, *7*(1), 1-8.

Lo, Y.-C., Chen, X.-J., Huang, C.-Y., Yuan, Y.-J., & Chang, J.-S. (2013). Dark fermentative hydrogen production with crude glycerol from biodiesel industry using indigenous hydrogen-producing bacteria. *international journal of hydrogen energy*, *38*(35), 15815-15822.

Lo, Y.-C., Lu, W.-C., Chen, C.-Y., & Chang, J.-S. (2010). Dark fermentative hydrogen production from enzymatic hydrolysate of xylan and pretreated rice straw by *Clostridium butyricum* CGS5. *Bioresource technology*, *101*(15), 5885-5891.

Lu, C., Zhang, Z., Zhou, X., Hu, J., Ge, X., Xia, C., Zhao, J., Wang, Y., Jing, Y., & Li, Y. (2018). Effect of substrate concentration on hydrogen production by photo-fermentation in the pilot-scale baffled bioreactor. *Bioresource technology*, *247*, 1173-1176.

Łukajtis, R., Hołowacz, I., Kucharska, K., Glinka, M., Rybarczyk, P., Przyjazny, A., & Kamiński, M. (2018). Hydrogen production from biomass using dark fermentation. *Renewable and sustainable energy reviews*, *91*, 665-694.

Lund, B., Brocklehurst, T., & Wyatt, G. (1981). Characterization of Strains of *Clostridium puniceum* sp. no v., a Pink-pigmented, Pectolytic Bacterium. *Microbiology*, *122*(1), 17-26.

Ma, Y., Huang, A., Zhu, D., Pan, G., & Wang, G. (2015). Biohydrogen production via the interaction of nitrogenase and anaerobic mixed-acid fermentation in marine bacteria. *international journal of hydrogen energy*, *40*(1), 176-183.

Maeda, T., Sanchez-Torres, V., & Wood, T. K. (2007a). Enhanced hydrogen production from glucose by metabolically engineered *Escherichia coli*. *Applied microbiology and biotechnology*, *77*(4), 879-890.

Maeda, T., Sanchez-Torres, V., & Wood, T. K. (2007b). *Escherichia coli* hydrogenase 3 is a reversible enzyme possessing hydrogen uptake and synthesis activities. *Applied microbiology and biotechnology*, *76*(5), 1035-1042.

Maeda, T., Sanchez-Torres, V., & Wood, T. K. (2012). Hydrogen production by recombinant *Escherichia coli* strains. *Microbial Biotechnology*, *5*(2), 214-225.

Maintinguer, S. I., Lazaro, C. Z., Pachiega, R., Varesche, M. B. A., Sequinel, R., & de Oliveira, J. E. (2017). Hydrogen bioproduction with *Enterobacter* sp. isolated from brewery wastewater. *international journal of hydrogen energy*, *42*(1), 152-160.

Marone, A., Massini, G., Patriarca, C., Signorini, A., Varrone, C., & Izzo, G. (2012). Hydrogen production from vegetable waste by bioaugmentation of indigenous fermentative communities. *international journal of hydrogen energy*, *37*(7), 5612-5622.

Masset, J., Calusinska, M., Hamilton, C., Hiligsmann, S., Joris, B., Wilmotte, A., & Thonart, P. (2012). Fermentative hydrogen production from glucose and starch using pure strains and artificial co-cultures of *Clostridium* spp. *Biotechnology for biofuels*, *5*, 1-15.

Masset, J., Hiligsmann, S., Hamilton, C., Beckers, L., Franck, F., & Thonart, P. (2010). Effect of pH on glucose and starch fermentation in batch and sequenced-batch mode with a recently isolated strain of hydrogen-producing *Clostridium butyricum* CWBI1009. *international journal of hydrogen energy*, *35*(8), 3371-3378.

Masuko, T., Minami, A., Iwasaki, N., Majima, T., Nishimura, S.-I., & Lee, Y. C. (2005). Carbohydrate analysis by a phenol–sulfuric acid method in microplate format. *Analytical biochemistry*, *339*(1), 69-72.

Matsumura, Y., Al-Saari, H., Mino, S., Nakagawa, S., Maruyama, F., Ogura, Y., Hayashi, T., Kurokawa, K., Sawabe, T., & Sawabe, T. (2015). Identification of a gene cluster responsible for hydrogen evolution in *Vibrio tritonius* strain AM2 with transcriptional analyses. *international journal of hydrogen energy*, *40*(30), 9137-9146.

Matsumura, Y., Sato, K., Al-saari, N., Nakagawa, S., & Sawabe, T. (2014). Enhanced hydrogen production by a newly described heterotrophic marine bacterium, *Vibrio tritonius* strain AM2, using seaweed as the feedstock. *international journal*

of hydrogen energy, *39*(14), 7270-7277.

Maynard, L., & Loosli, J. (1979). Animal Nutrition, 6th edn. ed McGraw-Hill Book Co. *New York, NY*.

Mehetre, G., Shah, M., Dastager, S. G., & Dharne, M. S. (2018). Untapped bacterial diversity and metabolic potential within Unkeshwar hot springs, India. *Archives of Microbiology*, *200*(5), 753-770.

Mei, N., Postec, A., Monnin, C., Pelletier, B., Payri, C. E., Ménez, B., Frouin, E., Ollivier, B., Erauso, G., & Quéméneur, M. (2016). Metagenomic and PCR-based diversity surveys of [FeFe]-hydrogenases combined with isolation of alkaliphilic hydrogen-producing bacteria from the serpentinite-hosted Prony Hydrothermal Field, New Caledonia. *Frontiers in microbiology*, *7*, 1301.

Mei, N., Zergane, N., Postec, A., Erauso, G., Ollier, A., Payri, C., Pelletier, B., Fardeau, M.-L., Ollivier, B., & Quéméneur, M. (2014). Fermentative hydrogen production by a new alkaliphilic *Clostridium* sp.(strain PROH2) isolated from a shallow submarine hydrothermal chimney in Prony Bay, New Caledonia. *international journal of hydrogen energy*, *39*(34), 19465-19473.

Meier-Kolthoff, J. P., Carbasse, J. S., Peinado-Olarte, R. L., & Göker, M. (2022). TYGS and LPSN: a database tandem for fast and reliable genome-based classification and nomenclature of prokaryotes. *Nucleic acids research*, *50*(D1), D801-D807.

Miller, G. L. (1959). Use of dinitrosalicylic acid reagent for determination of reducing sugar. *Analytical chemistry*, *31*(3), 426-428.

Mirzoyan, S., Romero-Pareja, P. M., Coello, M. D., Trchounian, A., & Trchounian, K. (2017). Evidence for hydrogenase-4 catalyzed biohydrogen production in *Escherichia coli*. *international journal of hydrogen energy*, *42*(34), 21697-21703.

Mishra, J., Khurana, S., Kumar, N., Ghosh, A. K., & Das, D. (2004). Molecular cloning, characterization, and overexpression of a novel [Fe]-hydrogenase isolated from a high rate of hydrogen producing *Enterobacter cloacae* IIT-BT 08. *Biochemical and biophysical research communications*, *324*(2), 679-685.

Mishra, P., Thakur, S., Singh, L., Krishnan, S., Sakinah, M., & Ab Wahid, Z. (2017). Fermentative hydrogen production from indigenous mesophilic strain *Bacillus anthracis* PUNAJAN 1 newly isolated from palm oil mill effluent. *international*

journal of hydrogen energy, *42*(25), 16054-16063.

Morales-Martínez, T. K., Medina-Morales, M. A., Ortíz-Cruz, A. L., Rodríguez-De la Garza, J. A., Moreno-Dávila, M., López-Badillo, C. M., & Ríos-González, L. (2020). Consolidated bioprocessing of hydrogen production from agave biomass by *Clostridium acetobutylicum* and bovine ruminal fluid. *international journal of hydrogen energy*, *45*(26), 13707-13716.

Morillo Pérez, J. A., García-Ribera, R., Quesada, T., Aguilera, M., Ramos-Cormenzana, A., & Monteoliva-Sánchez, M. (2008). Biosorption of heavy metals by the exopolysaccharide produced by Paenibacillus jamilae. *World Journal of Microbiology and Biotechnology*, *24*, 2699-2704.

Mullai, P., Rene, E. R., & Sridevi, K. (2013). Biohydrogen production and kinetic modeling using sediment microorganisms of pichavaram mangroves, India. *BioMed research international*, *2013*.

Murugan, R. S., Dinesh, G. H., Raja, R. K., Obeth, E. S. J., Bora, A., Samsudeen, N. M., Pugazhendhi, A., & Arun, A. (2021). Dark fermentative biohydrogen production by *Acinetobacter junii*-AH4 utilizing various industry wastewaters. *international journal of hydrogen energy*, *46*(20), 11297-11304.

Nguyen, T. A. D., Kim, J. P., Kim, M. S., Oh, Y. K., & Sim, S. J. (2008). Optimization of hydrogen production by hyperthermophilic eubacteria, *Thermotoga maritima* and *Thermotoga neapolitana* in batch fermentation. *international journal of hydrogen energy*, *33*(5), 1483-1488.

Nho, S. W., Cui, X., Kweon, O., Jin, J., Chen, H., Moon, M. S., Kim, S.-J., & Cerniglia, C. E. (2021). Phylogenetically diverse bacteria isolated from tattoo inks, an azo dye-rich environment, decolorize a wide range of azo dyes. *Annals of microbiology*, *71*, 1-11.

Nissilä, M. E., Lay, C.-H., & Puhakka, J. A. (2014). Dark fermentative hydrogen production from lignocellulosic hydrolyzates–a review. *biomass and bioenergy*, *67*, 145-159.

Niu, K., Zhang, X., Tan, W.-S., & Zhu, M.-L. (2010). Characteristics of fermentative hydrogen production with Klebsiella pneumoniae ECU-15 isolated from anaerobic sewage sludge. *international journal of hydrogen energy*, *35*(1), 71-80.

Ntaikou, I. (2021). Microbial production of hydrogen. In *Sustainable Fuel Technologies*

Handbook (pp. 315-337). Elsevier.

OAC, A. (1990). Official methods of analysis 15th ed. *Association of Official analytical chemists. Washington DC*.

Oceguera-Contreras, E., Aguilar-Juárez, O., Oseguera-Galindo, D., Macías-Barragán, J., Bolaños-Rosales, R., Mena-Enríquez, M., Arias-García, A., Montoya-Buelna, M., Graciano-Machuca, O., & De León-Rodríguez, A. (2019). Biohydrogen production by vermihumus-associated microorganisms using agro industrial wastes as substrate. *international journal of hydrogen energy*, *44*(20), 9856-9865.

Ochman, H., Elwyn, S., & Moran, N. A. (1999). Calibrating bacterial evolution. *Proceedings of the National Academy of Sciences*, *96*(22), 12638-12643.

Olukunle, O. F., Ayodeji, A. O., & Akinloye, P. O. (2021). Carboxymethyl Cellulase (CMCase) from UV-irradiation Mutated Bacillus cereus FOA-2 cultivated on Plantain (Musa parasidiaca) Stalk-based Medium: Production, Purification and Characterization. *Scientific African*, *11*, e00691.

Ondov, B. D., Treangen, T. J., Melsted, P., Mallonee, A. B., Bergman, N. H., Koren, S., & Phillippy, A. M. (2016). Mash: fast genome and metagenome distance estimation using MinHash. *Genome biology*, *17*(1), 1-14.

Öner, B. E., Akyol, Ç., Bozan, M., Ince, O., Aydin, S., & Ince, B. (2018). Bioaugmentation with Clostridium thermocellum to enhance the anaerobic biodegradation of lignocellulosic agricultural residues. *Bioresource technology*, *249*, 620-625.

Pachapur, V. L., Sarma, S. J., Brar, S. K., Le Bihan, Y., Buelna, G., & Verma, M. (2015). Biological hydrogen production using co-culture versus mono-culture system. *Environmental Technology Reviews*, *4*(1), 55-70.

Pachapur, V. L., Sarma, S. J., Brar, S. K., Le Bihan, Y., Buelna, G., & Verma, M. (2016). Surfactant mediated enhanced glycerol uptake and hydrogen production from biodiesel waste using co-culture of *Enterobacter aerogenes* and *Clostridium butyricum*. *Renewable Energy*, *95*, 542-551.

Pan, C.-M., Fan, Y.-T., Zhao, P., & Hou, H.-W. (2008). Fermentative hydrogen production by the newly isolated *Clostridium beijerinckii* Fanp3. *international journal of hydrogen energy*, *33*(20), 5383-5391.

Park, S.-C., & Won, S. (2018). Evaluation of 16S rRNA databases for taxonomic

assignments using a mock community. *Genomics & informatics*, *16*(4).

Pason, P., Tachaapaikoon, C., Panichnumsin, P., Ketbot, P., Waeonukul, R., Kosugi, A., & Ratanakhanokchai, K. (2020). One-step biohydrogen production from cassava pulp using novel enrichment of anaerobic thermophilic bacteria community. *Biocatalysis and Agricultural Biotechnology*, *27*, 101658.

Patowary, R., & Deka, H. (2020). Paenibacillus. In *Beneficial Microbes in Agro-Ecology* (pp. 339-361). Elsevier.

Pei, A. Y., Oberdorf, W. E., Nossa, C. W., Agarwal, A., Chokshi, P., Gerz, E. A., Jin, Z., Lee, P., Yang, L., & Poles, M. (2010). Diversity of 16S rRNA genes within individual prokaryotic genomes. *Applied and Environmental Microbiology*, *76*(12), 3886-3897.

Penniston, J., & Gueguim Kana, E. B. (2018). Impact of medium pH regulation on biohydrogen production in dark fermentation process using suspended and immobilized microbial cells. *Biotechnology & Biotechnological Equipment*, *32*(1), 204-212.

Peters, J. W., Schut, G. J., Boyd, E. S., Mulder, D. W., Shepard, E. M., Broderick, J. B., King, P. W., & Adams, M. W. (2015). [FeFe]-and [NiFe]-hydrogenase diversity, mechanism, and maturation. *Biochimica et Biophysica Acta (BBA)-Molecular Cell Research*, *1853*(6), 1350-1369.

Pi, J., Jawed, M., Wang, J., Xu, L., & Yan, Y. (2016). Mutational analysis of the hyc-operon determining the relationship between hydrogenase-3 and NADH pathway in *Enterobacter aerogenes*. *Enzyme and Microbial Technology*, *82*, 1-7.

Poehlein, A., Solano, J. D. M., Flitsch, S. K., Krabben, P., Winzer, K., Reid, S. J., Jones, D. T., Green, E., Minton, N. P., & Daniel, R. (2017). Microbial solvent formation revisited by comparative genome analysis. *Biotechnology for biofuels*, *10*(1), 1-15.

Poirier, S., Steyer, J.-P., Bernet, N., & Trably, E. (2020). Mitigating the variability of hydrogen production in mixed culture through bioaugmentation with exogenous pure strains. *international journal of hydrogen energy*, *45*(4), 2617-2626.

Pu, Y., Tang, J., Wang, X. C., Hu, Y., Huang, J., Zeng, Y., Ngo, H. H., & Li, Y. (2019). Hydrogen production from acidogenic food waste fermentation using untreated

inoculum: effect of substrate concentrations. *international journal of hydrogen energy*, *44*(50), 27272-27284.

Qi, N., Hu, X., Zhao, X., Li, L., Yang, J., Zhao, Y., & Li, X. (2018). Fermentative hydrogen production with peanut shell as supplementary substrate: effects of initial substrate, pH and inoculation proportion. *Renewable Energy*, *127*, 559-564.

Rahaman, S. M. B., Sarder, L., Rahaman, M. S., Ghosh, A. K., Biswas, S. K., Siraj, S., Huq, K. A., Hasanuzzaman, A. F. M., & Islam, S. S. (2013). Nutrient dynamics in the Sundarbans mangrove estuarine system of Bangladesh under different weather and tidal cycles. *Ecological Processes*, *2*(1), 1-13.

Rajagopalan, G., He, J., & Yang, K. L. (2014). Direct fermentation of xylan by *Clostridium* strain BOH3 for the production of butanol and hydrogen using optimized culture medium. *Bioresource technology*, *154*, 38-43.

Ranganathan, S., Nakai, K., & Schonbach, C. (2018). *Encyclopedia of Bioinformatics and Computational Biology: ABC of Bioinformatics*. Elsevier.

Reischl, B., Ergal, İ., & Simon, K.-M. R. (2018). Biohydrogen production characteristics of Desulfurococcus amylolyticus DSM 16532. *international journal of hydrogen energy*, *43*(18), 8747-8753.

Rorke, D., & Kana, E. G. (2016). Biohydrogen process development on waste sorghum (Sorghum bicolor) leaves: Optimization of saccharification, hydrogen production and preliminary scale up. *international journal of hydrogen energy*, *41*(30), 12941-12952.

Rydzak, T., Levin, D. B., Cicek, N., & Sparling, R. (2009). Growth phase-dependant enzyme profile of pyruvate catabolism and end-product formation in *Clostridium thermocellum* ATCC 27405. *Journal of Biotechnology*, *140*(3-4), 169-175.

Sahoo, K., & Dhal, N. (2009). Potential microbial diversity in mangrove ecosystems: a review.

Saratale, G. D., Saratale, R. G., Kim, S. H., & Kumar, G. (2018). Screening and optimization of pretreatments in the preparation of sugarcane bagasse feedstock for biohydrogen production and process optimization. *international journal of hydrogen energy*, *43*(25), 11470-11483.

Sarma, S., Anand, A., Dubey, V. K., & Moholkar, V. S. (2017). Metabolic flux network analysis of hydrogen production from crude glycerol by *Clostridium pasteurianum*. *Bioresource technology*, *242*, 169-177.

Sarma, S., Dubey, V. K., & Moholkar, V. S. (2016). Kinetic and thermodynamic analysis (with statistical optimization) of hydrogen production from crude glycerol using *Clostridium pasteurianum*. *international journal of hydrogen energy*, *41*(44), 19972-19989.

Schwengers, O., Jelonek, L., Dieckmann, M. A., Beyvers, S., Blom, J., & Goesmann, A. (2021). Bakta: rapid and standardized annotation of bacterial genomes via alignment-free sequence identification. *Microbial genomics*, *7*(11).

Sen, U., Shakdwipee, M., & Banerjee, R. (2008). Status of biological hydrogen production.

Shanmugam, S., Sun, C., Zeng, X., & Wu, Y.-R. (2018). High-efficient production of biobutanol by a novel *Clostridium* sp. strain WST with uncontrolled pH strategy. *Bioresource technology*, *256*, 543-547.

Shi, X.-Y., Jin, D.-W., Sun, Q.-Y., & Li, W.-W. (2010). Optimization of conditions for hydrogen production from brewery wastewater by anaerobic sludge using desirability function approach. *Renewable Energy*, *35*(7), 1493-1498.

Shin, H.-S., Youn, J.-H., & Kim, S.-H. (2004). Hydrogen production from food waste in anaerobic mesophilic and thermophilic acidogenesis. *international journal of hydrogen energy*, *29*(13), 1355-1363.

Singh, S., Sarma, P. M., & Lal, B. (2014). Biohydrogen production by Thermoanaerobacterium thermosaccharolyticum TERI S7 from oil reservoir flow pipeline. *international journal of hydrogen energy*, *39*(9), 4206-4214.

Singh, S., Sudhakaran, A. K., Sarma, P. M., Subudhi, S., Mandal, A. K., Gandham, G., & Lal, B. (2010). Dark fermentative biohydrogen production by mesophilic bacterial consortia isolated from riverbed sediments. *international journal of hydrogen energy*, *35*(19), 10645-10652.

Singh, V., Singh, H., & Das, D. (2019). Optimization of the medium composition for the improvement of hydrogen and butanol production using *Clostridium saccharoperbutylacetonicum* DSM 14923. *international journal of hydrogen energy*, *44*(49), 26905-26919.

Sinha, P., Roy, S., & Das, D. (2016). Genomic and proteomic approaches for dark fermentative biohydrogen production. *Renewable and sustainable energy reviews*, *56*, 1308-1321.

Sivagurunathan, P., Sen, B., & Lin, C.-Y. (2014). Batch fermentative hydrogen production by enriched mixed culture: combination strategy and their microbial composition. *Journal of bioscience and bioengineering*, *117*(2), 222-228.

Skonieczny, M. T., & Yargeau, V. (2009). Biohydrogen production from wastewater by Clostridium beijerinckii: effect of pH and substrate concentration. *international journal of hydrogen energy*, *34*(8), 3288-3294.

Smitkova, M., Janíček, F., & Riccardi, J. (2011). Life cycle analysis of processes for hydrogen production. *international journal of hydrogen energy*, *36*(13), 7844-7851.

Sompark, C., Singkhonrat, J., & Sakkayawong, N. (2021). Biotransformation of Reactive Red 141 by Paenibacillus terrigena KKW2-005 and Examination of Product Toxicity.

Srimawong, C., & Chulalaksananukul, W. (2022). Evaluating biohydrogen production by *Clostridium hydrogenum* sp. *nov*. strain CUEA01 isolated from mangrove sediments in Thailand. *international journal of hydrogen energy*, *47*(15), 9169-9182.

Srimawong, C., & Chulalaksananukul, W. (2023). Evaluation of hydrogen fermentation by a newly isolated alkaline tolerant *Clostridium felsineum* strain CUEA03. *international journal of hydrogen energy*, *48*(6), 2130-2144.

Stamatakis, A. (2014). RAxML version 8: a tool for phylogenetic analysis and post-analysis of large phylogenies. *Bioinformatics*, *30*(9), 1312-1313.

Stamatakis, A., Hoover, P., & Rougemont, J. (2008). A rapid bootstrap algorithm for the RAxML web servers. *Systematic biology*, *57*(5), 758-771.

Su, H., Cheng, J., Zhou, J., Song, W., & Cen, K. (2009). Combination of dark-and photo-fermentation to enhance hydrogen production and energy conversion efficiency. *international journal of hydrogen energy*, *34*(21), 8846-8853.

Survase, S. A., Nimbalkar, P., Jurgens, G., Granström, T., Chavan, P., & Bankar, S. B. (2020).

Efficient strategy to alleviate the inhibitory effect of lignin-derived compounds for enhanced butanol production. *ACS Sustainable Chemistry & Engineering*, *9*(3), 1172-1179.

Sybirna, K., & Bottin, H. (2013). New insights into the systems for heterologous synthesis and maturation of hydrogenases, the most efficient biohydrogen producers. *international journal of hydrogen energy*, *38*(30), 13164-13171.

Taguchi, F., Hasegawa, K., Saito-Taki, T., & Hara, K. (1996). Simultaneous production of xylanase and hydrogen using xylan in batch culture of *Clostridium* sp. strain X53. *Journal of fermentation and bioengineering*, *81*(2), 178-180.

Tan, J., Wang, D., Cao, H., Qiao, Y., Zhu, H., & Liu, X. (2018). Effect of local alkaline microenvironment on the behaviors of bacteria and osteogenic cells. *ACS Applied Materials & Interfaces*, *10*(49), 42018-42029.

Tran, K. T., Maeda, T., & Wood, T. K. (2014). Metabolic engineering of *Escherichia coli* to enhance hydrogen production from glycerol. *Applied microbiology and biotechnology*, *98*(10), 4757-4770.

Trchounian, K., Gevorgyan, H., Sawers, G., & Trchounian, A. (2021). Interdependence of *Escherichia coli* formate dehydrogenase and hydrogen-producing hydrogenases during mixed carbon sources fermentation at different pHs. *international journal of hydrogen energy*, *46*(7), 5085-5099.

Valdez-Vazquez, I., Castillo-Rubio, L. G., Pérez-Rangel, M., Sepúlveda-Gálvez, A., & Vargas, A. (2019). Enhanced hydrogen production from lignocellulosic substrates via bioaugmentation with *Clostridium* strains. *Industrial Crops and Products*, *137*, 105-111.

Valdez-Vazquez, I., Pérez-Rangel, M., Tapia, A., Buitrón, G., Molina, C., Hernández, G., & Amaya-Delgado, L. (2015). Hydrogen and butanol production from native wheat straw by synthetic microbial consortia integrated by species of *Enterococcus* and *Clostridium*. *Fuel*, *159*, 214-222.

Villanueva-Galindo, E., & Moreno-Andrade, I. (2021). Bioaugmentation on hydrogen production from food waste. *international journal of hydrogen energy*, *46*(51), 25985-25994.

Wang, J., & Yin, Y. (2018). Fermentative hydrogen production using various biomass-

based materials as feedstock. *Renewable and sustainable energy reviews*, *92*, 284-306.

Wang, J., & Yin, Y. (2021). *Clostridium* species for fermentative hydrogen production: An overview. *international journal of hydrogen energy*, *46*(70), 34599-34625.

Wang, S., Tang, H., Peng, F., Yu, X., Su, H., Xu, P., & Tan, T. (2019). Metabolite-based mutualism enhances hydrogen production in a two-species microbial consortium. *Communications biology*, *2*(1), 1-11.

Wang, X., Jin, B., & Mulcahy, D. (2008). Impact of carbon and nitrogen sources on hydrogen production by a newly isolated *Clostridium butyricum* W5. *international journal of hydrogen energy*, *33*(19), 4998-5005.

Ward, B. (2015). Bacterial energy metabolism. In *Molecular medical microbiology* (pp. 201-233). Elsevier.

Watanapokasin, R. Y., Boonyakamol, A., Sukseree, S., Krajarng, A., Sophonnithiprasert, T., Kanso, S., & Imai, T. (2009). Hydrogen production and anaerobic decolorization of wastewater containing Reactive Blue 4 by a bacterial consortium of *Salmonella subterranea* and *Paenibacillus polymyxa*. *Biodegradation*, *20*, 411-418.

Wattam, A. R., Davis, J. J., Assaf, R., Boisvert, S., Brettin, T., Bun, C., Conrad, N., Dietrich, E. M., Disz, T., & Gabbard, J. L. (2017). Improvements to PATRIC, the all-bacterial bioinformatics database and analysis resource center. *Nucleic acids research*, *45*(D1), D535-D542.

Wong, Y. M., Wu, T. Y., & Juan, J. C. (2014). A review of sustainable hydrogen production using seed sludge via dark fermentation. *Renewable and sustainable energy reviews*, *34*, 471-482.

Wu, X.-C., Shen, X.-B., Ding, R., Qian, C.-D., Fang, H.-H., & Li, O. (2010). Isolation and partial characterization of antibiotics produced by *Paenibacillus elgii* B69. *FEMS microbiology letters*, *310*(1), 32-38.

Xia, A., Jacob, A., Herrmann, C., & Murphy, J. D. (2016). Fermentative bio-hydrogen production from galactose. *Energy*, *96*, 346-354.

Xie, B., Cheng, J., Zhou, J., Song, W., & Cen, K. (2008). Cogeneration of hydrogen and methane from glucose to improve energy conversion efficiency. *international*

journal of hydrogen energy, *33*(19), 5006-5011.

Yin, Y., & Wang, J. (2016). Characterization and hydrogen production performance of a novel strain Enterococcus faecium INET2 isolated from gamma irradiated sludge. *international journal of hydrogen energy*, *41*(48), 22793-22801.

Yin, Y., & Wang, J. (2017). Isolation and characterization of a novel strain *Clostridium butyricum* INET1 for fermentative hydrogen production. *international journal of hydrogen energy*, *42*(17), 12173-12180.

Youn, S. H., Lee, K. M., Kim, K.-Y., Lee, S.-M., Woo, H. M., & Um, Y. (2016). Effective isopropanol–butanol (IB) fermentation with high butanol content using a newly isolated *Clostridium* sp. A1424. *Biotechnology for biofuels*, *9*(1), 1-15.

Zagrodnik, R., Duber, A., & Seifert, K. (2021). Hydrogen production during direct cellulose fermentation by mixed bacterial culture: The relationship between the key process parameters using response surface methodology. *Journal of Cleaner Production*, *314*, 127971.

Zhang, C., Li, T., & He, J. (2018). Characterization and genome analysis of a butanol–isopropanol-producing Clostridium beijerinckii strain BGS1. *Biotechnology for biofuels*, *11*, 1-11.

Zhang, Q., You, S., Li, Y., Qu, X., & Jiang, H. (2020). Enhanced biohydrogen production from cotton stalk hydrolysate of *Enterobacter cloacae* WL1318 by overexpression of the formate hydrogen lyase activator gene. *Biotechnology for biofuels*, *13*(1), 1-11.

Zhang, Z., Li, Y., Zhang, H., He, C., & Zhang, Q. (2017). Potential use and the energy conversion efficiency analysis of fermentation effluents from photo and dark fermentative bio-hydrogen production. *Bioresource technology*, *245*, 884-889.

Zhang, Z., Wang, Y., Hu, J., Wu, Q., & Zhang, Q. (2015). Influence of mixing method and hydraulic retention time on hydrogen production through photo-fermentation with mixed strains. *international journal of hydrogen energy*, *40*(20), 6521-6529.

Zhao, J., Song, W., Cheng, J., Liu, M., Zhang, C., & Cen, K. (2017). Improvement of fermentative hydrogen production using genetically modified *Enterobacter aerogenes*. *international journal of hydrogen energy*, *42*(6), 3676-3681.

Zhao, X., Li, D., Xu, S., Guo, Z., Zhang, Y., Man, L., Jiang, B., & Hu, X. (2017). *Clostridium*

guangxiense sp. *nov*. and *Clostridium neuense* sp. *nov*., two phylogenetically closely related hydrogen-producing species isolated from lake sediment. *International journal of systematic and evolutionary microbiology*, *67*(3), 710-715.

Zheng, H., Wang, Y., Feng, X., Li, S., Leong, Y. K., & Chang, J.-S. (2021). Renewable biohydrogen production from straw biomass–Recent advances in pretreatment/hydrolysis technologies and future development. *international journal of hydrogen energy*.

Zhu, D., Wang, G., Qiao, H., & Cai, J. (2008). Fermentative hydrogen production by the new marine *Pantoea agglomerans* isolated from the mangrove sludge. *international journal of hydrogen energy*, *33*(21), 6116-6123.

Zhu, H., Fu, B., Lu, S., Liu, H., & Liu, H. (2018). *Clostridium bovifaecis* sp. nov., a novel acetogenic bacterium isolated from cow manure. *International journal of systematic and evolutionary microbiology*, *68*(9), 2956-2959.

Ziara, R. M., Miller, D. N., Subbiah, J., & Dvorak, B. I. (2019). Lactate wastewater dark fermentation: the effect of temperature and initial pH on biohydrogen production and microbial community. *international journal of hydrogen energy*, *44*(2), 661-673.

APPENDICES

APPENDIX A

Culture medium

1. Modified DSMZ640

NH_4Cl 0.90 g

NaCl 0.90 g

$MgCl_2$ x 6 H_2O 0.40 g

KH_2PO_4 0.75 g

K_2HPO_4 1.50 g

Trypticase peptone (Polypeptone) 2.00 g

Yeast extract 1.00 g

$FeCl_3$ x 6 H_2O 2.5 mg

L-Cysteine HCl x H_2O 0.75 g

Distilled water 1000.00 ml

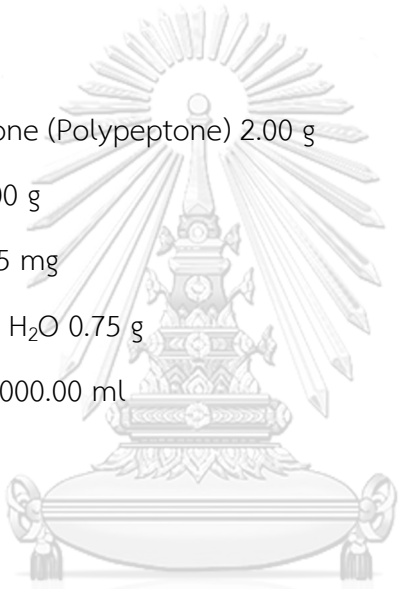

APPENDIX B

Energy recovery calculation

Table A-1 Energy content from complete combustion of various substrate

Carbon	Energy content (kJ/g)
glucose	15.59
xylose	15.60
xylan	15.60
soluble starch	15.59
casava starch	15.59
maltose	15.59
fructose	15.59
galactose	15.59
l-alabinose	15.60
manose	15.60
glycerol	16.05
cellubiose	15.59
avicel	15.59
sucrose	15.59

Specific enthalpy

Theopold, P. F., Klaus, & Richard Langley et al. (2020, November 6). Standard Thermodynamic Properties for Selected Substances. Retrieved May 24, 2021, from https://chem.libretexts.org/@go/page/43241

glucose

$$C_6H_{12}O_6 + 6O_2 \longrightarrow 6CO_2 + 6H_2O$$

$\Delta H_{rxn} = 6(\Delta H_f\ CO_2) + 6(\Delta H_f\ H_2O) - (\Delta H_f\ C_6H_{12}O_6) - 6(\Delta H_f\ O_2)$

$\Delta H_{rxn} = 6(-393.51) + 6(-285.83) - (-1268) - 6(0) = -2361.06-1714.98+1268 = -2808.04$ kJ/mol

= -2808.04 kJ/mol /180.16 g/mol = 15.59 kJ/g

xylose

$$C_5H_{10}O_5 + 5O_2 \longrightarrow 5CO_2 + 5H_2O$$

$\Delta H_{rxn} = 5(\Delta H_f\ CO_2) + 5(\Delta H_f\ H_2O) - (\Delta H_f\ C_5H_{10}O_5) - 5(\Delta H_f\ O_2)$

$\Delta H_{rxn} = 5(-393.51) + 5(-285.83) - (-1054.55) - 5(0) = -1967.55-1429.15+1054 = -2342.7$ kJ/mol

= - 2122.55 kJ/mol / 150.13 g/mol = 15.60 kJ/g

Glycerol

$$C_3H_8O_3 + 3.5O_2 \longrightarrow 3CO_2 + 4H_2O$$

$\Delta H_{rxn} = 3(\Delta H_f\ CO_2) + 4(\Delta H_f\ H_2O) - (\Delta H_f\ C_3H_8O_3) - 3.5(\Delta H_f\ O_2)$

ΔH_{rxn} = 3(-393.51) + 4(-285.83) - (-669.3) -3.5(0) = -1180.53 -1143.32+ 669.3 = -1478.51 kJ/mol

-1478.51 kJ/mol/92.09382 g/mol = 16.05 kJ/g

Table A-2 Energy content from complete combustion of products

Product	Energy content (kJ/g)
H_2	142.9 kJ/g (HHV)
Acetic acid (CH_3COOH)	14.56
Butyric acid ($C_4H_8O_2$)	24.78
Butanol ($C_4H_{10}O$)	36.78
Ethanol CH_3CH_2OH	39.16
Acetone C_3H_6O	31.33

H_2

$$2H_2 + O_2 \longrightarrow 2H_2O$$

$\Delta H_{rxn} = 2(\Delta H_f\ H_2O) - 2(\Delta H_f\ H_2) - (\Delta H_f\ O_2)$

ΔH_{rxn} = 2(-285.83) – 2(0) - (0) = -285.83 kJ/mol

-285.83 kJ/mol / 2 = 142.9 kJ/g or -285.83 kJ/mol

Acetic acid (CH_3COOH)

$CH_3COOH + 2O_2 \longrightarrow 2CO_2 + 2H_2O$

$\Delta H_{rxn} = 2(\Delta H_f\ CO_2) + 2(\Delta H_f\ H_2O) - (\Delta H_f\ CH_3COOH) - 2(\Delta H_f\ O_2)$

ΔH_{rxn} = 2(-393.51) + 2(-285.83) – (–484.3) - 2(0) = -787.02-571.66+484.3 = - 874.38 kJ/mol

- 874.38 kJ/mol / 60.052 g/mol = 14.56 kJ/g

Butyric acid -533.92

$C_4H_8O_2 + 5O_2 \longrightarrow 4CO_2 + 4H_2O$

$\Delta H_{rxn} = 4(\Delta H_f\ CO_2) + 4(\Delta H_f\ H_2O) – (\Delta H_f\ C4H8O2) - 5(\Delta H_f\ O_2)$

ΔH_{rxn} = 4(-393.51) + 4(-285.83) – (-533.92) - 5(0) = -1574.04 –1143.32 + 533.92 = - 2183.44 kJ/mol

-2183.44 kJ/mol / 88.11 g/mol = 24.78 kJ/g

Butanol ($C_4H_{10}O$) -277 $\Delta_fH°_{gas}$

$C_4H_{10}O + 6O_2 \longrightarrow 4CO_2 + 5H_2O$

$\Delta H_{rxn} = 4(\Delta H_f\ CO_2) + 5(\Delta H_f\ H_2O) – (\Delta H_f\ C_4H_{10}O) - 6(\Delta H_f\ O_2)$

ΔH_{rxn} = 4(-393.51) + 5(-285.83) – (-277) - 6(0) = -1574.04 – 1429 + 277 = - 2726.04 kJ/mol

- 2726.04 kJ/mol / 74.121 g/mol = 36.78 kJ/g

Ethanol -234

$C3H_2OH + 3O_2 \longrightarrow 3CO_2 + 3H_2O$

ΔH_{rxn} = 3(ΔH_f CO_2) + 3(ΔH_f H_2O) – (ΔH_f C3H2OH) - 3(ΔH_f O_2)

ΔH_{rxn} = 3(-393.51) + 3(-285.83) – (-234) - 3(0) = -1180.53 – 857.49 + 234 = -1804.02 kJ/mol

-1804.02 kJ/mol / 46.07 = 39.16 kJ/g

Acetone -218.5

$C_3H_6O + 4O_2 \longrightarrow 3CO_2 + 3H_2O$

ΔH_{rxn} = 3(ΔH_f CO_2) + 3(ΔH_f H_2O) – (ΔH_f C3H2OH) - 4(ΔH_f O_2)

ΔH_{rxn} = 3(-393.51) + 3(-285.83) – (-218.5) - 4(0) =-1180.53-857.49+218.5=-1819.53 kJ/mol/ 58.08 g/mol =31.33 kJ/g

APPENDIX C

H_2 gas detection and culculation

1. H_2 gas calculation

PV=nRT (25℃)

1/24.45 = 0.041

V = nRT/P

= 1*8.314472 *298/101.325

= 24.45 L

PV=nRT(0°)=22.41 =1/22.41=0.044

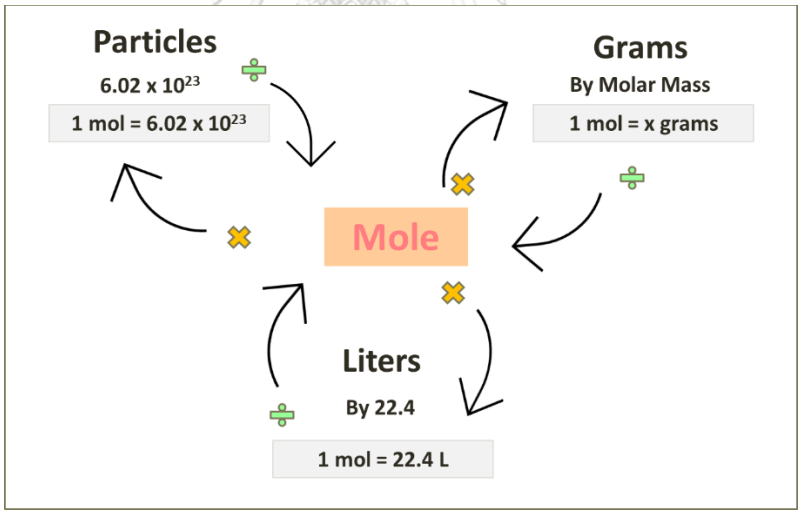

Fig. B-1 H_2 gas conversion diagram from different units.

2. Detection of standard H_2 gases by GC-TCD at varied concentrations in order to construct calibation curve of H_2 gas concentration.

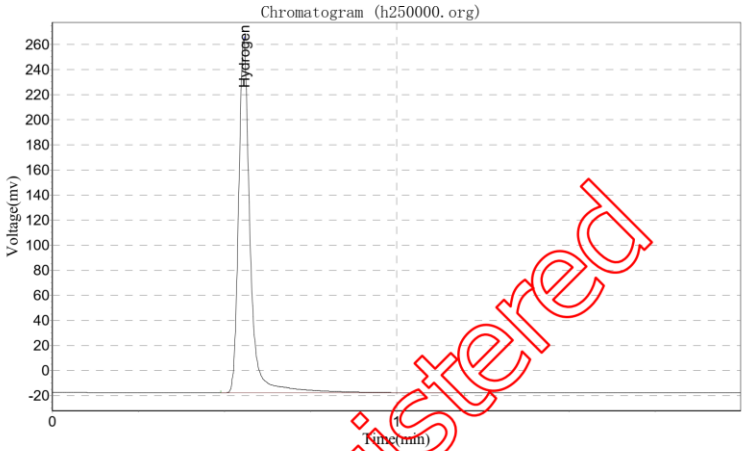

Results

Peak No.	Peak ID	Ret Time	Height	Area	Conc.
1	Hydrogen	0.557	272870.813	662431.250	22.2094
Total			272870.813	662431.250	22.2094

Fig. B-2 Chromatogram of H_2 gas at 25 percent concentration

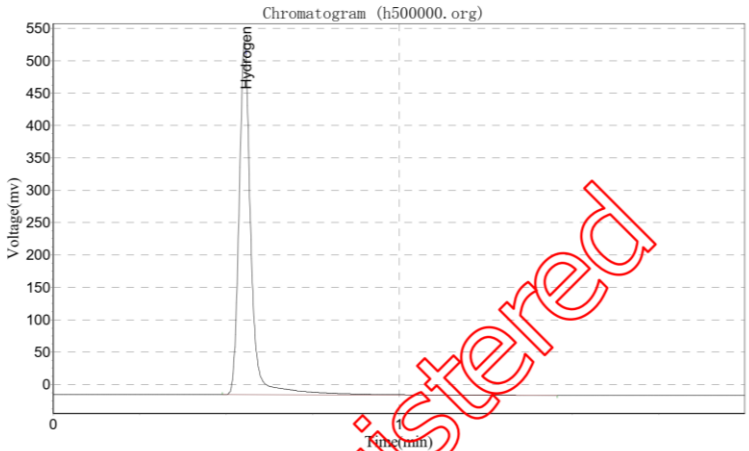

Results

Peak No.	Peak ID	Ret Time	Height	Area	Conc.
1	Hydrogen	0.557	537424.500	1317304.250	42.6646
Total			537424.500	1317304.250	42.6646

Fig. B-3 Chromatogram of H2 gas at 50 percent concentration

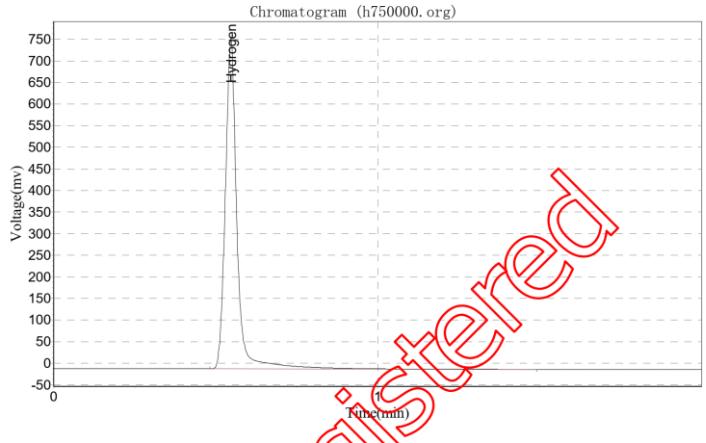

Results

eak No.	Peak ID	Ret Time	Height	Area	Conc.
1	Hydrogen	0.548	748500.188	1929711.250	61.7933
'otal			748500.188	1929711.250	61.7933

Fig. B-4 Chromatogram of H2 gas at 75 percent concentration

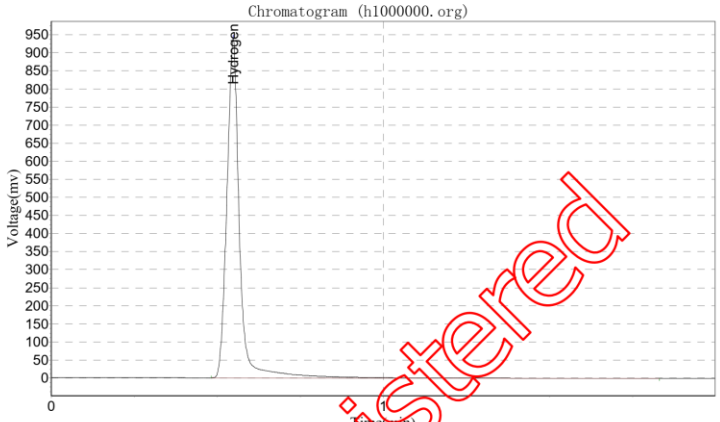

Results

Peak No.	Peak ID	Ret Time	Height	Area	Conc.
1	Hydrogen	0.548	912022.938	2508307.250	79.8659
Total			912022.938	2508307.250	79.8659

Fig. B-5 Chromatogram of H2 gas at 100 percent concentration

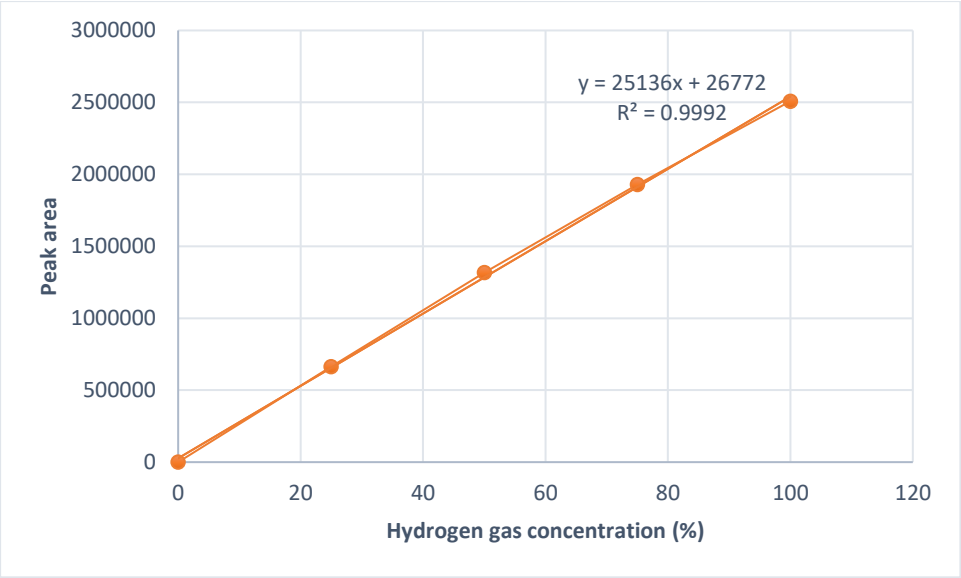

Fig. B-6 Calibration curve of H_2 concentration generated from standard H_2 gases

*Calibration was performed before each experiment of H_2 gas detection.

3. **H_2 gas sample detection**

Results

Peak No.	Peak ID	Ret Time	Height	Area	Conc.
1	Hydrogen	0.548	541375.313	1355480.625	43.8570
2		1.398	7458.333	86721.438	0.0000
Total			548833.646	1442202.063	43.8570

Fig. B-7 Chromatogram of CUEA01 (SW5A) gas sample obtained from GC-TCD.

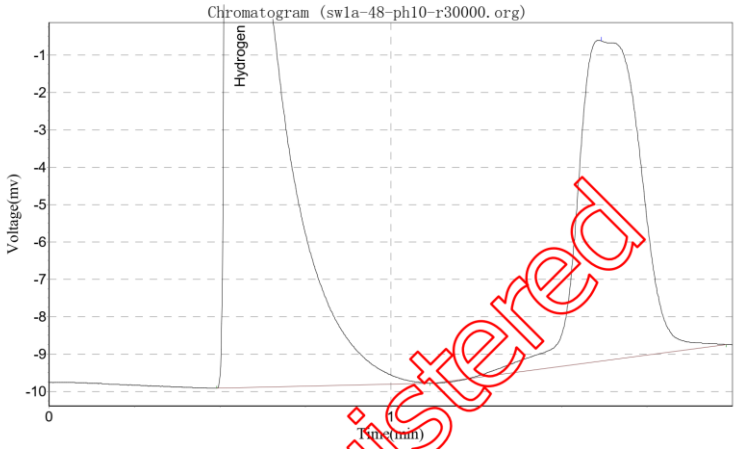

Results

Peak No.	Peak ID	Ret Time	Height	Area	Conc.
1	Hydrogen	0.557	540073.375	1322150.375	42.8159
2		1.015	8584.990	109040.852	0.0000
Total			548658.365	1431191.227	42.8159

Fig. B-8 Chromatogram of CUEA03 (SW1S) gas sample obtained from GC-TCD.

APPENDIX D

Volatile fatty acid detection

1. Volatile fatty acid

GC-FID

Analysis Date & Time : 28/03/2548 16:44:17
User Name : Admin
Vial# : 15
Sample Name : 72h_nonsuluble_starchl_r1
Sample ID :
Sample Type : Unknown
Injection Volume : 1.00
ISTD Amount :

Data Name : D:\Fai\carbon\72h_nonsuluble_starchl_r1.gcd
Method Name : D:\PUMgc\calibration curve new1.gcm

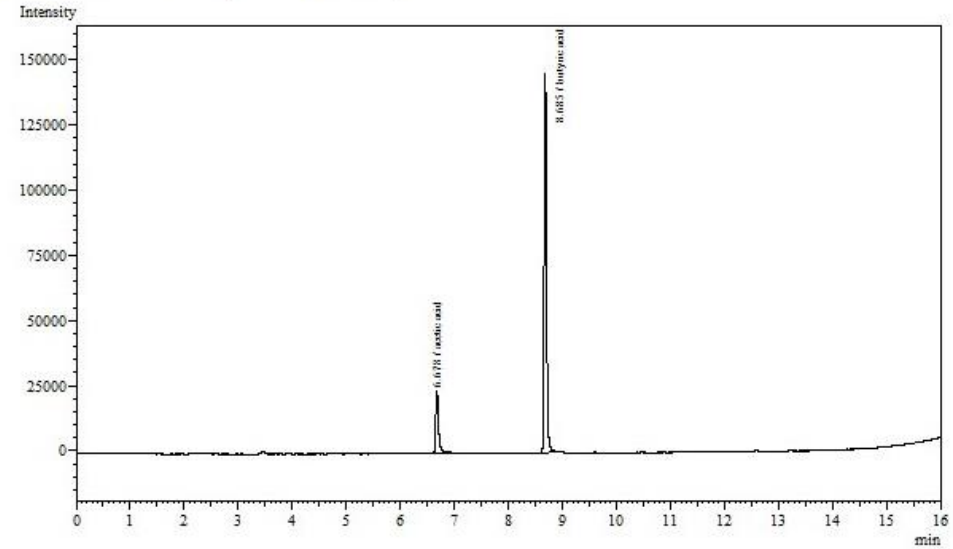

Peak#	Ret.Time	Area	Height	Conc.	Unit	Mark	ID#	Cmpd Name
1	6.678	90579	23671	1.497	g/L	S	4	acetic acid
2	8.685	448508	144693	5.055	g/L		7	butyric acid
Total		539087	168364					

Fig. C-1 Chromatogram of CUEA01 (SW5A) liquid sample obtained from GC-FID.

Analysis Date & Time : 01/10/2564 13:46:28
User Name : Admin
Vial# : 14
Sample Name : SW1S-lactose-72h-r1
Sample ID :
Sample Type : Unknown
Injection Volume : 1.00
ISTD Amount :

Data Name : D:\NuTTha\ABEtest11021\SW1S-lactose-72h-r1.gcd
Method Name : D:\PUMgc\calibration curve new1.gcm

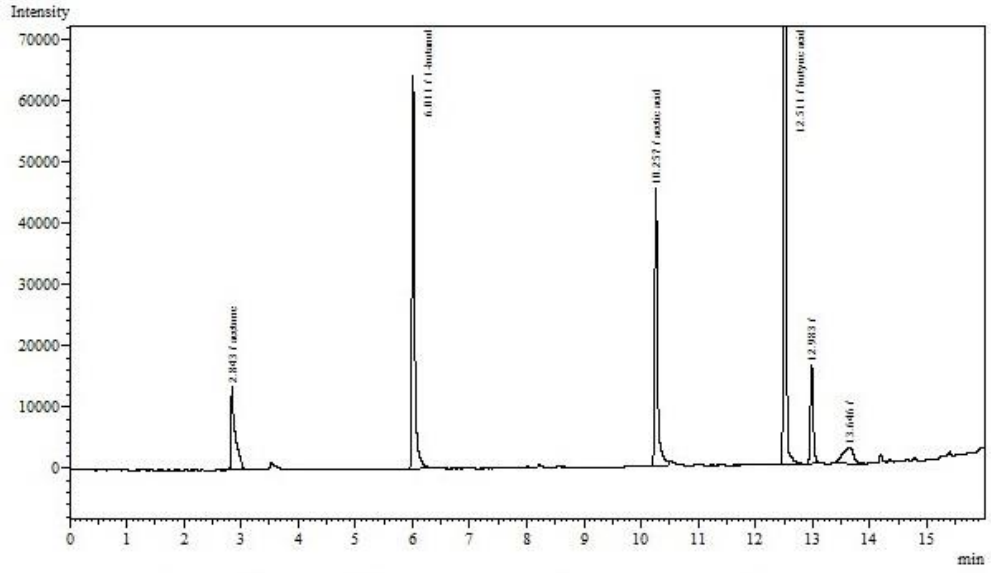

Peak#	Ret.Time	Area	Height	Conc.	Unit	Mark	ID#	Cmpd Name
1	2.843	67440	13377	0.642	g/L		1	acetone
2	6.011	205472	63482	0.831	g/L		3	1-butanol
3	10.257	154069	45229	2.100	g/L		4	acetic acid
4	12.511	417215	154461	4.843	g/L		7	butyric acid
5	12.983	55218	16002	0.000				
6	13.646	34067	2607	0.000				
Total		933481	295158					

Fig. C-2 Chromatogram of CUEA03 (SW1S) liquid sample obtained from GC-FID.

APPENDIX E

Sample collection sources

Table D-1 Samples collected from mangrove sediments in Thepha, Songkhla

Date	Samples	location	Sources	Characteristics	Temperature (°C)	pH	Note
29/07/61	SW1	717582 E, 759835 N	Pak Nam Thepha, Ban Khlong Pradu	brownish yellow water, foul odor, black clay	29.9	6.80	fishing boat parking
29/07/61	SW2	718565 E, 759241 N	Klong Thepa Beach, Ban Khlong Pradu	Closed-loop water source, wastewater, water covered with duckweeds, sandy soil	32.7	6.40	The old fish pond
29/07/61	SW3	716145 E, 758186 N	Thepha River, Ban Na Ko	Turbid brown water, black clay	30.0	6.60	The pier near Wat Sam Ong
29/07/61	SW4	721968 E, 757611 N	Klong Kwai, Ban Klong Kwai	Turbid, lots of bubbles, black and steel brown hard clays	30.9	6.2	Fishing boat mooring area near the shrimp farm
29/07/61	SW5	721061 E, 755735 N	Tuyong Canal, Ban Tuyong	still water, foamy, smells like rotten eggs, black clay	31.1	6.40	Mangrove forest area near the shrimp farm
29/07/61	SW6	725719 E, 757702 N	Koh Lae Nang Canal Ban Koh Lae Nang	Turbid water, black clay	30.8	6.50	The mangrove forest area has fish ponds surrounding it.
29/07/61	SW7	725916 E, 756174 N	Khlong Tha Yamu, Ban Tha Yamu	oily turbid green water, black clay	30.1	6.40	mangrove area

Date	Samples	location	Sources	Characteristics	Temperature (° C)	pH	Note
29/07/61	SK1	701819 E, 768542 N	Pak Khlong Sakom	Turbid water, black clay	34.1	6.71	Fishing port near the community
29/07/61	PK2	747521 E, 7 64206 N	Entrance of Pattani River	Turbid water, black clay	34.1	5.80	
29/07/61	SoBivr1	6.8527797, 101.0054754	Klong Pradu by the sea, next to the shrimp pond	black clay	-	5	The mangrove forest has Ta Kwai shells and dense mangrove trees.
29/07/61	SoBivr2	6.8528938, 101.0016462	Wat Pak Bang	clay soil mixed with sediment carried by water	-	5.6	mangrove forest
29/07/61	SoBivr3	6.8482851, 101.0161597	Watershed and Mangrove Forest Conservation Group, Klong Kwai	Clay	-	5.6	
29/07/61	RAS1	6.8527797, 101.0054754	Klong Pradu by the sea, next to the shrimp pond	Clay	-	-	

Table D-2 Samples collected from hot spring sediments in Theppanom hot spring, Mae Chaem, Chiang Mai and Mae Urm Long hot spring, Mae Sariang, Mae Hong Son.

Date	Samples	location	Sources	Characteristics	Temperature (° C)	pH	Note
16/12/61	TPNS1	18.27102, 98.39579	Theppanom hot spring, Chiang Mai	Sediment and soil under the stream	48		12
16/12/61	TPNS2	18.27102, 98.39579	Theppanom hot spring, Chiang Mai	sandy soil and grass roots	30		7

Date	Samples	location	Sources	Characteristics	Temperature (°C)	pH	Note
16/12/61	TPNS3		Theppanom hot spring, Chiang Mai				
16/12/61	TPNS4	18.27102,98.39568	Theppanom hot spring, Chiang Mai	Sediment	34		5
16/12/61	TPNS5	18.27246,98.39573	Theppanom hot spring, Chiang Mai	Orange sediment	44		5
16/12/61	TPNS6	18.27241,98.39586	Theppanom hot spring, Chiang Mai	Soil, sediment, spring mouth	71		5-7
16/12/61	TPNS7	18.2724, 98.39594	Theppanom hot spring, Chiang Mai	Sediment	78		5
16/12/61	TPNS8	18.27233,38.39604	Theppanom hot spring, Chiang Mai	Soil	85		5
16/12/61	MALS1	18.20685,98.00006	Mea Um Long Luang hot spring, Mae Hong Son	Soil, sediment	66, 71		5-10
16/12/61	MALS2	1820734,98.0003	Mea Um Long Luang hot spring, Mae Hong Son	Soil, sediment	62		5-10
16/12/61	MALS3	18.20734,98.00032	Mea Um Long Luang hot spring, Mae Hong Son	Soil, sediment	52		5-10
16/12/61	MALS4	18.20744,98.0003	Mea Um Long Luang hot spring, Mae Hong Son	Soil, sediment, spring mouth	72		5-10
16/12/61	MALS5	18.2079, 98.00027	Mea Um Long Luang hot spring, Mae Hong Son	Soil	28		5
16/12/61	MALS6	18.20693,98.00017	Mea Um Long	Soil under the	27		5

Date	Samples	location	Sources	Characteristics	Temperature (°C)	pH	Note
			Luang hot spring, Mae Hong Son	tree			
16/12/61	MALS3	18.20734,98.00032	Mea Um Long Luang hot spring, Mae Hong Son	Sediment and soil under the stream	52		
16/12/61	MALS4	18.20744, 98.0003	Mea Um Long Luang hot spring, Mae Hong Son		72		
16/12/61	MALGAS		Mea Um Long Luang hot spring, Mae Hong Son				gas bubbles pop up

Table D-3 Samples collected from Theppadungporn coconut plant, Sam Phran, Nakhon Pathom.

Date	Samples	location	Sources	Characteristics	Temperature (°C)	pH	Note
28/8/61	Wastewater	13.779398083453842, 100.47556180454096	Anaerobic tank in wastewater treatment	Cloudy, stink			
28/8/61	Wastewater	13.779398083453842, 100.47556180454096	aerobic tank in wastewater treatment	Cloudy, stink			

APPENDIX F

Methods and reagents for sugar detection

1. Reducing sugar concentration determination

Reducing sugar determination by 3, 5-dinitrosalicylic acid (DNS) method (Miller, 1959)

1.1 Reagents

3, 5-dinitrosalicylic acid	10 g
Sodium hydroxide	16 g
Potassium sodium tartrate	300 g

After mixed the component then adjusted to 1,000 ml by deionized water and kept away from light.

1.2 Method

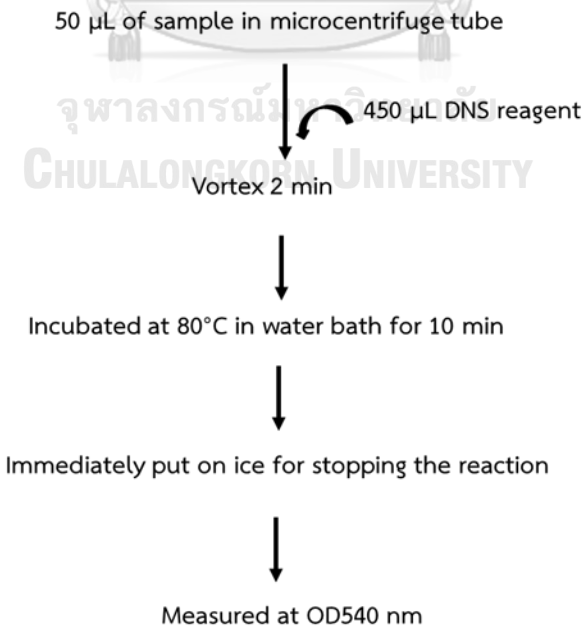

2. Carbohydrate concentration determination

The carbohydrate concentration was evaluated using phenol-sulferic acid method by (Masuko et al., 2005)

2.1 Reagents

-5% phenol

-concentrate sulfuric acid

2.2 Method

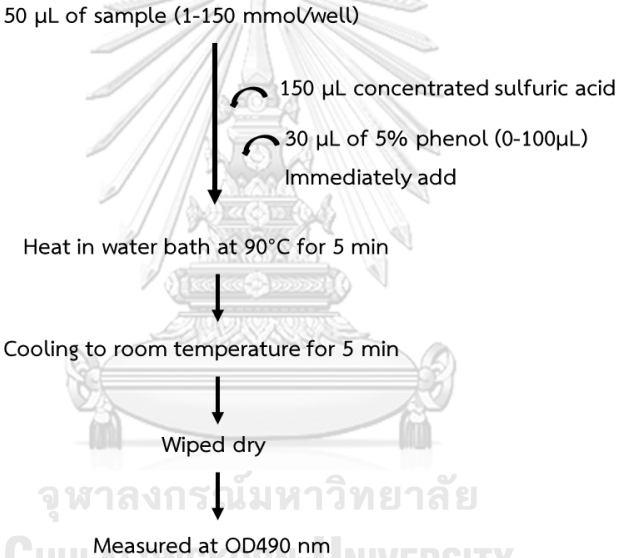

3. Glycerol concentration determination

The glycerol concentration was evaluated using the modified glycerol assay (Kuhn et al., 2015)

the method was combining two reaction principles — the Malaprade reaction and the Hantzsch reaction.

3.1 Reagents

Reagent 1: periodate reagent

-18 mg/L sodium periodate

-10%(v/v) acetic acid

-77 mg/L ammonium acetate (VWR)

The sodium periodate content of this reagent was estimated for a calibration curve ranging from 50 to 200 mg/L glycerol.

Reagent 2: acetylacetone reagent

1%(v/v) acetylacetone (VWR) in isopropyl alcohol This reagent had to be stored in the dark

3.2 Method

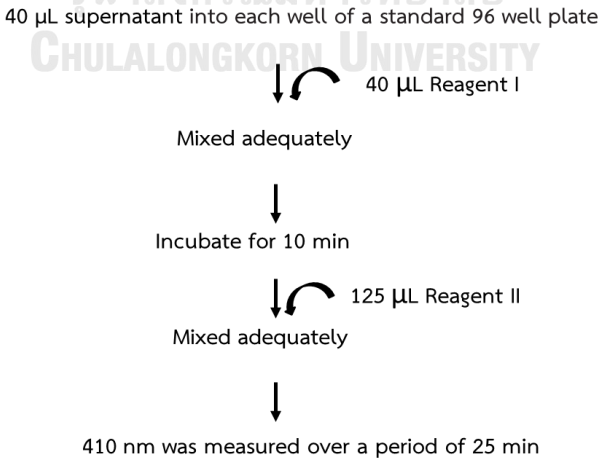

VITA

NAME	Chonticha Srimawong
DATE OF BIRTH	27 December 2535
PLACE OF BIRTH	Nakhon Ratchasim
INSTITUTIONS ATTENDED	Program in Biotechnology, Faculty of Science, Chulalongkorn University Institut Pascal, Polytech Clermont, Clermont Auvergne INP, Clermont Auvergne University Program in Biology, Faculty of Science, Srinakharinwirot University
HOME ADDRESS	200 M. 5 Nong Nam Daeng, Pak Chong, Nakhon Ratchasima, 30130
PUBLICATION	Srimawong, C., & Chulalaksananukul, W. (2022). Evaluating biohydrogen production by Clostridium hydrogenum sp. nov. strain CUEA01 isolated from mangrove sediments in Thailand. international journal of hydrogen energy, 47(15), 9169-9182. Srimawong, C., & Chulalaksananukul, W. (2023). Evaluation of hydrogen fermentation by a newly isolated alkaline tolerant Clostridium felsineum strain CUEA03. international journal of hydrogen energy, 48(6), 2130-2144.